Submitted to
manuscript (Please, provide the manuscript number!)

Effective Exact Solution Framework for Routing Optimization with Time Windows and Travel Time Uncertainty

Zhenzhen Zhang
Department of Management Science, School of Economics and Management, Tongji University, Shanghai 200092, China

Yu Zhang*
Department of Supply Chain Management, School of Business Administration, Southwestern University of Finance and Economics, Chengdu 611130, China

Roberto Baldacci
Department of Electrical, Electronic, and Information Engineering "Guglielmo Marconi", University of Bologna, Italy

We consider a vehicle routing problem with time windows under uncertain travel times where the goal is to determine routes for a fleet of homogeneous vehicles to arrive at the locations of customers within their stipulated time windows to the maximum extent, while ensuring that the total travel cost does not exceed a prescribed budget. Specifically, a novel performance measure that accounts for the riskiness associated with late arrivals at the customers, called the *generalized riskiness index* (GRI), is optimized. The GRI covers several existing riskiness indices as special cases and generates new ones. We demonstrate its salient managerial and computational properties to better motivate it. We propose alternative set partitioning-based models of the problem. To obtain the optimal solution, we develop an exact solution framework combining route enumeration and branch-price-and-cut algorithms, in which the GRI is dealt with in route enumeration and column generation subproblems. By exploiting the properties of both the GRI and budget constraint, we mainly reduce the solution space without loss of optimality. The proposed method is tested on a collection of instances derived from the literature. The results show that a new instance of the GRI outperforms several existing riskiness indices in mitigating lateness. The exact method can solve instances with up to 100 nodes to optimality, and can consistently solve instances involving up to 50 nodes, outperforming state-of-the-art methods by more than doubling the manageable instance size.

Key words: vehicle routing, uncertain travel times, riskiness indices, route enumeration, branch-price-and-cut

History: May 7, 2022

* Corresponding author, waltyuzhang@gmail.com.

1. Introduction

A basic Vehicle Routing Problem (VRP), also called a Capacitated VRP (CVRP), is at the core of the field of transportation and logistics planning, and has been attracting extensive studies over the decades (e.g., Dantzig and Ramser 1959, Laporte 2009, Baldacci et al. 2010, Toth and Vigo 2014, Vidal et al. 2020). The task of a CVRP consists of routing a fleet of homogeneous vehicles to deliver goods to (or collect them from) a set of customer locations, to ensure that the vehicle capacity is not exceeded.

Additionally, when customers need to be serviced within prescribed time windows, a CVRP is generalized to a VRP with Time Windows (VRPTW), possibly the most important variant of VRPs. As a special case of a VRPTW, a VRP with Deadlines (VRPD) does not impose the earliest times for service commencement. In a scenario in which there is only one uncapacitated vehicle, a VRP, VRPD, and VRPTW are reduced to a Traveling Salesman Problem (TSP), TSP with Deadlines (TSPD), and TSP with Time Windows (TSPTW), respectively. A VRPTW has a wide range of industrial applications, from school bus scheduling (Park and Kim 2010) to courier delivery (Sungur et al. 2010) to dial-a-ride services (Ho et al. 2018). To solve a VRPTW, various solution methods have been proposed, including exact algorithms and heuristics. Examples of the former are branch-and-cut (BC), branch-and-price (BP), branch-price-and-cut (BPC), and route enumeration (e.g., Baldacci et al. 2012, Pecin et al. 2017, Costa et al. 2019). Heuristics methods include tabu search, variable neighborhood search, and genetic algorithms (e.g., Cordeau et al. 2002, Bräysy and Gendreau 2005a,b, Vidal et al. 2014, Vidal 2017).

However, many VRPTW studies assume *deterministic* travel times, leading to potential violations of the time window requirements in the real world of *uncertainty*. In particular, late arrivals may degrade service levels, and in the long term, cause losses of customers and revenues. To consider the uncertainty in travel times and provide quality services, the methods to determine the following must be established: i) model uncertain travel times, ii) measure the time window violation level, and iii) solve the resultant VRPTW with computational effectiveness. The next section presents a review of the relevant literature on routing problems under uncertain travel times.

1.1. Literature review

In this section, we focus on the uncertainty in travel times (and service times), although the presence of customers (Bertsimas et al. 1990, Campbell and Thomas 2008) and the quantities of demands (Secomandi and Margot 2009, Gounaris et al. 2013, Dinh et al. 2018, Ghosal and Wiesemann 2020, Subramanyam et al. 2021) may also be uncertain. For more comprehensive reviews on VRP under uncertainty, we refer interested readers to Ritzinger et al. (2016), Gendreau et al. (2016), Oyola et al. (2018, 2017), De Maio et al. (2021). In particular, distributionally robust chance-constrained

optimization has been investigated by Gounaris et al. (2013), Dinh et al. (2018), and Ghosal and Wiesemann (2020). Ghosal and Wiesemann (2020) studied a VRP in which the customer demands are modeled as a random vector whose distribution is only known to belong to an ambiguity set, and proposed cutting-plane techniques to enforce robust feasibility, which were embedded into a BC framework.

In the following, we present the categories of some representative studies that deal with uncertain travel times in a VRPTW, which are also outlined in Table 1. For each study, the table lists the type of problem investigated, method to deal with the time window constraints, model of uncertainty, measure adopted to weight a time window violation, solution method, and size of the instances solved by the corresponding solution method.

Dynamic programming Kao (1978) proposed a preference-order dynamic programming to solve a TSPD that maximizes the on-time completion probability. For tractability, the arc travel times were assumed to be independently normally distributed. Subsequently, Sniedovich (1981) pointed out that the above method is inexact. Carraway et al. (1989) solved this issue by developing an exact generalized dynamic programming method. To our knowledge, dynamic programming-type methods were not adopted subsequently for studying the family of VRPTW under stochastic and dynamic travel times, possibly owing to their curse of dimensionality in addressing practical-size problems.

Chance-constrained stochastic programming For studying a VRPD, Laporte et al. (1992) proposed a chance-constrained model that minimizes the operational cost (i.e., the sum of the fixed and travel costs of the vehicles) while limiting the late completion probability within a threshold. Note that for a given routing solution, even checking the feasibility of a chance constraint is NP-hard when the arc travel times show a general distribution (Nemirovski and Shapiro 2006). Nonetheless, Laporte et al. (1992) remarked that a chance constraint poses no problem when the arc travel times have finite supports of small cardinalities or are independently and normally distributed.

Kenyon and Morton (2003) proposed to maximize the joint probability of on-time completions of all vehicles in a VRPD. They presented the relationship, in terms of their objective values, with another model that minimizes the expected completion time. The arc travel times were depicted via samples. They developed two BC algorithms to solve the problem: one applicable to the case of a small sample space, and a second inexact algorithm to a large sample space case. Adulyasak and Jaillet (2016) revisited the above problem, proposing a multi-commodity flow formulation and developing a BC algorithm, which could solve the generated instances having 80 nodes over an incomplete graph with a node having an average outdegree of 3.

Table 1 Summary of related work on VRPTW under uncertain travel times

Reference	Problem	Hard constraints	Model of uncertainty	Measure of time window violation	Solution method	Instances solved
Kao (1978)	stochastic TSPD	-	normal distribution	lateness probability	preference order dynamic programming	4 nodes
Laporte et al. (1992)	stochastic VRPD	-	discrete distribution	lateness probability, expected lateness	BC	20 nodes, 3 vehicles
Verweij et al. (2003)	stochastic TSPD	-	general distribution	expected lateness	Sample Average Approximation (SAA), Benders decomposition	101 nodes, incomplete graph
Kenyon and Morton (2003)	stochastic VRPD	-	general distribution	lateness probability	SAA, BC	28 nodes, 2 vehicles, incomplete graph
Taş et al. (2014)	stochastic VRPTW	-	Gamma distribution	expected earliness and lateness	BP	Solomon-based, vehicle capacity = 50, 100 nodes (suboptimally)
Errico et al. (2016)	stochastic VRPTW	time windows	discrete distribution	no violation	BPC	Solomon-based, 50 nodes
Lee et al. (2012)	robust VRPD	deadlines	budgeted uncertainty set	no violation	BP	Solomon-based, 25 nodes
Agra et al. (2013)	robust VRPTW	time windows	polytope uncertainty set	no violation	BC, column-and-row generation	56 ports, 20-50 cargoes
Munari et al. (2019)	robust VRPTW	time windows	budgeted uncertainty set	no violation	BPC	Solomon-based, 100 nodes (58% optimally)
Bartolini et al. (2021)	robust TSPTW	time windows	knapsack uncertainty set	no violation	column generation, route enumeration	80 nodes
Adulyasak and Jaillet (2016)	distrib. robust VRPTW	-	distribution, mean and support, moments	lateness probability, requirement violation index	Benders decomposition	80 nodes, incomplete graph
Jaillet et al. (2016)	distrib. robust TSPTW	-	distribution, mean and support, moments	requirement violation index	Benders decomposition	40 nodes, incomplete graph
Zhang et al. (2019a)	distrib. robust TSPTW	earliest service	general distribution, mean and covariance	essential riskiness index	Benders decomposition	12 nodes
Zhang et al. (2021)	distrib. robust VRPTW	earliest service	empirical distribution, Wasserstein ball	service fulfillment risk index	BC	Solomon-based, 25 nodes

Li et al. (2010) studied a chance-constrained VRPTW, in which the earliest arrival time constraints are *hard*, i.e., the vehicles have to wait if arriving before the time windows and services can still be rendered after the time windows. They adopted a tabu search to solve it, where the feasibilities of the chance-constraints for on-time services were examined by simulations. As an alternative, Ehmke et al. (2015) propose a normal approximation method to estimate the arrival time distribution and to examine the feasibility of a chance-constrained VRP.

Stochastic programming with recourse In addition to their chance-constrained model, Laporte et al. (1992) proposed a two-index recourse model and a three-index counterpart that minimize the sum of the operational and penalty costs for the expected tardiness, where the travel times are governed by discrete distributions. They developed a BC algorithm to solve this VRPD. In their models, the "recourse" is simply an observation of the tardiness (Birge and Louveaux 2011). For solving a TSPD counterpart, Verweij et al. (2003) proposed a Benders decomposition method and showed that the computational time is insensitive to the number of travel time samples.

Russell and Urban (2007) studied a VRP with *soft* time windows in which a service is rendered even in early arrival cases. Their multiple objectives included minimizing the number of used vehicles, total travel distance, and penalty incurred by time window violations. They assumed that the travel times follow the Erlang distributions and derived closed-form expressions for the expected tardiness and earliness. Moreover, a tabu search was developed to solve the problem.

Taş et al. (2013) investigated the objective of minimizing the weighted sum of the operational and penalty costs in a VRP with soft time windows. Assuming Gamma distributions of the arc travel times, they also derived closed-form expressions for the expected tardiness and earliness, and solved the problem by a tabu search. In a subsequent research, they developed a BP algorithm to solve the same problem (Taş et al. 2014). In their numerical study, they solved Solomon-based instances having 100 nodes without closing the optimality gaps.

Errico et al. (2016) studied a VRP with *hard* time windows under stochastic service times in which the time windows can never be violated; they remarked that this "hard" feature makes solving the problem extremely challenging. In their set partitioning model, they proposed two recourse policies to recover the operational infeasibility when the first-stage planned routes begin to violate the time windows. Subsequently, Errico et al. (2016) developed a BPC algorithm that can solve Solomon-based instances with 50 nodes.

We refer interested readers to Gendreau et al. (2014) for a comprehensive discussion of these methods.

Robust optimization Lee et al. (2012) investigated a robust VRPD under uncertain arc travel times within a cardinality constrained uncertainty set (Bertsimas and Sim 2004). Their model minimizes the total travel cost while ensuring that the deadlines are satisfied for all travel times in the uncertainty set. They developed a BP algorithm and solved Solomon-based instances with 25 nodes. Han et al. (2014) also studied a VRPD with consideration of a different, scenario-based uncertainty set for arc travel times. They established a BC algorithm and solve Solomon-based instances with 25 nodes.

A robust VRPTW under uncertain arc travel times within a cardinality constrained uncertainty set is more challenging to solve than a robust VRPD. In this problem, arriving earlier than the time window entails waiting and arriving later is prohibited. Agra et al. (2012) proposed a compact, layered formulation, which allows a tractable reformulation of the above robust VRPTW; however, it is computationally heavy. Subsequently, Agra et al. (2013) proposed resource and path inequality-based formulations; they develop BC and column-and-row generation algorithms, respectively, which could solve generated instances with 50 nodes. Munari et al. (2019) developed an efficient BPC algorithm that embeds a novel dynamic programming recursive equation to resolve the issue of uncertainty; they optimally solve 58% of Solomon-based instances with 100 nodes.

Bartolini et al. (2021) studied a robust TSPTW in which the arc travel times are within a knapsack-constrained uncertainty set. They devised an exact method based on column generation and route enumeration. An extension of the *ng*-route relaxation technique (Baldacci et al. 2011) enabled them to solve instances with 80 nodes. Wang et al. (2021) focused on a robust VRP, in which the customer demands and vehicle travel times are assumed to be random variables. The authors considered different classes of uncertainty sets–cardinality constrained sets, budget sets, ellipsoidal sets and discrete sets–and explored BPC algorithms that combine robust cutting-plane techniques with state-of-the-art deterministic BPC solvers. The BPC algorithms were tested on instances derived from VRP benchmark sets involving up to 150 nodes.

Distributionally robust optimization Distributionally robust optimization (DRO) can incorporate distributional ambiguity, i.e., the probability distributions of uncertain parameters are assumed to belong to an ambiguity set (a set of distributions sharing common properties). It can determine solutions that are lesser conservative than those computed by robust optimization-based methods.

Jaillet et al. (2016) introduced an innovative framework to solve a TSP with soft time windows. In particular, they proposed a new decision criterion, called requirement violation index (RVI), inspired by the riskiness index (RI) (Aumann and Serrano 2008), to measure the time window violation level. They developed a multi-commodity flow formulation and a Benders decomposition

method. In their method, the routes are optimized over known distributions of the arc travel times for which moment generating functions exist or over the worst-case distribution satisfying incomplete information, such as means, variances, and supports. Adulyasak and Jaillet (2016) extended the above study to a VRP with soft time windows and developed an improved BC algorithm.

However, the framework of Jaillet et al. (2016) cannot deal with *hard* earliest service time constraints owing to some technical factors. To address the above issue, Zhang et al. (2019a) established a multi-commodity TSPTW formulation in which the service start time is expressed as a convex piecewise affine function of the arc travel times. They further proposed a decision criterion, known as the essential riskiness index (ERI), which although possesses salient properties similar to the RVI, can deal with hard earliest service time constraints. They showed a method to optimize routes when the samples or means and covariance matrix of the arc travel times are known. They proposed a Benders decomposition method to solve small instances of the problem. Furthermore, Zhang et al. (2021) extended the decision criterion to the service fulfillment risk index (SRI), which can model differentiated customer services. They assumeed the travel times to follow a worst-case distribution that is proximal, measured by the Wasserstein distance, to an empirical distribution, and develop an efficient BC algorithm that solves Solomon-based instances with 25 nodes.

In a related investigation, Rostami et al. (2021) studied a VRP (without time windows) under stochastic and correlated arc travel times, with only known means and a covariance matrix. They minimized the weighed sum of the means and variances of the vehicular travel times for obtaining reliable travel times. Their proposed BPC algorithm could solve instances with 75 nodes.

1.2. Our contributions and overview of paper

In this study, we consider a VRPTW under uncertain travel times, in which the goal is to determine routes for a fleet of homogeneous vehicles to arrive at the locations of customers within their stipulated time windows to the maximum extent. Moreover, this should be achieved while ensuring that the total route cost does not exceed a prescribed budget. The problem is to optimize a performance measure that accounts for the riskiness associated with late arrivals at the customers.

The following are the contributions of this study:

- We develop new mathematical formulations for the above problem based on a set partitioning model that exploit the properties of the different riskiness indices reported in the literature and of the budget constraint. More specifically, the RVI of Jaillet et al. (2016), ERI of Zhang et al. (2019a), and SRI of Zhang et al. (2021) can be dealt with as special cases of the objective functions of the new models.
- We establish a reasonably general riskiness index, termed the *generalized riskiness index* (GRI), which covers some existing ones as special cases: the RVI, ERI, and SRI. We demonstrate its salient

managerial and computational properties to better motivate the GRI. To illustrate its generality, we choose a specific function in the definition of the GRI, resulting in a new measurement, termed the convex piecewise riskiness index (CPRI).

- We develop a novel exact solution framework to solve the considered VRPTW under uncertain travel times. Our framework combines route enumeration and BPC algorithms, where the chosen riskiness index is dealt with in route enumeration and column generation subproblems. Leveraging the properties of both the riskiness indices and budget constraint, we mainly reduce the size of the candidate route set without loss of optimality.
- We demonstrate that our solution framework can optimally solve Solomon-based instances with up to 100 nodes, representing the best performance reported in the existing literature. In particular, the exact method can consistently solve instances involving up to 50 nodes, outperforming the method of Zhang et al. (2021) by more than doubling the manageable instance size. We also show that our newly proposed CPRI can better mitigate lateness than the existing ones: the RVI, ERI, and SRI.
- To our knowledge, this study is the first of this type on solving the family of VRPs using DRO. This study not only supplements the optimization techniques for DRO but also enhances the corresponding solution methods, and given the flexibility of the set partitioning model in dealing with additional routing constraints, extends the practical applications of DRO.

The remainder of this paper is organized as follows. In §2 we introduce our set partitioning-based formulation for the considered VRPTW under uncertain travel times, in which the riskiness index used to measure lateness is elaborated in §3. Subsequently, we present our exact solution framework in §4, followed by the algorithm details in §5. In §6, we discuss extensive computational studies conducted to demonstrate the computational efficiency and the efficacy of the decision criterion. In §7, we present the conclusions of this study and point out future research directions.

2. Problem definition and riskiness index-based mathematical formulations

The VRPTW with uncertain travel times considered in this study is defined on a digraph $G=(V,A)$, where $V=\{0,1,\ldots,n+m\}$ is a set of $n+m+1$ vertices and A is an arc set. Vertex 0 represents the depot and vertex set V is partitioned as $V=\{0\}\cup V_c\cup V_d$ where set $V_c=\{1,\ldots,n\}$ corresponds to n customers. For description convenience, we introduce m dummy depots $V_d=\{n+1,\ldots,n+m\}$ positioned at the same location as depot 0, and we regard depots 0 and V_d as the start depot and set of the end depots, respectively. Each vertex $i\in V$ is associated with a demand q_i (we assume $q_0=0$ and $q_i=0$, $\forall i\in V_d$) and a time window $[e_i,l_i]$, where e_i and l_i represent the earliest and latest times, respectively, to serve vertex i. Arc set A is defined as $A=\{(0,i):\forall i\in V_c\}\cup\{(i,j):\forall i,j\in V_c, i\neq j\}\cup\{(i,j):\forall i\in V_c, j\in V_d\}$.

A fleet of m identical vehicles of capacity Q stationed at the depot has to fulfill customer demands. Each arc $(i,j) \in A$ is associated with a travel cost d_{ij} and let $\tilde{t}_{ij}$ be the consolidated nonnegative random variable associated with the random travel time for traversing arc (i,j). In the following, (i,j) and a are used interchangeably to represent an arc in set A.

A vehicle route $R = (0, i_1, \ldots, i_\nu, i_{\nu+1})$, where $\nu \geq 1$ and $i_{\nu+1} \in V_d$, is a simple path in G starting from depot 0, visiting customers $\{i_1, \ldots, i_\nu\}$ such that the total demand of the visited customers does not exceed the vehicle capacity Q, and ends at vertex or depot $i_{\nu+1}$. We consider the *hard earliest* time window case where if the route arrives at a vertex i before e_i the service is delayed to time e_i, and an arrival later than l_i is allowed; however, the latter results in a poor customer service. The cost of route R is the sum of the travel costs of the arc set traversed by the route.

We define a VRPTW solution as a set of at most m routes such that each customer is visited exactly once by exactly one route and the total route cost is within a budget $B > 0$. Given the uncertain nature of the problem, to improve service quality, the objective should penalize tardiness and ensure that the fleet of vehicles arrives at the locations of the customers within their stipulated time windows to the maximum extent. The next section elucidates this in more detail.

2.1. Riskiness index-based mathematical formulations

In this section, we first present a review of the riskiness index-based mathematical formulations reported in the literature and subsequently describe a new set partitioning-based formulation for the studied VRPTW.

Let $\mathcal{R}$ be the index set of all feasible VRPTW routes, and for $r \in \mathcal{R}$, we denote the corresponding route with R_r, and represent the set of vertices visited and arcs traversed by the route as $V(R_r)$ and $A(R_r)$, respectively. Let $\mathcal{P}$ be the index set of all feasible VRPTW solutions, where a solution $p \in \mathcal{P}$ is defined by a set $\{r_1^p, \ldots, r_{h_p}^p\} \subset \mathcal{R}$ of $h_p \leq m$ routes. Without loss of generality, we assume that route R_s, $s = 1, \ldots, h_p$, ends at depot $n + s$.

Each solution $p \in \mathcal{P}$ is associated with a characteristic or incident vector $\boldsymbol{x} \in \{0,1\}^{|A|}$, where $x_{ij} = 1$ if arc (i,j) is traversed by one of the routes of p, i.e., $(i,j) \in A(R_s)$ for some $s \in \{r_1^p, \ldots, r_{h_p}^p\}$, and 0 otherwise. Let $\mathcal{S} = \{\boldsymbol{x}^p\}_{p \in \mathcal{P}}$ be a set of all characteristic vectors associated with the solutions in $\mathcal{P}$, where $\boldsymbol{x}^p \in \mathcal{S}$ denotes the characteristic vector of solution $p \in \mathcal{P}$.

To quantify the riskiness associated with the violation of deadlines, recent studies (Jaillet et al. 2016, Zhang et al. 2019a, 2021) have demonstrated the issue of the commonly used "lateness probability" (to be detailed in §3.1), and thus, have focused on objective functions based on particular riskiness indices. More specifically, consider riskiness index computed by a function $\rho(\bar{\xi}_i(\boldsymbol{x}, \tilde{\boldsymbol{t}})) : \mathcal{V} \mapsto [0, +\infty]$ that evaluates the service riskiness at vertex $i \in V$, where function $\bar{\xi}_i(\boldsymbol{x}, \tilde{\boldsymbol{t}})$ is the *delay function* at vertex i (see §EC.2 of the e-companion to this paper) and $\mathcal{V}$ is the space of real-valued random variables. The following model is used to minimize the sum of riskiness indices:

$$\min \quad \sum_{i \in V} \rho(\bar{\xi}_i(\boldsymbol{x}, \tilde{\boldsymbol{t}})) \tag{1a}$$

$$\text{s.t.} \quad \boldsymbol{c}^\top \boldsymbol{x} \leq B, \tag{1b}$$

$$\boldsymbol{x} \in \mathcal{S}. \tag{1c}$$

Objective function (1a) minimizes the sum of the riskiness indices over all vertices with deadlines where constraint (1b) ensures that the total travel cost does not exceed the prescribed budget B.

Zhang et al. (2021) introduced the SRI (see §3) and proposed a mixed-integer linear reformulation of model (1) (see §EC.2). In particular, set $\mathcal{S}$ is represented by a set of constraints of a two-index (vehicle flow) formulation for a directed capacitated VRP proposed by Laporte et al. (1986). Moreover, an additional set of the constraints of exponential size is used to correctly consider the SRI in the objective function. Jaillet et al. (2016) and Zhang et al. (2019a) established the RI and the ERI for a TSPD and a TSPTW, respectively. They also proposed to solve (1); however, the procedure involved modeling the set of characteristic vectors, $\mathcal{S}$, as a set of characteristic vectors $(\boldsymbol{x}, \boldsymbol{s})$, where $\boldsymbol{x} \in \{0,1\}^{|A|}$ and $\boldsymbol{s} \in \mathbb{R}^{|A| \times |V|}$ are associated with the constraints of the multi-commodity flow formulation proposed by Claus (1984) for an Asymmetric TSP.

Given a solution $p \in \mathcal{P}$ and a realization $\boldsymbol{t}$ of travel times $\tilde{\boldsymbol{t}}$, we can determine the service start times of the vertices by computing for each route $s \in \{r_1^p, \ldots, r_{h_p}^p\}$ with $R_s = (i_0 = 0, i_1, \ldots, i_\nu, i_{\nu+1})$ in the following recursive expression:

$$\tau_{i_k}(R_s, \boldsymbol{t}) = \max\{\tau_{i_{k-1}}(R_s, \boldsymbol{t}) + t_{i_{k-1} i_k}, e_{i_k}\}, \quad k = 1, \ldots, \nu + 1, \tag{2}$$

where $\tau_0(R_s, \boldsymbol{t}) = e_0$. The following property states that the service start time of a node can be represented as a convex piecewise affine function of $\boldsymbol{t}$.

Proposition 1 *Given a route $r \in \mathcal{R}$ with $R_r = (i_0 = 0, i_1, i_2, \ldots, i_{\nu-1}, i_\nu, i_{\nu+1})$ and a realization of $\tilde{\boldsymbol{t}}$, denoted by $\boldsymbol{t}$, the service start time for each node $i_k \in V(R_r)$ is determined by the function*

$$\tau_{i_k}(R_r, \boldsymbol{t}) = \max_{h=0,\ldots,k} \left\{ e_{i_h} + \sum_{l=h}^{k-1} t_{i_l i_{l+1}} \right\}. \tag{3}$$

Proof. The proof is provided in §EC.4.1 of the e-companion of this paper. □

Based on the service start time function, we define the *delay function* at vertex $i \in V(R_r)$ as follows

$$\xi_i(R_r, \boldsymbol{t}) = \tau_i(R_r, \boldsymbol{t}) - l_i, \tag{4}$$

which is also a convex piecewise affine in $\boldsymbol{t}$, and hence, a late service at vertex i occurs if and only if $\xi_i(R_r, \boldsymbol{t}) > 0$. Because travel times $\tilde{\boldsymbol{t}}$ are uncertain, delay function $\xi_i(R_r, \tilde{\boldsymbol{t}})$ is also uncertain.

Based on the above definitions, the sum of the riskiness indices over all vertices with deadlines can be written as follows:

$$\sum_{s\in\left\{r_1^p,\ldots,r_{h_p}^p\right\}}\sum_{i\in V(R_s)}\rho(\xi_i(R_s,\tilde{\boldsymbol{t}}))=\sum_{s\in\left\{r_1^p,\ldots,r_{h_p}^p\right\}}\zeta_s(\rho,\tilde{\boldsymbol{t}}), \tag{5}$$

where $\zeta_s(\rho,\tilde{\boldsymbol{t}})=\sum_{i\in V(R_s)}\rho(\xi_i(R_s,\tilde{\boldsymbol{t}}))$ is the total riskiness index of route R_s.

Let c_r be the cost of route $r\in\mathcal{R}$ computed as $c_r=\sum_{a\in A(R_r)}c_a$, and let a_{ir} be a binary coefficient equal to 1 if vertex $i\in V(R_r)$, and 0 otherwise. Let y_r be a binary variable equal to 1 if and only if route r is in the optimal solution. Model (1) can be reformulated as follows:

$$(F_\rho(\mathcal{R}))\quad \min \sum_{r\in\mathcal{R}}\zeta_r(\rho,\tilde{\boldsymbol{t}})y_r \tag{6a}$$

$$\text{s.t.} \sum_{r\in\mathcal{R}}a_{ir}y_r=1,\quad \forall i\in V_c, \tag{6b}$$

$$\sum_{r\in\mathcal{R}}y_r\le m, \tag{6c}$$

$$\sum_{r\in\mathcal{R}}c_r y_r\le B, \tag{6d}$$

$$y_r\in\{0,1\},\quad \forall r\in\mathcal{R}. \tag{6e}$$

Constraints (6b) specify that each customer $i\in V_c$ has to be visited by exactly one route. Constraint (6c) requires that at most m routes are selected whereas Constraint (6d) imposes that the total cost is within the budget B.

With respect to the model proposed by Zhang et al. (2021) showing a polynomial number of variables and an exponential number of constraints (see §EC.2), model (6) shows a polynomial number of constraints. Moreover, it embeds the computation of function $\rho(\cdot)$ into the definition of the route set $\mathcal{R}$. Therefore, its complexity strongly depends on the definition of function $\rho(\cdot)$ and the size of the route set $\mathcal{R}$. The next section discusses the study of the different riskiness indices together with their salient properties whereas §4 describes the reformulations of model $F_\rho(\mathcal{R})$ and presents the solution framework adopted to solve the model.

3. Riskiness indices

In this section, we discuss in detail the riskiness index $\rho(\xi_i(R,\tilde{\boldsymbol{t}}))$ in model (6). For notational convenience, we use shorthand $\tilde{\xi}$ interchangeably to represent the uncertain delay $\xi_i(R,\tilde{\boldsymbol{t}})$ at some node $i\in V$ for some given route R. The uncertainty is modeled by a state-space Ω and a $\sigma-$algebra $\mathcal{F}$ of events in Ω. $\mathbb{P}$ denotes the distribution of the uncertain parameters in $(\Omega,\mathcal{F})$, where $\mathbb{P}[\cdot]$ denotes the probability of some event, and $\mathbb{E}_{\mathbb{P}}[\tilde{\xi}]$ represents the expectation of the uncertain parameter $\tilde{\xi}$ under probability distribution $\mathbb{P}$. The distribution itself may also be uncertain and is contained in an ambiguity set $\mathbb{F}$.

3.1. Review of riskiness indices in routing optimization

To measure the lateness level under uncertainty, Kenyon and Morton (2003) and Adulyasak and Jaillet (2016) adopted a lateness probability criterion, $\mathbb{P}[\tilde{\xi} > 0]$. However, it cannot distinguish different lateness magnitudes having the same lateness probability (e.g., a route in which $\mathbb{P}[\tilde{\xi} = 10] = 5\%$ and $\mathbb{P}[\tilde{\xi} \le 0] = 95\%$, and another in which $\mathbb{P}[\tilde{\xi} = 20] = 5\%$ and $\mathbb{P}[\tilde{\xi} \le 0] = 95\%$). Verweij et al. (2003) and Taş et al. (2014) alternatively employed expected lateness duration, $\mathbb{E}_{\mathbb{P}}[\max\{\tilde{\xi}, 0\}]$, which can account for the lateness magnitude; however, it does not provide insight into the lateness probability. Recently, Zhang et al. (2021) proposed the following riskiness index that captures both the lateness probability and its magnitude. We presents an example to illustrate this issue in §EC.3.

Definition 1 *(*Service Fulfillment Risk Index, SRI*) Given a random delay $\tilde{\xi} \in \mathcal{V}$ governed by probability distribution $\mathbb{P}$ within ambiguity set $\mathbb{F}$, the SRI is defined as*

$$\rho_{SRI}(\tilde{\xi}) = \min\left\{\alpha \ge 0 \;\middle|\; \sup_{\mathbb{P}\in\mathbb{F}} \mathbb{E}_{\mathbb{P}}\left[(\tilde{\xi}+\alpha)^+\right] \le \gamma\alpha \right\}, \tag{7}$$

where $\gamma \in (0,1]$ corresponds to some service level and $(x)^+ = \max\{x, 0\}$.

Zhang et al. (2021) elucidate the following managerial and computational properties of the SRI for any $\tilde{\xi}, \tilde{\xi}_1$, and $\tilde{\xi}_2 \in \mathcal{V}$:

i) *Satisficing:* $\rho_{SRI}(\tilde{\xi}) = 0$ if and only if $\mathbb{P}[\tilde{\xi} \le 0] = 1$ for all $\mathbb{P} \in \mathbb{F}$.

ii) *Infeasibility:* If the worst-case Conditional Value-at-Risk (CVaR), $\mathbb{F}\text{-CVaR}_{1-\gamma}(\tilde{\xi}) > 0$, then $\rho_{SRI}(\tilde{\xi}) = +\infty$. Here, $\mathbb{F}\text{-CVaR}_{1-\gamma}(\tilde{\xi})$ is defined as

$$\mathbb{F}\text{-CVaR}_{1-\gamma}(\tilde{\xi}) = \min_{\beta\in\mathbb{R}} \left\{\beta + \frac{1}{\gamma} \sup_{\mathbb{P}\in\mathbb{F}} \mathbb{E}_{\mathbb{P}}[(\tilde{\xi}-\beta)^+]\right\}.$$

iii) *Convexity:* $\rho_{SRI}\left(\lambda\tilde{\xi}_1 + (1-\lambda)\tilde{\xi}_2\right) \le \lambda\rho_{SRI}(\tilde{\xi}_1) + (1-\lambda)\rho_{SRI}(\tilde{\xi}_2)$ for all $\lambda \in [0,1]$.

iv) *Probability envelope:* For all $\theta \ge 0$ and $\mathbb{P} \in \mathbb{F}$, we have

$$\mathbb{P}\left[\tilde{\xi} > \rho_{SRI}(\tilde{\xi})\theta\right] \le \frac{\gamma}{1+\theta}. \tag{8}$$

Recall that the uncertain delay, $\tilde{\xi}$, is defined in (EC.2) or (4) as difference between the uncertain service start time and the deadline. Thus, the property of satisficing indicates that the SRI is zero, its best possible value, if and only if the service start time is earlier than the deadline almost surely for all probability distributions in the ambiguity set. Because the worst-case CVaR is translation-invariant (Zhu and Fukushima 2009), $\mathbb{F}\text{-CVaR}_{1-\gamma}(\tilde{\xi}) > 0$ is equivalent to $\mathbb{F}\text{-CVaR}_{1-\gamma}$(the service start time) $>$ the deadline. Thus, the property of infeasibility asserts that if the worst-case CVaR of the service start time is later than the deadline, then the corresponding route is infeasible. Convexity is desired in the optimization computation. The probability envelope ensures that the

probability of the service start time exceeding the deadline with an additional duration, $\rho_{SRI}(\tilde{\xi})\theta$, is upper bounded by a threshold $\gamma/(1+\theta)$, for all $\theta \geq 0$ and all $\mathbb{P} \in \mathbb{F}$. When $\theta = 0$, the lateness probability, $\mathbb{P}[\tilde{\xi} > 0] \leq \gamma$ for all $\mathbb{P} \in \mathbb{F}$. Subsequently in Example 2, we provide a concrete example to illustrate this property.

The SRI generalizes an earlier riskiness index proposed by Zhang et al. (2019a), which is defined as follows.

Definition 2 *(*Essential Riskiness Index, ERI*) Given a random delay $\tilde{\xi} \in \mathcal{V}$ governed by probability distribution $\mathbb{P}$ within ambiguity set $\mathbb{F}$, the ERI is defined as*

$$\rho_{ERI}(\tilde{\xi}) = \min\left\{\alpha \geq 0 \;\middle|\; \sup_{\mathbb{P}\in\mathbb{F}} \mathbb{E}_{\mathbb{P}}\left[(\tilde{\xi}+\alpha)^{+}\right] \leq \alpha\right\}. \tag{9}$$

Indeed, the SRI reduces to the ERI when $\gamma = 1$. Thus, the ERI also possesses the above properties when $\gamma = 1$. Specifically, for any $\tilde{\xi}, \tilde{\xi}_1$ and $\tilde{\xi}_2 \in \mathcal{V}$, we have

i) *Satisficing:* $\rho_{ERI}(\tilde{\xi}) = 0$ if and only if $\mathbb{P}[\tilde{\xi} \leq 0] = 1$ for all $\mathbb{P} \in \mathbb{F}$.

ii) *Infeasibility:* If $\sup_{\mathbb{P}\in\mathbb{F}} \mathbb{E}_{\mathbb{P}}[\tilde{\xi}] > 0$, then $\rho_{ERI}(\tilde{\xi}) = +\infty$.

iii) *Convexity:* $\rho_{ERI}(\lambda\tilde{\xi}_1 + (1-\lambda)\tilde{\xi}_2) \leq \lambda\rho_{ERI}(\tilde{\xi}_1) + (1-\lambda)\rho_{ERI}(\tilde{\xi}_2)$ for all $\lambda \in [0,1]$.

iv) *Probability envelope:* For all $\theta \geq 0$ and $\mathbb{P} \in \mathbb{F}$, we have

$$\mathbb{P}\left[\tilde{\xi} > \rho_{ERI}(\tilde{\xi})\theta\right] \leq \frac{1}{1+\theta}. \tag{10}$$

With regard to the condition of infeasibility, we note that $\mathbb{F}\text{-CVaR}_{1-\gamma}(\tilde{\xi}) = \sup_{\mathbb{P}\in\mathbb{F}} \mathbb{E}_{\mathbb{P}}[\tilde{\xi}]$ when $\gamma = 1$ (Rockafellar and Uryasev 2002). By introducing another dimension, $\gamma \in (0,1]$, of flexibility, the SRI can model differentiated service levels for different customers. The correspondence of γ to the service level is shown by fact that the ERI provides a trivial lateness probability bound, $\mathbb{P}[\tilde{\xi} > 0] \leq 1, \forall \mathbb{P} \in \mathbb{F}$, whereas the SRI provides a non-trivial one, $\mathbb{P}[\tilde{\xi} > 0] \leq \gamma, \forall \mathbb{P} \in \mathbb{F}$, when $\gamma \in (0,1)$.

This direction of riskiness index-based research in routing optimization originates from the study by Jaillet et al. (2016), who propose the following riskiness index.

Definition 3 *(*Requirement Violation Index, RVI*) Given a random delay $\tilde{\xi} \in \mathcal{V}$ governed by probability distribution $\mathbb{P}$ within ambiguity set $\mathbb{F}$, the RVI is defined as*

$$\rho_{RVI}(\tilde{\xi}) = \inf\left\{\alpha > 0 \;\middle|\; \sup_{\mathbb{P}\in\mathbb{F}} \mathbb{E}_{\mathbb{P}}\left[\exp(\tilde{\xi}/\alpha)\right] \leq 1\right\}. \tag{11}$$

The RVI, based on the Riskiness Index of Aumann and Serrano (2008) in economics literature, has been introduced by Jaillet et al. (2016) into vehicle routing under uncertain travel times and/or demands. Jaillet et al. (2016) show the following salient properties of the RVI, for any $\tilde{\xi}, \tilde{\xi}_1$, and $\tilde{\xi}_2 \in \mathcal{V}$:

i) *Satisficing:* $\rho_{RVI}(\tilde{\xi}) = 0$ if and only if $\mathbb{P}[\tilde{\xi} \leq 0] = 1$ for all $\mathbb{P} \in \mathbb{F}$.

ii) *Infeasibility:* If $\sup_{\mathbb{P}\in\mathbb{F}} \mathbb{E}_{\mathbb{P}}[\tilde{\xi}] > 0$, then $\rho_{RVI}(\tilde{\xi}) = +\infty$.

iii) *Convexity:* $\rho_{RVI}(\lambda\tilde{\xi}_1 + (1-\lambda)\tilde{\xi}_2) \leq \lambda\rho_{RVI}(\tilde{\xi}_1) + (1-\lambda)\rho_{RVI}(\tilde{\xi}_2)$ for all $\lambda \in [0,1]$.

iv) *Probability envelope:* For all $\theta > 0$ and $\mathbb{P} \in \mathbb{F}$, we have

$$\mathbb{P}[\tilde{\xi} > \theta] \leq \exp\big(-\theta/\rho_{RVI}(\tilde{\xi})\big). \tag{12}$$

These properties are highly analogous to those of the ERI, with a difference in the shape of the probability envelope, which is elucidated subsequently using Example 2. However, to achieve computationally tractable models, the RVI requires the arc travel times to be *independently* distributed and the time windows to be *soft*, i.e., the vehicles should start services immediately even if arriving before the required earliest service times. These limitations motivate Zhang et al. (2019a, 2021) to propose the ERI and SRI for solving a VRPTW with *hard* earliest service time constraints and possibly correlated travel times.

3.2. Generalized Riskiness Index

Given the similarity in the salient properties and the difference in the mathematical forms of the RI and the ERI (and its generalization, the SRI), it is natural to question whether there exist other decision criteria of alternative mathematical forms that possess similar properties and would perform even better in mitigating lateness. Thus, we extend the boundaries and propose such a reasonably general decision criterion, showing the hidden relations between the RI, ERI, and SRI.

Definition 4 *(*Generalized Riskiness Index, GRI*) Given a random delay $\tilde{\xi} \in \mathcal{V}$ governed by probability distribution $\mathbb{P}$ within ambiguity set $\mathbb{F}$, we define the GRI as*

$$\rho_{GRI}(\tilde{\xi}) = \inf\left\{\alpha > 0 \;\middle|\; \sup_{\mathbb{P}\in\mathbb{F}} \mathbb{E}_{\mathbb{P}}\big[\phi(\tilde{\xi}/\alpha)\big] \leq \gamma\right\}, \tag{13}$$

where $\gamma \in (0,1]$ corresponds to some service level, and $\phi(\cdot)$ is a disutility function that is convex, non-decreasing, non-negative, and satisfies $\phi(0) = 1$, $\phi(\xi) \geq \xi + 1$ for all $\xi \in \mathbb{R}$, and $\phi(\xi) \to 0^+$ as $\xi \to -\infty$.

The GRI has the following desired properties.

Theorem 1 *For any $\tilde{\xi}, \tilde{\xi}_1$, and $\tilde{\xi}_2 \in \mathcal{V}$, we have:*

i) Monotonicity: If $\mathbb{P}[\tilde{\xi}_1 \geq \tilde{\xi}_2] = 1$ for all $\mathbb{P} \in \mathbb{F}$, then $\rho_{GRI}(\tilde{\xi}_1) \geq \rho_{GRI}(\tilde{\xi}_2)$.

ii) Satisficing: If $\mathbb{P}[\tilde{\xi} < 0] = 1$ for all $\mathbb{P} \in \mathbb{F}$, then $\rho_{GRI}(\tilde{\xi}) = 0$.

iii) Infeasibility: If $\sup_{\mathbb{P}\in\mathbb{F}} \mathbb{E}_{\mathbb{P}}[\tilde{\xi}] > 0$, then $\rho_{GRI}(\tilde{\xi}) = +\infty$.

iv) Positive homogeneity: $\rho_{GRI}(k\tilde{\xi}) = k\rho_{GRI}(\tilde{\xi})$ for all $k > 0$.

v) Convexity: $\rho_{GRI}\big(\lambda\tilde{\xi}_1+(1-\lambda)\tilde{\xi}_2\big)\le\lambda\rho_{GRI}\big(\tilde{\xi}_1\big)+(1-\lambda)\rho_{GRI}\big(\tilde{\xi}_2\big)$ *for all* $\lambda\in[0,1]$.

vi) Subadditivity: $\rho_{GRI}\big(\tilde{\xi}_1+\tilde{\xi}_2\big)\le\rho_{GRI}\big(\tilde{\xi}_1\big)+\rho_{GRI}\big(\tilde{\xi}_2\big)$.

vii) Probability envelope: For all $\theta>0$ *and* $\mathbb{P}\in\mathbb{F}$, *we have*

$$\mathbb{P}\big[\tilde{\xi}>\theta\big]\le\frac{\gamma}{\phi\big(\theta/\rho_{GRI}(\tilde{\xi})\big)}. \tag{14}$$

Proof. The proof is provided in §EC.4.2 of the e-companion to this paper. □

From a managerial standpoint, the monotonicity property indicates that a later service start time leads to a larger (or at least an equal) value of the GRI, implying a worse performance. In terms of the satisficing property, if the service start time is earlier than the deadline almost surely, the GRI is equal to zero, its best possible value. The infeasibility property indicates that if there exists some distribution in the ambiguity set such that the expected service start time is later than the deadline, the corresponding route is infeasible. Positive homogeneity implies that the GRI increases proportionally with the uncertain delay. For instance, consider an uncertain delay $\tilde{\xi}_1$ with $\mathbb{P}[\tilde{\xi}_1=-10]=90\%$ and $\mathbb{P}[\tilde{\xi}_1=10]=10\%$ and another one, $\tilde{\xi}_2=2\tilde{\xi}_1$. In this scenario, the GRI considers $\tilde{\xi}_2$ twice riskier than $\tilde{\xi}_1$; however, the lateness probability criterion does not distinguish them, such that even if $\tilde{\xi}_1$ is late for 10 minutes and $\tilde{\xi}_2$ for 20 minutes, they have the same lateness probability, 10%. Subadditivity suggests that the riskiness of the combined delays does not exceed the sum of the riskiness associated with the individual delays. Probability envelope suggests that the lateness probability with respect to the sum of deadline and any duration decays at a certain rate, which is subsequently illustrated in Example 2.

From a computational viewpoint, the monotonicity and infeasibility properties help in the design of effective solution methods (see §4), and, as will be explained in §3.3, the convexity facilitates evaluating the GRI.

In the following, we discuss the relations and differences between the GRI and the aforementioned riskiness indices—RI, ERI and SRI. First, in the terms of the mathematical forms, the GRI covers these riskiness indices as special cases. This is illustrated, based on the observation that when $\phi(\xi)=\exp(\xi)$ and $\gamma=1$, the GRI recovers the RVI in (11); when $\phi(\xi)=(\xi+1)^+$, the GRI recovers the SRI in (7), and when additionally $\gamma=1$, the GRI recovers the ERI in (9). Second, from the aspect of the possessed properties, our Theorem 1 shows the additional properties–monotonicity, positive homogeneity, and subadditivity–possessed by the RVI, ERI, and SRI that were not exhibited previously by Jaillet et al. (2016), Zhang et al. (2019a, 2021). However, our satisficing property of the GRI is slightly weaker than those of the RVI, ERI, and SRI; this can be viewed as consequence to compensate the generality of GRI.

In addition to the aforementioned riskiness indices, by choosing alternative disutility functions $\phi(\cdot)$ in the GRI, new ones can be obtained. Among them are a class of convex piecewise functions.

Definition 5 *(*Convex Piecewise Riskiness Index, CPRI*) A CPRI is a GRI in which the disutility function has the form*

$$\phi(\xi) = \sum_{k\in[K]} \phi_k(\xi)\mathbb{1}\{\xi \in \Xi_k\},$$

where $\Xi_k, k \in [K]$, form a K-partition of the support of ξ, and $\phi_k(\xi), k \in [K]$, are a set of convex functions.

In the following, we present a concrete example.

Example 1 *(CPRI) When $\phi_{CPRI}(\xi) = 0\mathbb{1}\{\xi < -1\} + (\xi+1)\mathbb{1}\{-1 \le \xi < 0\} + \exp(\xi)\mathbb{1}\{\xi \ge 0\}$, the resultant CPRI is expressed as:*

$$\rho_{CPRI}(\tilde{\xi}) = \inf\left\{\alpha > 0 \;\middle|\; \sup_{\mathbb{P}\in\mathbb{F}} \mathbb{E}_{\mathbb{P}}\left[\phi_{CPRI}(\tilde{\xi}/\alpha)\right] \le \gamma \right\}.$$

One can verify that such choice of $\phi_{CPRI}(\xi)$ satisfies the conditions required by the definition of the GRI, and thus, it possesses the properties of GRI.

It would be interesting to compare the probability envelopes induced by the different GRIs. To this end, we present the following example.

Example 2 *Let us consider a random delay $\tilde{\xi}$ following a two-point distribution: $\mathbb{P}[\tilde{\xi} = -10] = 50\%$ and $\mathbb{P}[\tilde{\xi} = 5] = 50\%$; thus, ambiguity set $\mathbb{F}$ is a singleton comprising this distribution. Using the algorithm to be presented in §EC.5, we calculate that $\rho_{RVI}(\tilde{\xi}) \approx 10.39, \rho_{ERI}(\tilde{\xi}) = 5, \rho_{SRI}(\tilde{\xi}) = 6.25$ and $\rho_{CPRI}(\tilde{\xi}) \approx 8.51$, where $\gamma = 0.9$ is set for the SRI and CPRI. The induced probability envelopes, calculated using (14), are shown in Figure 1. In this example, all probability envelopes are generally not tight compared with the exact one, except those of the ERI, SRI, and CPRI when $\theta = 5$. Among them, the SRI appears to be the tightest when $\theta \in [0, 5]$ whereas the CPRI is the tightest when $\theta \in [5, 30]$. The RVI and the CPRI decay exponentially, whereas the ERI and the SRI decays reciprocally.*

We remark that although each probability envelope is not tight, it can account for both the lateness probability and its magnitude, thereby guiding the search direction for vehicle routes during optimization.

3.3. Evaluating Generalized Riskiness Index

We aim to develop a computationally efficient method to evaluate the GRI, $\rho_{GRI}(\tilde{\xi})$, or equivalently $\rho_{GRI}(\xi(R, \tilde{\boldsymbol{t}}))$, given some route R and some ambiguity set $\mathbb{F}$ of distribution $\mathbb{P}$ governing the uncertain arc travel times, $\tilde{\boldsymbol{t}}$. This is a key procedure in the design of effective solution methods for model (6) (see §4).

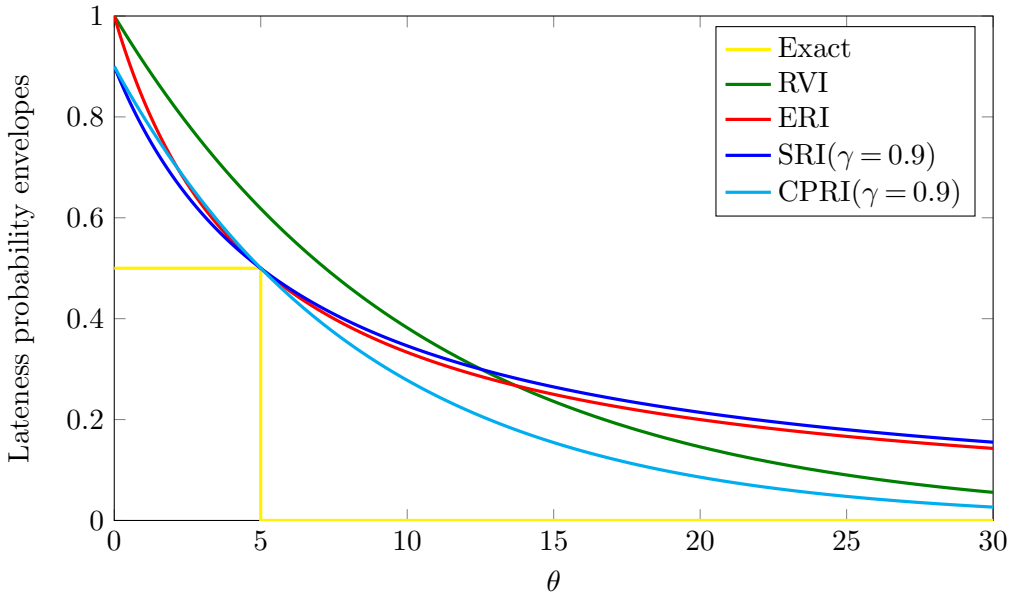

Figure 1 **Lateness probability envelopes**

First, we discuss a review of the methods for evaluating the RVI, ERI, and SRI under different models of the arc travel times. For evaluating the RVI, Jaillet et al. (2016) suggested a bisection algorithm to be feasible when $\tilde{\boldsymbol{t}}$ are independently distributed and each $\tilde{t}_{ij}, (i,j) \in A$, follows a known or an ambiguous distribution. The known distribution has a well-defined moment generating function, whereas the ambiguous distribution has known bounds and a mean value, or has known moment information. For evaluating the ERI, Zhang et al. (2019a) derived a closed-form solution when $\tilde{\boldsymbol{t}}$ follow from an empirical distribution. Alternatively, they solve a semidefinite program when the ambiguous distribution is characterized by the means and covariance of $\tilde{\boldsymbol{t}}$. Subsequently, Zhang et al. (2021) derived a closed-form solution when $\tilde{\boldsymbol{t}}$ are governed by an ambiguous distribution in proximity, as measured by the Wasserstein distance, to an empirical distribution. However, their methods rely on distinct structures of the corresponding riskiness indices, which may not be trivially extended to evaluate our GRI.

In this study, we consider using an empirical distribution to model the uncertain travel times $\tilde{\boldsymbol{t}}$. It is supposed that we have N samples of $\tilde{\boldsymbol{t}}$, denoted by $\boldsymbol{t}^{\omega}$, where $\omega \in \Omega$ and $\Omega = \{1, 2, \cdots, N\}$. The empirical distribution, $\mathbb{P}$, is defined as a discrete uniform distribution over the samples, i.e., $\mathbb{P}[\tilde{\boldsymbol{t}} = \boldsymbol{t}^{\omega}] = 1/N, \forall \omega \in \Omega$. In this setting, the ambiguity set, $\mathbb{F}$, in (13) is defined as the singleton $\{\mathbb{P}\}$ containing the empirical distribution. This modeling choice originates from two reasons. From a managerial viewpoint, in the big data era, one can acquire data much easier; thus, historical travel time data can be employed as samples, which is a useful and natural modeling of the travel times. From a computational perspective, this choice allows a computationally efficient algorithm

to evaluate the GRI, which will be shown subsequently. However, despite these advantages, this modeling choice fails to consider the ambiguity in the travel times.

Based on an empirical distribution, the GRI can be rewritten as

$$\rho(\tilde{\xi}) = \inf\{\alpha > 0 \mid \psi(\alpha) \leq \gamma\}, \tag{15}$$

where $\psi(\alpha) = N^{-1}\sum_{\omega\in\Omega}\phi(\xi^{\omega}/\alpha)$, and ξ^{ω} is the delay function under sample $\omega \in \Omega$. To evaluate the GRI, we first need a convexity result.

Proposition 2 *The function $\psi(\alpha)$ is convex in $\alpha > 0$.*

Proof. The proof is presented in §EC.4.3 of the e-companion of this paper. □

By virtue of the convexity property, we can evaluate the GRI by a bisection search, detailed in Algorithm 1 presented in §EC.5 of the e-companion to this paper. Because Algorithm 1 is generally applicable for evaluating the GRI, it is also applicable to the special case, SRI. Zhang et al. (2021) propose a closed-form solution to evaluate the SRI. We are interested in investigating the loss of the computational efficiency of Algorithm 1 relative to that of the closed-form solution. We defer the computational results to §EC.6, which demonstrate that Algorithm 1 is, unexpectedly, approximately five times faster than the closed-form solution that embeds a sorting procedure with complexity $O(N \log N)$.

4. Exact solution framework

In this section, we first describe the reformulations of model $F_\rho(\mathcal{R})$ that mainly reduce the size of route set $\mathcal{R}$ without loss of optimality. This is realized by leveraging (i) the *infeasibility* property, a property shared by all the riskiness indices described in the previous section, and (ii) the cost budget constraint (6d). Subsequently, we present an overview of the solution framework adopted to solve the resulting models, whose implementation details are described in §5. Hereafter, $z(x)$ denotes the optimal solution cost of model x.

Based on the *infeasibility* property in Theorem 1, the set of routes $\mathcal{R}$ can be replaced by a set of routes $\mathcal{R}_\rho$ defined as $\mathcal{R}_\rho = \{r \in \mathcal{R} : \rho(\xi_i(R_r, \tilde{\boldsymbol{t}})) < +\infty, \forall i \in V(R_r)\}$. Understandably, $\mathcal{R}_\rho \subseteq \mathcal{R}$, and under the assumption that model $F_\rho(\mathcal{R})$ allows a bounded optimal solution, the optimal solution cost, $z(F_\rho(\mathcal{R}_\rho))$, of model $F_\rho(\mathcal{R}_\rho)$ equals $z(F_\rho(\mathcal{R}))$. We follow the convention and assume that $z(F_\rho(\mathcal{R}_\rho)) = +\infty$ if model $F_\rho(\mathcal{R}_\rho)$ has no feasible solution.

However, examining the condition in $\mathcal{R}_\rho$ requires some efforts, e.g., invoking Algorithm 1 in §EC.5. Alternatively, we can employ a lesser restrictive but computationally amiable condition, to discard the infeasible routes. Specifically, let $\boldsymbol{\mu} = \mathbb{E}_{\mathbb{P}}(\tilde{\boldsymbol{t}})$ be the expectation of $\tilde{\boldsymbol{t}}$ under probability distribution $\mathbb{P}$ representing the mean travel times. Let $\mathcal{R}_{cap}$ be the set of feasible routes satisfying

the capacity constraints only. Given a route $r \in \mathcal{R}_{cap}$ and travel times $\boldsymbol{\mu}$, the service start times of route $R_r = (i_0 = 0, i_1, i_2, \ldots, i_{\nu-1}, i_\nu, i_{\nu+1})$ under mean travel times $\boldsymbol{\mu}$ can be computed as

$$\tau_{i_k}(R_r, \boldsymbol{\mu}) = \max\{\tau_{i_{k-1}}(R_r, \boldsymbol{\mu}) + \mu_{i_{k-1}i_k}, e_{i_k}\}, \quad k = 1, \ldots, \nu+1. \tag{16}$$

Let $\overline{\mathcal{R}} \subseteq \mathcal{R}_{cap}$ be the set of routes in $\mathcal{R}_{cap}$ satisfying the time window constraints based on the mean travel times $\boldsymbol{\mu}$, i.e., $\overline{\mathcal{R}} = \{r \in \mathcal{R}_{cap} : e_i \leq \tau_i(R_r, \boldsymbol{\mu}) \leq l_i, \forall i \in V(R_r)\}$. Thus, the following proposition holds.

Proposition 3 $\mathcal{R}_\rho \subseteq \overline{\mathcal{R}} \subseteq \mathcal{R}$.

Proof. The proof is provided in §EC.4.4 of the e-companion of this paper. □

Based on the above proposition, set $\mathcal{R}_\rho$ can be redefined as $\mathcal{R}_\rho = \{r \in \overline{\mathcal{R}} : \rho(\xi_i(R_r, \tilde{\boldsymbol{t}})) < +\infty, \forall i \in V(R_r)\}$. Route set $\mathcal{R}_\rho$ can be further reduced by exploiting the properties of the budget constraint (6d) based on the following model:

$$(FB(\mathcal{R}_\rho)) \quad \min \sum_{r \in \mathcal{R}_\rho} c_r y_r \tag{17a}$$

$$\text{s.t. } (6b), (6c), (6e). \tag{17b}$$

Let $\overline{\boldsymbol{u}} \in \mathbb{R}^{|V_c|+1}$ be the vector of the dual variables associated with the linear programming (LP) relaxation of model $FB(\mathcal{R}_\rho)$, where variables $\overline{u}_i \in \mathbb{R}$, $i \in V_c$, are associated with constraints (6b) whereas variable $\overline{u}_0 \leq 0$ is associated with constraint (6c). Thus, the following theorem holds.

Theorem 2 *Let $\overline{\boldsymbol{u}}$ be a feasible solution of the dual of the LP relaxation of model $FB(\mathcal{R}_\rho)$ of cost $\overline{z}$. Define the reduced cost of a route $r \in \mathcal{R}_\rho$ with respect to the dual solution $\overline{\boldsymbol{u}}$ as $\overline{c}_r = c_r - \sum_{i \in V_c} a_{ir}\overline{u}_i - \overline{u}_0$. Any optimal solution $\boldsymbol{y}^*$ of $FB(\mathcal{R}_\rho)$ with cost $z(FB(\mathcal{R}_\rho))$ less than or equal to the budget B cannot contain any route $r \in \mathcal{R}_\rho$ such that $\overline{c}_r > B - \overline{z}$.*

Proof. The proof is provided in §EC.4.5 of the e-companion of this paper. □

Based on the above theorem, given a feasible dual solution $\overline{\boldsymbol{u}}$ of the LP relaxation of model $FB(\mathcal{R}_\rho)$ of cost $\overline{z}$, we define set $\overline{\mathcal{R}}_\rho = \{r \in \mathcal{R}_\rho : \overline{c}_r \leq B - \overline{z}\}$. Understandably, $\overline{\mathcal{R}}_\rho \subseteq \mathcal{R}_\rho$ and $z(F_\rho(\overline{\mathcal{R}}_\rho)) = z(F_\rho(\mathcal{R}_\rho))$.

The exact solution framework combines a route enumeration technique and BPC algorithms to solve model (6) effectively. It comprises the following steps:

1. *Compute the initial dual solution.* A feasible dual solution $\overline{\boldsymbol{u}}$ of the LP relaxation of model $FB(\overline{\mathcal{R}})$ of cost $\overline{z}$ is computed (see §5.1.2). Note that the route set, $\overline{\mathcal{R}}$, accounts for the capacity constraints and the time window constraints based on the mean travel times.

2. *Route enumeration.* Using the dual solution, $\overline{\boldsymbol{u}}$, the largest route set, $\overline{\mathcal{R}}_\rho = \{r \in \mathcal{R}_\rho : \bar{c}_r \leq B - \bar{z}\}$ such that $|\overline{\mathcal{R}}_\rho| \leq \Delta_{max}$, where Δ_{max} is a user-defined parameter, is generated (see §EC.7.2). In addition to the capacity constraints, time window constraints on the mean travel times, and infeasibility property, the generation of set $\overline{\mathcal{R}}_\rho$ relies on the reduction stated by Theorem 2.
3. *Finding an optimal solution.* We have the following three cases:
   a) $|\overline{\mathcal{R}}_\rho| < \Delta_{mip}$: Model $F_\rho(\overline{\mathcal{R}}_\rho)$ is solved using a general purpose mixed-integer programming (MIP) solver, where Δ_{mip} is a user-defined parameter.
   b) $\Delta_{mip} \leq |\overline{\mathcal{R}}_\rho| < \Delta_{max}$: Model $F_\rho(\overline{\mathcal{R}}_\rho)$ is solved using a BPC algorithm based on the enumerated set of routes $\overline{\mathcal{R}}_\rho$ (see §5.2).
   c) $|\overline{\mathcal{R}}_\rho| \geq \Delta_{max}$: Model $F_\rho(\mathcal{R}_\rho)$ is solved using a BPC algorithm (see §5.3).

The next section describes the implementation details of the exact method based on the above solution framework.

5. Algorithm details

In this section, we present the details of the exact method used to solve the considered VRPTW under a given sample set $\Omega = \{1, 2, \cdots, N\}$. First, we describe the procedure for computing the lower bounds in a column-and-row generation appproach (§5.1), which is also used to compute the initial dual solution required in Step 1 of the solution framework. Subsequently, we present the methods by which models $F_\rho(\overline{\mathcal{R}}_\rho)$ (§5.2) and $F_\rho(\mathcal{R}_\rho)$ (§5.3) employed in Steps 3.b) and 3.c), respectively, are solved to optimality. We detail the route enumeration procedure used in Step 2 in the e-companion to this paper (see §EC.7.2).

5.1. Column-and-row generation

Because formulations $FB(\overline{\mathcal{R}})$ and $F_\rho(\mathcal{R}_\rho)$ feature exponentially many columns, they are suitable to be solved by a column generation (CG) method (for a general introduction to CG, we refer the interested reader to Lübbecke and Desrosiers (2005)). Moreover, state-of-the-art methods for dealing with complex VRPs rely on valid inequalities used to reinforce the LP relaxation of set partitioning-based models (e.g., Poggi and Uchoa 2014, Costa et al. 2019). Therefore, we designed the following *column-and-row generation* procedure.

The LP relaxation corresponds to formulation $FB(\overline{\mathcal{R}})$ (or $F_\rho(\mathcal{R}_\rho)$) that is solved by a column-and-row generation approach, in which, at each iteration, the primal simplex algorithm is used to solve the restricted master problem (RMP) and provide a primal and a dual solution. Subsequently, a *column generation* step is performed, by which the pricing (sub)problem is solved to determine the negative reduced cost columns (or variables). If no negative reduced cost columns are found, the current primal solution is the optimal for the master problem; otherwise, one or several negative reduced cost columns are added to the RMP, and a new iteration is conducted. If the current primal

solution is the optimal one, a *row generation* step is performed, in which the valid inequalities (see below) are separated by a cutting plane approach. The cutting plane algorithm terminates when no additional valid inequalities are identified, and a new column-and-row generation iteration is executed. The lower bound computation stops when both the column and row generation algorithms terminate without finding new columns/rows to be added to the RMP.

5.1.1. Valid inequalities. The following families of the valid inequalities are used to strengthen the LP relaxation of formulations $FB(\overline{\mathcal{R}})$ and $F_\rho(\mathcal{R}_\rho)$. Let b_{ijr} be a binary coefficient equal to 1 if and only if arc $(i,j) \in A$ is traversed by the route $r \in \mathcal{R}$. In addition, $\delta^+(S) = \{(i,j) \in A \ : \ i \in S, j \in V \setminus S\}$ denotes the cutset of set $S \subseteq V_c$.

Two-path inequalities (2PIs). Given a subset S of the customer set, V_c, such that the customers in S cannot be serviced by a single vehicle because of the time windows under the mean travel times, $\boldsymbol{\mu}$, the following inequality as proposed by Kohl et al. (1999) imposes a lower bound of 2 on the arcs entering set S, where set $\mathcal{B}$ is either $\overline{\mathcal{R}}$ or $\mathcal{R}_\rho$.

$$\sum_{(i,j)\in\delta^+(S)} \sum_{r\in\mathcal{B}} b_{ijr} y_r \geq 2. \tag{18}$$

Capacity inequalities (CIs). Rounded capacity inequalities, originally proposed for a CVRP by Laporte and Nobert (1983), impose a lower bound on the number of vehicles required to service a subset S of the customer set V_c, and are defined as follows

$$\sum_{(i,j)\in\delta^+(S)} \sum_{r\in\mathcal{B}} b_{ijr} y_r \geq \left\lceil \frac{1}{Q} \sum_{i\in S} q_i \right\rceil, \tag{19}$$

where set $\mathcal{B}$ is either $\overline{\mathcal{R}}$ or $\mathcal{R}_\rho$.

Subset-row inequalities (SR3Is). Let $\mathcal{C} \subseteq \{C \subseteq V_c : |C| = 3\}$ be a subset of all customer triplets, and let $\mathcal{B}(C) \subseteq \mathcal{B}$ be the subset of the routes serving at least two customers in C (i.e., $\mathcal{B}(C) = \{r \in \mathcal{B} : |V(R_r) \cap C| \geq 2\}$), where set $\mathcal{B}$ is either $\overline{\mathcal{R}}$ or $\mathcal{R}_\rho$. The SR3Is are defined as

$$\sum_{r\in\mathcal{B}(C)} y_r \leq 1, \quad \forall C \in \mathcal{C}. \tag{20}$$

The SR3Is correspond to a subset of SR and the clique inequalities used by Jepsen et al. (2008) for a VRPTW and by Baldacci et al. (2008) for a CVRP, respectively.

To separate 2PIs (18) and CIs (19), the shrinking heuristic and route-based connected component heuristic separation procedures (Archetti et al. 2011), tabu search (Cordeau 2006), and the partial enumeration method (Desaulniers 2010) are used. We refer the reader to the corresponding studies for additional details. The SR3Is (20) are separated by complete enumeration.

5.1.2. Computing initial dual solution. To further improve the effectiveness of the route enumeration phase, the procedure adopted to compute an initial dual solution considers model $FB(\overline{\mathcal{R}})$ strengthened with the valid inequalities described in the previous section.

Let $u_i \in \mathbb{R}$, $\forall i \in V_c$, and $u_0 \leq 0$ denote the dual variables associated with constraints (6b) and (6c) of the LP relaxation of formulation $FB(\overline{\mathcal{R}})$, respectively. In addition, let $\mathcal{S} = \{S \subseteq V_c : |S| \geq 2\}$, and let $\mathcal{S}_P \subseteq \mathcal{S}$, $\mathcal{S}_C \subseteq \mathcal{S}$, and $\mathcal{C} \subseteq \{C \subseteq V_c : |C| = 3\}$ denote the sets of the 2PIs, CIs and SR3Is associated with the RMP, respectively. The corresponding dual variables are $\pi_S \geq 0$, $\forall S \in \mathcal{S}_P$, $\eta_S \geq 0$, $\forall S \in \mathcal{S}_C$, and $\varphi_T \leq 0$, $\forall T \in \mathcal{C}$. Therefore, in our implementation, the computed dual solution is represented by dual vectors $(\boldsymbol{u}, \boldsymbol{\pi}, \boldsymbol{\eta}, \boldsymbol{\varphi})$, instead of dual vector $\overline{\boldsymbol{u}}$.

Formulation $FB(\overline{\mathcal{R}})$ strengthened with the 2PIs, CIs, and SR3Is, corresponds to a valid formulation for a deterministic VRPTW with travel times as the mean travel times $\boldsymbol{\mu}$. Therefore, to compute an initial dual solution of the LP relaxation of model $FB(\overline{\mathcal{R}})$, we adopt the above-mentioned column-and-row generation procedure, following similar procedures used to compute dual bounds for VRPs (see, for example Baldacci et al. 2011, Pecin et al. 2017, Zhang et al. 2019b). In particular, the pricing problem associated with formulation $FB(\overline{\mathcal{R}})$ is solved as an elementary shortest path problem with resource constraints (ESPPRC) (Irnich and Desaulniers 2005) using a state-of-the-art algorithm based on a *bi-directional search* (Righini and Salani 2006), an *ng-set based decremental state space relaxation* (Martinelli et al. 2014) and *completion bounds* (Baldacci et al. 2011). The algorithm also relies on heuristic pricing to further accelerate the computation. For a review and discussion on these techniques, the reader is referred to Poggi and Uchoa (2014) and Costa et al. (2019).

Note that the computation of the dual solution, $(\boldsymbol{u}, \boldsymbol{\pi}, \boldsymbol{\eta}, \boldsymbol{\varphi})$, disregards the infeasibility property that is fully exploited in route set $\mathcal{R}_\rho$. Nevertheless, we find calculating the dual solution based on formulation $FB(\overline{\mathcal{R}})$, instead of formulation $FB(\mathcal{R}_\rho)$, and exploiting the infeasibility property in Step 2 of the algorithm during the route enumeration phase as computationally convenient.

5.2. Solving $F_\rho(\overline{\mathcal{R}}_\rho)$

In the route enumeration phase, we allow the generation of up to Δ_{max} routes, which in practice cannot be dealt with directly by an MIP solver when the number of routes generated is greater than or equal to Δ_{mip}. Note, Δ_{mip} is chosen to ensure that model $F_\rho(\overline{\mathcal{R}}_\rho)$ can be effectively solved by a general purpose MIP solver. If the number of routes generated is greater than or equal to Δ_{mip} and less than Δ_{max}, the routes are stored in a pool and model $F_\rho(\overline{\mathcal{R}}_\rho)$ is solved by a BPC algorithm where the pricing problem is solved by inspecting the pool of routes. This method has several advantages, because it allows the separation of nonrobust cuts without impacting the complexity of the pricing algorithm. *Nonrobust* cuts are those for which the values of the corresponding dual

variables cannot be translated into costs in the pricing subproblem, such as the SR3Is (see Poggi and Uchoa 2014). In addition, the above method allows alternative branching rules. Implicit pricing techniques were also used by Baldacci et al. (2011) and Contardo and Martinelli (2014).

In our implementation, using the column-and-row generation procedure based only on the SR3Is is found as computationlly convenient. In addition, to derive integer solutions, we adopt the following two branching decisions, which are examined in sequence: (i) branching on the number of vehicles leaving the depot, and (ii) branching on customer pairs, i.e., either customers i and j must be on the same route or different routes, based on the branching scheme proposed by Ryan and Foster (1981) for applications that can be formulated as set partitioning problems.

To compute the primal bounds, and thereby accelerate the convergence of the BPC algorithm, we use two heuristic algorithms. The first heuristic is a local search algorithm (LSA) based on the heuristic algorithm proposed by Zhang et al. (2021) for a VRPTW under the SRI. The LSA starts from an initial solution constructed by a greedy heuristic (*cheapest insertion*), which is further improved by a local search procedure. The move operators commonly used for VRPs are employed, such as *relocate*, *swap*, and *2-opt*. We also extend the study of Zhang et al. (2021) to deal with a generic riskiness index $\rho(\cdot)$, where the algorithm considers solutions that are feasible in terms of the capacity and function $\rho(\cdot)$ (infeasibility property). Moreover, the budget constraint is penalized in the objective function as $\sum_{r\in\overline{\mathcal{R}}_\rho}\zeta_r(\rho,\tilde{\boldsymbol{t}})y_r + M\max\{\sum_{r\in\overline{\mathcal{R}}_\rho}c_r y_r - B, 0\}$, where M is a large constant. Function $\zeta_r(\rho,\tilde{\boldsymbol{t}})$ is computed as $\zeta_r(\rho,\tilde{\boldsymbol{t}}) = \sum_{i\in V(R_r)}\rho(\xi_i(R_r,\tilde{\boldsymbol{t}}))$, where $\rho(\xi_i(R_r,\tilde{\boldsymbol{t}}))$ computes the riskiness index associated with vertex i and is determined using Algorithm 1.

The second heuristic is a primal heuristic, which is applied at each node of the BPC enumeration tree and builds a feasible VRPTW solution using the incumbent fractional RMP solution. Let $\boldsymbol{y}^*$ be the current fractional solution of the RMP and let $\hat{\mathcal{R}}_\rho \subset \overline{\mathcal{R}}_\rho$ be the set of patterns composing the RMP. The primal heuristic performs the following steps by starting from an empty solution $\mathcal{R}'$:

1) A subset $\mathcal{R}'_\rho \subseteq \hat{\mathcal{R}}_\rho$ of routes is selected such that $\mathcal{R}'_\rho = \{r \in \hat{\mathcal{R}}_\rho : y^*_r \geq 0\}$, and it is sorted in decreasing $\boldsymbol{y}^*$ values.
2) Based on the order, the following steps are performed: (a) The first route, $r' \in \mathcal{R}'_\rho$, is selected and fixed into the solution if $\sum_{r\in\mathcal{R}'} c_r \leq B - c_{r'}$, i.e., $\mathcal{R}' = \mathcal{R}' \cup \{r'\}$; (b) From set $\mathcal{R}'_\rho$ route r' and all routes r'' such that $((V(R_{r'}) \cap V_c) \cap (V(R_{r''}) \cap V_c) \neq \emptyset$ are removed if route r' is added into solution; (c) Steps (a) and (b) are repeated until $\mathcal{R}'_\rho = \emptyset$ or $|\mathcal{R}'| = m$.
3) Let $\overline{V_c} \subset V_c$ be the set of customers not covered by solution $\mathcal{R}'$. If $\overline{V_c} = \emptyset$, then solution $\mathcal{R}'$ is a feasible solution. Otherwise, the VRPTW instance defined by the set of customers, $\overline{V_c}$, maximum number of vehicles equal to $m - |\mathcal{R}'|$, and budget $B - \sum_{r\in\mathcal{R}'} c_r$ is considered. The resulting (reduced) VRPTW instance is solved using the LSA, and let $\mathcal{R}''$ be the corresponding solution.
4) If the routes in $\mathcal{R}''$ form a feasible set, then VRPTW solution $\mathcal{R}' \cup \mathcal{R}''$ of cost $\sum_{r\in\mathcal{R}'\cup\mathcal{R}''}\zeta_r(\rho,\tilde{\boldsymbol{t}})$ is defined.

5.3. Solving $F_\rho(\mathcal{R}_\rho)$

Whenever the cardinality of route set $\overline{\mathcal{R}}_\rho$ is greater than or equal to Δ_{max}, formulation $F_\rho(\mathcal{R}_\rho)$ is solved to optimality using the BPC algorithm. The BPC algorithm uses state-of-the-art techniques designed for deterministic VRPTWs by Baldacci et al. (2011), Pecin et al. (2017) and Zhang et al. (2019b).

The lower bounds at the different nodes of the enumeration tree are computed using the column-and-row generation procedure described above, where the 2PIs (18), CIs (19) and SR3Is (20) are used to strengthen the lower bounds. As branching decisions, we employ commonly adopted branching strategies for the VRPs, which can be devised by considering the arc-flow variables of the compact formulation (Lysgaard et al. 2004): (i) branching on the number of vehicles, (ii) branching on the cutsets, and (iii) branching on the arcs. To compute primal bounds, we also use the LSA described in the previous section.

We relegate the description of the pricing algorithm to §EC.7.1, which involves the computation of the $\rho(\cdot)$ associated with the objective function of formulation $F_\rho(\mathcal{R}_\rho)$.

6. Computational experiments

In this section, we present the extensive experimental analysis conducted with three main aims. First, we discuss the evaluation of the performance of the exact method described in §5 on instances derived from the literature (see §6.2) and the comparison of its results with those obtained by Zhang et al. (2021) (see §6.3). Second, we report a comparison of the newly proposed CPRI with decision criteria from the literature (see §6.4). Third, we present the evaluation of the performance of the exact method to solve a DRO model based on the SRI and a Wasserstein distance-based ambiguity set (see §6.5). Additionally, in the e-companion to this paper, we present the analysis of the effectiveness of the different components of the algorithm (see §EC.8.2), and we describe the performed sensitivity analysis on important algorithm parameters such as the value of the budget, B, and the number, N, of samples (see §EC.8.3).

The algorithm was implemented in Java language, and IBM ILOG CPLEX 12.10 (IBM CPLEX 2021) was used as the LP solver in the BPC algorithms, as described in §5.2 and §5.3, and as the MIP solver to solve the reduced model, $F_\rho(\overline{\mathcal{R}}_\rho)$, in Step 3.a of the exact algorithm presented in §4. The experiments were performed on an AMD EPYC 7532 CPU (2.4 GHz) workstation equipped with 128 GB RAM running with a Windows 10 64-bit operating system (single-thread execution).

Hereafter, the exact algorithm proposed in this paper and detailed in §5 is denoted as EXM. Based on some preliminary experiments aimed at evaluating the performance of the EXM, we set parameters $\Delta_{mip} = 100,000$ and $\Delta_{max} = 15,000,000$. Moreover, we impose a time limit of 4 hours (14,400 seconds) for the execution of the EXM. Below, we first describe the benchmark instances used in our experiments.

6.1. Benchmark instances

The benchmark instances used in our experiments correspond to the set of instances used by Zhang et al. (2021), which were derived from the commonly used Solomon's deterministic VRPTW instances (Solomon 1987).

The Solomon instances are classified into six classes (c1, rc1, and r1 with tight time windows and strict vehicle capacity, and c2, rc2, and r2 with wide time windows and a loose vehicle capacity). Prefixes "c", "r", and "rc" denote *clustered*, *random*, and *mixed clustered-random* type of instances, respectively. For experiments aimed at evaluating the service level under an uncertain environment, Zhang et al. (2021) chosed to use only the instances with tight time windows, i.e., r1, c1, and rc1 set of instances, for a total of 29 instances. Moreover, because the original Solomon instances involve 100 nodes, Zhang et al. (2021) generated instances with 25 and 50 nodes by selecting the first 25 or 50 nodes from the original 100 node instances. Therefore, we consider a total of $29 \times 3 = 87$ instances involving 25, 50, and 100 nodes.

Zhang et al. (2021) obtained the uncertain travel times based on an asymmetric two-point distribution. More specifically, the travel time, $\tilde{t}_a$, for each arc $a \in A$ is assumed to follow an asymmetric two-point distribution supported on $\mu_a - \sigma_a/\sqrt{3}$ and $\mu_a + \sqrt{3}\sigma_a$ with respective probabilities of 0.75 and 0.25. Here, the original travel time of arc a is used as the mean, μ_a, and the standard deviation, $\sigma_a = \lambda_a \mu_a$, with λ_a randomly chosen from interval [0.1, 0.5]. The original travel cost and time between two nodes are computed base on the Euclidean distance. As commonly presented in the literature, the distance and travel time between two nodes are rounded down to the first decimal place (e.g., Jepsen et al. 2008, Baldacci et al. 2011, Pecin et al. 2017).

In the experiments, unless otherwise stated, the riskiness index used for the EXM algorithm is the CPRI, and the number, N, of the samples is set as 200. Moreover, for each instance, the value of the budget, B, was set as $1.05 \times opt$, where opt is the optimal solution cost of the deterministic VRPTW solution computed by the method of Zhang et al. (2019b) using the travel times of the original Solomon instance.

6.2. Results of EXM under CPRI

This section presents the results of the EXM based on the new CPRI obtained by solving the benchmark instances.

Table 2 summarizes the results obtained. For each group of instances, the table provides the number of instances in the group ("#inst"). For Step 1, column $\%lb$ provides the average percentage deviation of the initial lower bounds, lb, computed as $100 \times lb/B$. For Step 2, column $|\overline{\mathcal{R}}_\rho|$ reports the average cardinality of the set of routes generated by the route enumeration phase, computed over the instances for which $|\overline{\mathcal{R}}_\rho| < \Delta_{max}$. Concerning Step 3, column "#opt." gives the number

Table 2 Summary results of EXM under CPRI

		Step 1		Step 2		Step 3				
n	#inst	$\%lb$	t	$\lvert\overline{\mathcal{R}}_\rho\rvert$	t	#opt	MIP	iBPC	BPC	t
25	29	95.1	1.2	3112.4	2.0	29	29	0	0	0.4
50	29	95.2	9.8	198251.5	103.4	27	17	10	2	76.9
100	29	95.0	360.9	2757508.3	203.3	7	0	6	23	4368.5

of instances solved to otpimality and the next three columns report statistics about the type of methods used in solving the group of instances: "MIP" (general MIP solver, Step 3.a), "iBPC" (implicit BPC, Step 3.b), and "BPC" (BPC, Step 3.c). Finally, for each step of the EXM, the table reports the corresponding average computing times ("t"). For Step 2 and 3, the computing times are computed over the set of instances solved to optimality. Detailed results are reported in §EC.8.1.

The obtained results can be summarized as follows: The EXM algorithm solves to optimality all 25 node instances, all but two 50 node instances and seven 100 node instances. Almost all instances involving 25 and 50 nodes are solved using the MIP and iBPC methods, and in §EC.8.2 we show that they outperform the direct use of the BPC method. The detailed results show that for two instances involving 50 nodes and for all but six instances with 100 nodes, the EXM generates more than Δ_{max} routes during the execution of Step 2; thus, the BPC method is used to solve model $F_\rho(\mathcal{R}_\rho)$. The computing times of the EXM noticeably show that its effectiveness is related to the cardinality of the set of routes, $\overline{\mathcal{R}}_\rho$, which, in turn, is related to the difficulty of solving the pricing problem associated with the corresponding instance. It is worth noting that the EXM (see the detailed results) fails to compute the feasible solutions for some instances for which it reaches the imposed time limit, and this can be due to the imposed budget constraint, which is highly restrictive. In §EC.8.3, we also present the analysis of the impact by varying the budget, B.

6.3. Comparison with Zhang et al. (2021) under SRI

In this section, we discuss the comparison of the results of the EXM with those obtained by Zhang et al. (2021) using the SRI. The results of Zhang et al. (2021) using their BC algorithm are based on instances involving 25 nodes and are summarized by Table 3. In the table, columns $\%gap$ and t_{tot} list the final percentage gap and the total computing time of their BC (computing time in seconds on an Intel(R) Core(TM) CPU i7-7700 clocked at 3.60 GHz), respectively. For the EXM algorithm, in addition to the notations already introduced, the table lists the time spent in computing the SRI ("t_{SRI}") and the time spent at Step 2 to generate the route set, $\overline{\mathcal{R}}_\rho$ ("t_{RE}"). The last line of the table reports the average values. To compute the SRI, we use the closed-form expression described by Zhang et al. (2021).

Table 3 Comparison of different approaches on the SRI

	Zhang et al. (2021)		EXM					
Name	$\%gap$	t_{tot}	$\%gap$	$\lvert\overline{\mathcal{R}}_\rho\rvert$	t_{SRI}	t_{RE}	Method	t_{tot}
c101	0.00	0.08	0.00	1389	0.65	0.42	MIP	1.20
c102	0.00	1.90	0.00	8264	3.98	5.50	MIP	7.13
c103	0.00	0.02	0.00	2329	4.77	6.64	MIP	9.32
c104	0.00	0.02	0.00	18066	22.50	31.46	MIP	35.04
c105	0.00	0.02	0.00	2073	0.65	0.66	MIP	1.83
c106	0.00	0.11	0.00	1718	0.67	0.56	MIP	1.27
c107	0.00	0.02	0.00	4115	0.83	1.08	MIP	1.99
c108	0.00	0.02	0.00	2930	1.00	1.28	MIP	2.48
c109	0.00	0.02	0.00	1953	2.79	3.57	MIP	5.29
r101	0.00	0.14	0.00	288	0.40	0.18	MIP	0.84
r102	2.22	>1800	0.00	1423	0.79	0.87	MIP	1.95
r103	0.00	0.00	0.00	1621	0.81	0.96	MIP	2.02
r104	0.00	0.02	0.00	2151	1.02	1.23	MIP	2.70
r105	0.00	2.34	0.00	673	0.49	0.41	MIP	1.15
r106	100.00	>1800	0.00	2039	0.95	1.11	MIP	3.24
r107	100.00	>1800	0.00	2340	0.99	1.14	MIP	2.91
r108	0.00	0.02	0.00	4424	1.59	2.02	MIP	6.28
r109	0.00	126.22	0.00	1087	0.71	0.69	MIP	1.63
r110	0.00	0.02	0.00	6933	1.38	1.64	MIP	4.61
r111	100.00	>1800	0.00	2239	0.99	1.22	MIP	3.18
r112	0.00	0.02	0.00	3947	1.86	2.28	MIP	8.49
rc101	0.00	40.08	0.00	1338	0.55	0.58	MIP	2.28
rc102	0.00	106.58	0.00	1313	1.52	1.97	MIP	2.80
rc103	100.00	>1800	0.00	1228	2.07	2.80	MIP	4.01
rc104	100.00	>1800	0.00	7095	11.64	16.18	MIP	18.15
rc105	0.00	1098.86	0.00	1436	0.67	0.86	MIP	1.72
rc106	0.00	1614.22	0.00	852	1.03	1.15	MIP	2.05
rc107	0.00	889.78	0.00	924	2.09	2.65	MIP	3.73
rc108	100.00	>1800	0.00	715	7.39	10.53	MIP	12.01
		176.39			2.36	3.08		4.81

The comparison shows that the proposed EXM algorithm outperforms the BC algorithm of Zhang et al. (2021) in terms of the number of instances solved to optimality. By also considering the machines used by the two methods for the instances solved to optimality, the EXM is two orders of magnitude faster than the BC algorithm. All instances are solved by the EXM using an MIP route enumeration-based method; therefore, it is proven to be particularly effective for this set of instances.

6.4. Comparison of CPRI with decision criteria from literature

In this section, we discuss the investigation of the performance of the CPRI and RVI, ERI, and SRI using different indicators. Our analysis follows those of Zhang et al. (2019a) and Zhang et al. (2021); however, it extends their schemes by considering larger instances with 50 nodes. More importantly, it is based on the computation of the optimal solutions, and thus, is more accurate in terms of evaluating the different indicators.

Table 4 Comparison of decision criteria

	RVI							ERI						
Name	z^*	t_{RVI}	t_{tot}	$SumExp$	$MaExp$	$SumProb$	$MaxProb$	z^*	t_{ERI}	t_{tot}	$SumExp$	$MaExp$	$SumProb$	$MaxProb$
c101	7.18	0.37	2.70	0.94	0.47	0.30	0.14	1.25	1.22	3.19	0.94	0.47	0.30	0.14
c102	6.95	1.51	14.11	0.00	0.00	0.00	0.00	1.25	17.76	29.46	0.00	0.00	0.00	0.00
c103	1.10	21.43	228.61	0.00	0.00	0.00	0.00	0.23	364.70	565.44	0.00	0.00	0.00	0.00
c105	0.00	0.47	4.90	0.00	0.00	0.00	0.00	0.00	1.74	4.18	0.00	0.00	0.00	0.00
c106	18.35	0.75	22.92	0.00	0.00	0.00	0.00	6.17	2.58	22.49	0.00	0.00	0.00	0.00
c107	0.00	0.33	4.55	0.00	0.00	0.00	0.00	0.00	2.74	8.30	0.00	0.00	0.00	0.00
c108	0.00	0.78	31.21	0.00	0.00	0.00	0.00	0.00	6.52	43.01	0.00	0.00	0.00	0.00
c109	0.00	5.47	42.97	0.00	0.00	0.00	0.00	0.00	57.84	99.82	0.00	0.00	0.00	0.00
r101	56.64	0.54	2.51	3.04	3.04	0.26	0.26	18.72	0.77	2.56	3.04	3.04	0.26	0.26
r102	57.59	10.39	50.87	0.00	0.00	0.00	0.00	19.36	10.30	25.99	0.00	0.00	0.00	0.00
r103	49.19	104.81	219.24	4.47	3.59	0.63	0.25	15.76	110.54	257.85	0.68	0.68	0.25	0.25
r104	27.06	515.23	1232.62	0.74	0.74	0.26	0.26	6.80	539.09	1373.49	1.18	0.45	0.24	0.09
r105	8.02	1.68	10.04	0.01	0.01	0.06	0.06	1.58	1.85	9.18	0.01	0.01	0.06	0.06
r106	13.78	33.20	100.53	0.71	0.41	0.19	0.09	2.92	34.37	102.87	0.40	0.17	0.12	0.07
r107	31.20	188.50	635.15	1.90	1.90	0.34	0.34	5.10	199.43	637.44	0.49	0.20	0.16	0.07
r109	7.74	29.37	92.85	0.62	0.59	0.26	0.26	1.01	32.98	93.17	0.67	0.51	0.12	0.09
r110	10.79	30.83	90.22	0.02	0.02	0.01	0.01	1.83	40.82	103.74	0.15	0.14	0.05	0.05
r111	6.03	130.22	338.72	0.25	0.25	0.08	0.08	0.55	141.63	386.25	0.00	0.00	0.00	0.00
r112	13.98	412.82	1416.56	0.00	0.00	0.00	0.00	1.71	516.95	2085.80	0.00	0.00	0.00	0.00
rc101	18.00	1.29	9.39	0.74	0.74	0.25	0.25	6.48	1.61	12.48	0.74	0.74	0.25	0.25
rc102	61.09	32.39	118.64	0.00	0.00	0.00	0.00	19.63	28.68	140.81	0.00	0.00	0.00	0.00
rc103	56.21	76.67	782.10	1.83	1.50	0.28	0.20	14.37	74.69	548.73	1.66	1.13	0.26	0.14
rc104	18.50	105.64	259.17	0.73	0.49	0.18	0.10	3.62	119.52	269.95	0.70	0.49	0.17	0.10
rc105	36.95	7.61	38.46	0.00	0.00	0.00	0.00	12.02	9.18	62.33	0.00	0.00	0.00	0.00
rc107	59.96	31.17	82.13	4.46	4.46	0.25	0.25	17.94	39.63	87.09	4.46	4.46	0.25	0.25
rc108	57.83	62.25	170.14	5.80	2.56	0.92	0.26	15.65	98.63	204.34	8.30	3.99	0.67	0.25
	24.01	69.45	230.82	1.01	0.80	0.16	0.11	6.69	94.45	276.15	0.90	0.63	0.12	0.08

	SRI							CPRI						
Name	z^*	t_{SRI}	t_{tot}	$SumExp$	$MaExp$	$SumProb$	$MaxProb$	z^*	t_{CPRI}	t_{tot}	$SumExp$	$MaExp$	$SumProb$	$MaxProb$
c101	1.41	0.97	2.61	0.94	0.47	0.30	0.14	7.40	0.26	2.16	0.94	0.47	0.30	0.14
c102	1.40	16.17	27.54	0.00	0.00	0.00	0.00	7.17	0.99	11.46	0.00	0.00	0.00	0.00
c103	0.25	352.09	553.50	0.00	0.00	0.00	0.00	1.13	17.57	236.49	0.00	0.00	0.00	0.00
c105	0.00	1.66	4.31	0.00	0.00	0.00	0.00	0.00	0.42	4.88	0.00	0.00	0.00	0.00
c106	7.08	2.49	21.35	0.00	0.00	0.00	0.00	18.68	0.59	22.53	0.00	0.00	0.00	0.00
c107	0.00	2.22	6.97	0.00	0.00	0.00	0.00	0.00	0.31	4.66	0.00	0.00	0.00	0.00
c108	0.00	5.62	40.98	0.00	0.00	0.00	0.00	0.00	0.52	34.78	0.00	0.00	0.00	0.00
c109	0.00	59.17	94.90	0.00	0.00	0.00	0.00	0.00	3.86	45.83	0.00	0.00	0.00	0.00
r101	21.60	0.74	2.52	3.04	3.04	0.26	0.26	50.64	0.42	2.14	3.04	3.04	0.26	0.26
r102	22.34	9.81	24.32	0.00	0.00	0.00	0.00	53.57	4.18	29.43	0.00	0.00	0.00	0.00
r103	18.50	98.00	236.29	0.43	0.34	0.08	0.06	46.67	47.35	177.83	0.00	0.00	0.00	0.00
r104	7.94	513.78	1249.64	1.18	0.45	0.24	0.09	26.77	287.88	1256.01	0.40	0.40	0.07	0.07
r105	1.78	2.76	12.62	0.01	0.01	0.06	0.06	8.26	0.96	9.41	0.01	0.01	0.06	0.06
r106	3.33	32.83	96.64	0.59	0.59	0.25	0.25	14.15	17.73	133.81	0.00	0.00	0.00	0.00
r107	5.79	192.03	425.29	1.65	1.43	0.29	0.24	29.71	100.31	469.75	0.00	0.00	0.00	0.00
r109	1.13	28.98	103.30	0.00	0.00	0.00	0.00	7.98	15.27	117.57	0.62	0.59	0.26	0.26
r110	2.06	38.32	88.82	0.00	0.00	0.00	0.00	10.77	17.80	89.26	0.02	0.02	0.01	0.01
r111	0.62	139.58	335.49	0.00	0.00	0.00	0.00	6.17	66.80	323.40	0.25	0.25	0.08	0.08
r112	1.92	508.08	1414.40	0.67	0.52	0.14	0.09	14.25	240.58	1252.27	0.70	0.40	0.18	0.09
rc101	7.52	1.42	13.66	0.74	0.74	0.25	0.25	18.05	0.73	11.16	0.74	0.74	0.25	0.25
rc102	23.11	27.34	129.09	0.00	0.00	0.00	0.00	58.50	15.37	104.85	0.00	0.00	0.00	0.00
rc103	16.51	74.70	545.42	1.66	1.13	0.26	0.14	56.10	38.39	286.87	1.83	1.50	0.28	0.20
rc104	4.13	115.52	254.04	0.70	0.49	0.17	0.10	18.77	52.08	220.35	0.73	0.49	0.18	0.10
rc105	14.31	9.53	50.28	0.00	0.00	0.00	0.00	33.98	4.64	38.02	0.00	0.00	0.00	0.00
rc107	21.01	40.37	84.13	4.46	4.46	0.25	0.25	57.91	11.15	59.83	4.46	4.46	0.25	0.25
rc108	18.00	91.77	191.16	8.30	3.99	0.67	0.25	51.56	30.87	144.59	6.85	6.57	0.43	0.25
	7.76	91.00	231.13	0.94	0.68	0.12	0.08	23.01	37.58	195.74	0.79	0.73	0.10	0.08

To evaluate the performance of the solutions under the different indices, we perform an out-of-sample evaluation by generating 10,000 independent samples of $\tilde{\boldsymbol{t}}$. As the basic indicators, we consider for each $i \in V$, the lateness probability, $\mathbb{P}[\xi_i(\boldsymbol{x}, \tilde{\boldsymbol{t}}) > 0]$ and the expected lateness, $\mathbb{E}[(\xi_i(\boldsymbol{x}, \tilde{\boldsymbol{t}}))^+]$, as well as the following derived indicators:

- $SumProb$, the sum of the lateness probabilities computed as $\sum_{i \in V} \mathbb{P}[\xi_i(\boldsymbol{x}, \tilde{\boldsymbol{t}}) > 0]$.
- $MaxProb$, the maximum lateness probability computed as $\max_{i \in V} \mathbb{P}[\xi_i(\boldsymbol{x}, \tilde{\boldsymbol{t}}) > 0]$.
- $SumExp$, the sum of the expected lateness durations computed as $\sum_{i \in V} \mathbb{E}[(\xi_i(\boldsymbol{x}, \tilde{\boldsymbol{t}}))^+]$.
- $MaxExp$, the maximum expected lateness duration computed as $\max_{i \in V} \mathbb{E}[(\xi_i(\boldsymbol{x}, \tilde{\boldsymbol{t}}))^+]$.

For comparison, the RVI is computed by a bisection approach mentioned in Jaillet et al. (2016), the ERI and SRI are computed using the original closed forms (Zhang et al. 2019a, 2021), whereas the CPRI is computed using Algorithm 1. It is worth noting that the analyses of Zhang et al. (2019a) and Zhang et al. (2021) have already shown the advantages of using the ERI and the SRI for methods aimed at minimizing alternative objective functions. Examples of these functions are the total travel or routing cost (i.e., solving the deterministic VRPTW), sum of the expected lateness durations, and sum of the lateness probabilities. Consequently, our comparison focuses on the direct comparison of the different indices.

The results of the different indicators are tabulated in Table 4. The results are based on the 26 instances involving 50 nodes that can be solved to optimality under all indices. For each instance and each index, the table reports the optimal solution cost ("z^*"), the total time spent in computing the indices ("t_x", $x \in \{RVI, ERI, SRI, CPRI\}$), total computing time of EXM ("t_{tot}"), and values of the different indicators. The last line under each section of the table reports the average values.

Figure 2 illustrates the results of the normalized values of the indicators for the different indices. As shown, the CPRI, SRI, ERI outperform the RVI on average in mitigating the lateness. In fact, the performance of the various indicators for the CPRI, SRI, and ERI are on average superior to that of the RVI. The SRI and the ERI display similar average performance. The CPRI achieves smallest $SumProb$, $MaxProb$, and $SumExp$ among all indices, and it shows a slightly higher average maximum expected lateness duration for the worst-case node ($MaxExp$) with respect to the SRI and the ERI. Therefore, the CPRI shows a good balanced performance on all on-time service indicators.

Concerning the total computing times, the EXM under the CPRI is the fastest method, being approximately 30% faster than the ERI based-computation and approximately 15% faster than both the RVI and SRI based-computations, respectively.

Summarizing, our analysis shows that the new CPRI has salient features from the aspects of both computation and performance. In addition, the EXM algorithm can be a useful tool for decision makers interested in designing routing plans that provide on-time services with maximum efficiency while limiting the budgeted routing costs.

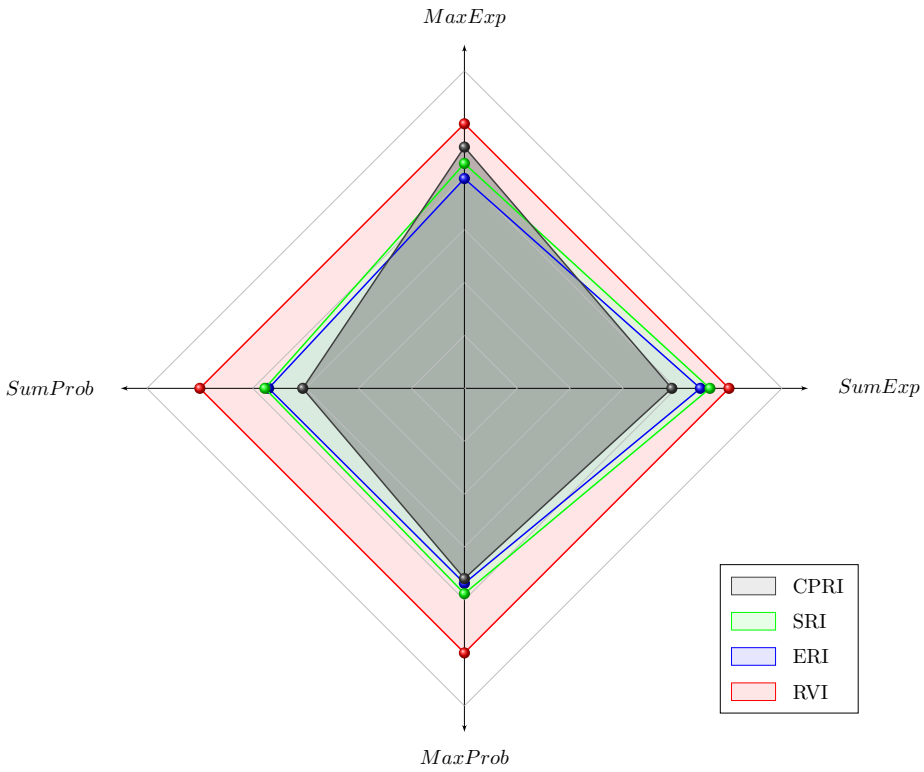

Figure 2 **Normalized values of the indicators for the CPRI, SRI, ERI and RVI**

6.5. Solving DRO models using EXM

In this section, we report the results of the EXM for solving a DRO model based on the SRI and a Wasserstein distance-based ambiguity set defined as follows: Suppose the true distribution, $\mathbb{P}$, lies in a Wasserstein ball of radius $\theta \in \mathbb{R}_+$ that is centered at the empirical distribution, $\mathbb{P}^\dagger$. Then, the Wasserstein ambiguity set is defined as

$$\mathbb{F}(\theta) = \left\{ \mathbb{P} \in \mathcal{P}(\mathcal{W}) \;\middle|\; \begin{array}{l} \tilde{\boldsymbol{t}} \sim \mathbb{P}, \tilde{\boldsymbol{t}}^\dagger \sim \mathbb{P}^\dagger, \\ d_{\mathcal{W}}(\mathbb{P}, \mathbb{P}^\dagger) \leq \theta, \end{array} \right\},$$

where $\mathcal{P}(\mathcal{W})$ represents the set of all probability distributions supported on set $\mathcal{W} \subseteq \mathbb{R}^I$ and $d_{\mathcal{W}}(\mathbb{P}, \mathbb{P}^\dagger) : \mathcal{P} \times \mathcal{P} \to [0, +\infty)]$ computes the type-1 Wasserstein distance.

As mentioned in Section 3.3, Zhang et al. (2021) derived a closed-form solution when $\tilde{\boldsymbol{t}}$ are governed by the Wasserstein distance and designed an efficient algorithm for its computation. They demonstrated that incorporating the distributional ambiguity over the empirical distributions helps improve the out-of-sample performance of indicators. Therefore, the aim of study presented in this section is to investigate the effectiveness of the EXM in incorporating the distributional ambiguity based on the SRI and the Wasserstein ambiguity set. We consider the 50 node instances solved to optimality by the EXM under the SRI, and we vary the Wasserstein ball radius, $\theta \in$

$\{0.0, 0.05, 0.1.0.5, 1.0\}$, where $\theta = 0$ ignores the distributional ambiguity and corresponds to the sample average approximation.

The obtained results are listed by Table 5. For each value of θ, the table provides the results of the EXM based on the notations already introduced for the previous tables. The table also reports the average values over the different columns.

The obtained results show that the performance of the EXM remains stable under the different values of θ. A larger radius θ implies a higher effectiveness of the infeasibility property in reducing the solution space in which customers receive poor service. This is validated by the decreasing average cardinalities of the sets of routes, $\overline{\mathcal{R}}_\rho$, for increasing θ values, with a reduction of approximatedly 10% from the $\theta = 0$ and $\theta = 1.0$ cases. Specifically, the effectiveness of the EXM is improved under DRO because its performance strongly relies on the infeasibility property.

7. Conclusions and future research

Routing optimization under uncertain travel times has generated the interest of many researchers in recent years, both owing to the practical importance of this class of problems and their intrinsic difficulty. In particular, the recent literature has focused on methods aimed at mitigating late service riskiness using decision criteria to measure it. The main interest in such criteria is that they account for both the probability and magnitude of the lateness and also consider the distributional ambiguity of uncertain travel times.

In this context, we studied a vehicle routing problems with time windows (VRPTW) under empirical travel times. We introduced a new decision criterion, the *generalized riskiness index* (GRI), and its special case, the *convex piecewise riskiness index* (CPRI). As main results of our study, we demonstrate its salient managerial and computational properties and show that the new index covers some indices recently proposed in the literature as special cases. Moreover, by exploiting the structure of the new index, we establish a new mathematical set partitioning-based formulation and a novel exact solution framework combining route enumeration and state-of-the-art branch-price-and-cut algorithms to solve the formulation.

The new solution framework is extensively tested on VRPTW instances derived from the literature. Our computational experiments demonstrate the effectiveness of the proposed algorithm in solving instances with up to 100 nodes, more than doubling the manageable instance size with respect to state-of-the-art algorithms. We also present that the newly proposed index can better mitigate lateness compared to existing ones. Moreover, it is shown that the new solution framework can effectively solve distributionally robust models, and thus, to the best of our knowledge, it is the first exact column generation-based method to be used to solve VRPs in the context of distributionally robust optimization.

Table 5 Incorporating distributional ambiguity into EXM: effect of the Wasserstein distance

	$\theta = 0.0$					$\theta = 0.05$					$\theta = 0.1$				
Name	z^*	$\lvert\overline{\mathcal{R}}_\rho\rvert$	t_{SRI}	t_{RE}	t_{tot}	z^*	$\lvert\overline{\mathcal{R}}_\rho\rvert$	t_{SRI}	t_{RE}	t_{tot}	z^*	$\lvert\overline{\mathcal{R}}_\rho\rvert$	t_{SRI}	t_{RE}	t_{tot}
c101	1.41	13949	0.97	1.19	2.61	4.49	13949	1.31	1.63	3.38	7.58	13901	1.36	1.62	3.20
c102	1.40	55074	16.17	22.11	27.54	4.49	55171	18.18	24.58	30.56	7.57	55305	17.06	23.44	27.95
c103	0.25	296641	352.09	528.65	553.50	3.32	297007	369.61	551.67	571.26	6.38	297048	361.77	546.56	566.93
c105	0.00	32351	1.66	2.30	4.31	3.06	32294	2.67	3.94	6.80	6.11	32190	2.68	3.82	6.56
c106	7.08	44544	2.49	3.57	21.35	10.20	44543	3.85	5.57	24.60	13.33	44475	3.55	5.28	24.68
c107	0.00	25231	2.22	2.76	6.97	3.06	25231	2.37	2.91	7.23	6.11	25210	2.97	3.73	8.00
c108	0.00	34002	5.62	8.10	40.98	3.06	33833	6.30	9.04	34.97	6.11	33741	6.32	9.02	38.86
c109	0.00	101284	59.17	83.79	94.90	3.06	101306	54.86	77.70	91.85	6.11	101333	64.04	87.35	103.28
r101	21.60	5027	0.74	0.73	2.52	25.34	5002	0.71	0.75	2.51	29.07	4966	0.66	0.66	2.35
r102	22.34	53657	9.81	13.38	24.32	25.95	53403	8.56	11.33	21.28	29.56	52881	9.71	12.80	23.61
r103	18.50	275340	98.00	143.00	236.29	21.95	273724	90.35	129.50	221.04	25.39	272890	97.10	138.01	231.74
r104	7.94	1092277	513.78	736.63	1249.64	11.23	1087001	491.08	696.50	1109.21	14.52	1081302	502.30	707.98	1379.65
r105	1.78	18817	2.76	3.41	12.62	5.15	18789	2.69	3.56	11.71	8.52	18643	2.83	3.77	11.27
r106	3.33	151828	32.83	45.41	96.64	6.68	151138	33.53	45.03	86.82	10.02	150659	30.80	42.63	93.88
r107	5.79	465929	192.03	292.91	425.29	9.09	463716	191.36	281.65	401.42	12.38	462051	185.54	276.36	515.51
r109	1.13	174656	28.98	40.02	103.30	4.42	173721	28.88	39.27	99.77	7.71	172925	29.57	40.18	143.49
r110	2.06	161066	38.32	53.35	88.82	5.32	160443	36.92	51.32	87.81	8.58	159742	40.25	55.85	93.74
r111	0.62	436830	139.58	195.35	335.49	3.86	434041	133.81	193.47	313.23	7.10	432458	128.63	186.46	296.83
r112	1.92	1152489	508.08	786.62	1414.40	5.11	1147628	505.94	770.56	1442.49	8.31	1143192	491.52	759.91	1318.39
rc101	7.52	12365	1.42	1.75	13.66	10.96	12274	2.00	2.55	15.79	14.40	12214	2.08	2.48	14.73
rc102	23.11	53806	27.34	37.32	129.09	26.59	53710	27.77	37.12	118.80	30.07	53424	28.09	37.76	116.51
rc103	16.51	64314	74.70	105.37	545.42	19.77	64156	70.48	100.29	736.27	23.03	63840	71.50	99.80	1174.47
rc104	4.13	23606	115.52	249.17	254.04	7.25	23571	116.05	240.41	244.65	10.37	23435	122.29	246.25	250.67
rc105	14.31	28279	9.53	12.51	50.28	17.77	28250	9.51	12.42	57.14	21.24	28156	9.44	12.27	51.73
rc107	21.01	12156	40.37	63.23	84.13	24.35	12112	39.32	61.38	82.84	27.69	12051	39.38	61.06	82.47
rc108	18.00	14099	91.77	158.86	191.16	21.25	14034	84.15	143.26	174.61	24.49	14000	94.21	156.66	187.87
	7.76	184601	91.00	138.13	231.13	11.03	183848	89.70	134.52	230.69	14.30	183155	90.22	135.45	260.32

	$\theta = 0.5$					$\theta = 1.0$				
Name	z^*	$\lvert\overline{\mathcal{R}}_\rho\rvert$	t_{SRI}	t_{RE}	t_{tot}	z^*	$\lvert\overline{\mathcal{R}}_\rho\rvert$	t_{SRI}	t_{RE}	t_{tot}
c101	32.23	12952	1.46	1.84	3.52	63.15	12761	1.46	1.66	3.36
c102	32.22	54834	17.81	24.22	28.83	63.11	54855	17.87	24.57	29.55
c103	30.86	292423	338.91	509.37	529.99	61.48	292167	343.00	522.31	548.55
c105	30.56	31742	1.75	2.44	5.30	61.11	30939	2.40	3.31	5.91
c106	38.39	43898	3.65	5.44	24.55	69.62	43167	3.76	5.29	23.80
c107	30.56	25004	2.36	2.80	6.90	61.11	24989	2.77	3.66	7.97
c108	30.56	32531	6.21	8.61	38.43	61.11	32014	6.00	8.62	38.74
c109	30.56	101581	55.51	79.49	90.60	61.11	101828	59.25	83.04	95.40
r101	59.11	4689	0.81	0.76	3.13	96.91	4328	0.82	0.82	2.50
r102	58.58	51214	9.40	12.88	28.17	95.08	45679	7.20	9.72	39.96
r103	52.86	260412	94.91	133.88	195.83	87.37	239458	89.32	123.60	174.40
r104	41.23	1015860	476.06	681.38	1230.75	73.72	961635	430.69	613.03	1060.39
r105	35.47	17831	2.92	3.50	11.08	69.32	17001	2.59	3.44	11.24
r106	36.82	143957	32.90	44.59	73.46	70.58	137455	27.37	37.89	76.25
r107	38.76	446719	187.30	278.38	520.18	71.88	427355	185.10	270.66	478.01
r109	34.05	166953	30.83	41.67	93.14	66.99	158731	29.70	40.25	126.15
r110	34.70	152526	39.37	55.38	90.41	67.39	145633	38.40	52.74	108.66
r111	33.04	415939	130.05	185.23	342.29	65.10	391029	126.59	179.61	301.99
r112	33.86	1105909	477.51	735.80	1710.17	65.82	1060525	436.43	685.66	1419.98
rc101	41.96	11832	1.89	2.19	10.26	76.87	11231	1.92	2.25	11.82
rc102	57.84	51762	25.16	34.46	110.69	92.98	49417	24.57	33.12	99.12
rc103	49.17	61525	69.22	97.73	312.28	82.11	59261	67.64	93.33	677.95
rc104	35.39	22469	117.80	240.15	245.01	66.79	21191	117.17	233.83	238.26
rc105	48.97	27131	9.18	11.89	48.64	83.69	25793	8.33	10.77	45.55
rc107	54.49	11683	39.60	60.87	82.15	88.49	11206	36.55	56.16	76.86
rc108	50.57	13542	88.83	147.56	178.95	83.67	13081	93.00	154.11	184.12
	40.49	176035	86.98	130.87	231.34	73.33	168182	83.07	125.13	226.40

Several interesting future research directions originating from this study can be considered. First, the adopted set partitioning-based model can be easily adapted to deal with other routing constraints, simply by considering such constraints in the route generation phase. Second, the computational efficiency to evaluate the GRI depends mainly on the selection of both the disutility function and ambiguity set about uncertain arc travel times, making it challenging to achieve. Although its solution algorithm applies to any disutility function, it is limited to an ambiguity set containing only an empirical distribution of travel times. Therefore, it would be interesting to also investigate other model selections of the ambiguity set, such as (generalized) moment-based ambiguity sets (e.g., Delage and Ye 2010, Wiesemann et al. 2014, Chen et al. 2020) and statistical distance-based ambiguity sets (e.g., Ben-Tal et al. 2013, Jiang and Guan 2018, Gao and Kleywegt 2016, Esfahani and Kuhn 2018). It is unclear which choices of the combination of the disutility function and the ambiguity set will lead to an efficient method for evaluating the GRI, which can be explored in the future. Finally, the applications for which the different decision criteria can be used to evaluate the target fulfillment riskiness are quite broad and include, for instance, portfolio optimization, inventory control, and appointment scheduling. Moreover, previous studies have shown the usefulness and wide applicability of a set partitioning model in modeling various applications, including railroad and airline crew scheduling, information retrieval, stock cutting, assembly line balancing, capital equipment decisions, and facility location problems. Therefore, our set partitioning-based model embedding riskiness indices can be a useful modeling tool to deal with other challenging optimization problems under uncertainty. Thus, our future research direction will also be to investigate these applications.

Acknowledgements

Yu Zhang is the corresponding author. This research was partially supported by the National Natural Science Foundation of China (Grants 72101187, 72021002, and 71901180).

References

Adulyasak, Y., P. Jaillet. 2016. Models and algorithms for stochastic and robust vehicle routing with deadlines. *Transportation Science* **50**(2) 608–626.

Agra, A., M. Christiansen, R. Figueiredo, L. M. Hvattum, M. Poss, C. Requejo. 2012. Layered formulation for the robust vehicle routing problem with time windows. *Lecture Notes in Computer Science*. Springer Science Business Media, 249–260.

Agra, A., M. Christiansen, R. Figueiredo, L. M. Hvattum, M. Poss, C. Requejo. 2013. The robust vehicle routing problem with time windows. *Computers & Operations Research* **40**(3) 856–866.

Archetti, C., M. Bouchard, G. Desaulniers. 2011. Enhanced branch and price and cut for vehicle routing with split deliveries and time windows. *Transportation Science* **45**(3) 285–298.

Aumann, R. J., R. Serrano. 2008. An economic index of riskiness. *Journal of Political Economy* **116**(5) 810–836.

Baldacci, R., N. Christofides, A. Mingozzi. 2008. An exact algorithm for the vehicle routing problem based on the set partitioning formulation with additional cuts. *Mathematical Programming* **115** 351–385.

Baldacci, R., E. Bartolini, A. Mingozzi, R. Roberti. 2010. An exact solution framework for a broad class of vehicle routing problems. *Computational Management Science* **7**(3) 229–268.

Baldacci, R., A. Mingozzi, R. Roberti. 2011. New route relaxation and pricing strategies for the vehicle routing problem. *Operations Research* **59**(5) 1269–1283.

Baldacci, R., A. Mingozzi, R. Roberti. 2012. Recent exact algorithms for solving the vehicle routing problem under capacity and time window constraints. *European Journal of Operational Research* **218**(1) 1–6.

Bartolini, E., D. Goeke, M. Schneider, M. Ye. 2021. The robust traveling salesman problem with time windows under knapsack-constrained travel time uncertainty. *Transportation Science* **55**(2) 371–394.

Ben-Tal, A., D. Den Hertog, A. De Waegenaere, B. Melenberg, G. Rennen. 2013. Robust solutions of optimization problems affected by uncertain probabilities. *Management Science* **59**(2) 341–357.

Bertsimas, D., M. Sim. 2004. The price of robustness. *Operations Research* **52**(1) 35–53.

Bertsimas, D. J., P. Jaillet, A. R. Odoni. 1990. A priori optimization. *Operations Research* **38**(6) 1019–1033.

Birge, J. R., F. Louveaux. 2011. *Introduction to stochastic programming*. Springer Science & Business Media.

Bräysy, O., M. Gendreau. 2005a. Vehicle routing problem with time windows, part I: Route construction and local search algorithms. *Transportation Science* **39**(1) 104–118.

Bräysy, O., M. Gendreau. 2005b. Vehicle routing problem with time windows, part II: Metaheuristics. *Transportation Science* **39**(1) 119–139.

Campbell, A. M., B. W. Thomas. 2008. Probabilistic traveling salesman problem with deadlines. *Transportation Science* **42**(1) 1–21.

Carraway, R. L., T. L. Morin, H. Moskowitz. 1989. Generalized dynamic programming for stochastic combinatorial optimization. *Operations Research* **37**(5) 819–829.

Chen, Z., M. Sim, P. Xiong. 2020. Robust stochastic optimization made easy with rsome. *Management Science* **66**(8) 3329–3339.

Claus, A. 1984. A new formulation for the travelling salesman problem. *SIAM Journal on Algebraic Discrete Methods* **5**(1) 21–25.

Contardo, C., R. Martinelli. 2014. A new exact algorithm for the multi-depot vehicle routing problem under capacity and route length constraints. *Discrete Optimization* **12** 129–146.

Cordeau, J.-F. 2006. A branch-and-cut algorithm for the dial-a-ride problem. *Operations Research* **54**(3) 573–586.

Cordeau, J.-F., G. Desaulniers, J. Desrosiers, M. M. Solomon, F. Soumis. 2002. VRP with time windows. *The Vehicle Routing Problem*. Society for Industrial & Applied Mathematics (SIAM), 157–193.

Costa, L., C. Contardo, G. Desaulniers. 2019. Exact branch-price-and-cut algorithms for vehicle routing. *Transportation Science* **53**(4) 946–985.

Dantzig, G. B., J. H. Ramser. 1959. The truck dispatching problem. *Management Science* **6**(1) 80–91.

De Maio, A., D. Laganà, R. Musmanno, F. Vocaturo. 2021. Arc routing under uncertainty: Introduction and literature review. *Computers & Operations Research* **135** 105442.

Delage, E., Y. Ye. 2010. Distributionally robust optimization under moment uncertainty with application to data-driven problems. *Operations Research* **58**(3) 595–612.

Desaulniers, G. 2010. Branch-and-price-and-cut for the split-delivery vehicle routing problem with time windows. *Operations Research* **58**(1) 179–192.

Dinh, T., R. Fukasawa, J. Luedtke. 2018. Exact algorithms for the chance-constrained vehicle routing problem. *Mathematical Programming* **172**(1) 105–138.

Ehmke, J. F., A. M. Campbell, T. L. Urban. 2015. Ensuring service levels in routing problems with time windows and stochastic travel times. *European Journal of Operational Research* **240**(2) 539–550.

Errico, F., G. Desaulniers, M. Gendreau, W. Rei, L.-M. Rousseau. 2016. A priori optimization with recourse for the vehicle routing problem with hard time windows and stochastic service times. *European Journal of Operational Research* **249**(1) 55–66.

Esfahani, P. M., D. Kuhn. 2018. Data-driven distributionally robust optimization using the wasserstein metric: Performance guarantees and tractable reformulations. *Mathematical Programming* **171**(1) 115–166.

Gao, R., A. J. Kleywegt. 2016. Distributionally robust stochastic optimization with wasserstein distance. *arXiv preprint arXiv:1604.02199* .

Gendreau, M., O. Jabali, W. Rei. 2014. Chapter 8: Stochastic vehicle routing problems. *MOS-SIAM Series on Optimization*. Society for Industrial and Applied Mathematics, 213–239.

Gendreau, M., O. Jabali, W. Rei. 2016. 50th anniversary invited article–future research directions in stochastic vehicle routing. *Transportation Science* **50**(4) 1163–1173.

Ghosal, S., W. Wiesemann. 2020. The distributionally robust chance-constrained vehicle routing problem. *Operations Research* **68**(3) 716–732.

Gounaris, C. E., W. Wiesemann, C. A. Floudas. 2013. The robust capacitated vehicle routing problem under demand uncertainty. *Operations Research* **61**(3) 677–693.

Han, J., C. Lee, S. Park. 2014. A robust scenario approach for the vehicle routing problem with uncertain travel times. *Transportation Science* **48**(3) 373–390.

Ho, S. C., W. Y. Szeto, Y.-H. Kuo, J. M. Leung, M. Petering, T. W. Tou. 2018. A survey of dial-a-ride problems: Literature review and recent developments. *Transportation Research Part B: Methodological* **111** 395–421.

IBM CPLEX. 2021. *IBM ILOG CPLEX 12.10 callable library*.

Irnich, S., G. Desaulniers. 2005. Shortest path problems with resource constraints. G. Desaulniers, J. Desrosiers, M. M. Solomon, eds., *Column Generation*. Springer, 33 – 65.

Jaillet, P., J. Qi, M. Sim. 2016. Routing optimization under uncertainty. *Operations Research* **64**(1) 186–200.

Jepsen, M., B. Petersen, S. Spoorendonk, D. Pisinger. 2008. Subset-row inequalities applied to the vehicle-routing problem with time windows. *Operations Research* **56**(2) 497–511.

Jiang, R., Y. Guan. 2018. Risk-averse two-stage stochastic program with distributional ambiguity. *Operations Research* **66**(5) 1390–1405.

Kao, E. P. C. 1978. A preference order dynamic program for a stochastic traveling salesman problem. *Operations Research* **26**(6) 1033–1045.

Kenyon, A. S., D. P. Morton. 2003. Stochastic vehicle routing with random travel times. *Transportation Science* **37**(1) 69–82.

Kohl, N., J. Desrosiers, O. B. G. Madsen, M. M. Solomon, F. Soumis. 1999. 2-path cuts for the vehicle routing problem with time windows. *Transportation Science* **33**(1) 101–116.

Laporte, G., Y. Nobert. 1983. A branch and bound algorithm for the capacitated vehicle routing problem. *Operations-Research-Spektrum* **5**(2) 77–85.

Laporte, G. 2009. Fifty years of vehicle routing. *Transportation Science* **43**(4) 408–416.

Laporte, G., F. Louveaux, H. Mercure. 1992. The vehicle routing problem with stochastic travel times. *Transportation Science* **26**(3) 161–170.

Laporte, G., H. Mercure, Y. Nobert. 1986. An exact algorithm for the asymmetrical capacitated vehicle routing problem. *Networks* **16**(1) 33–46.

Lee, C., K. Lee, S. Park. 2012. Robust vehicle routing problem with deadlines and travel time/demand uncertainty. *Journal of the Operational Research Society* **63**(9) 1294–1306.

Li, X., P. Tian, S. C. Leung. 2010. Vehicle routing problems with time windows and stochastic travel and service times: Models and algorithm. *International Journal of Production Economics* **125**(1) 137–145.

Lübbecke, M. E., J. Desrosiers. 2005. Selected topics in column generation. *Operations Research* **53** 1007–1023.

Lysgaard, J., A. N. Letchford, R. W. Eglese. 2004. A new branch-and-cut algorithm for the capacitated vehicle routing problem. *Mathematical Programming* **100**(2) 423–445.

Martinelli, R., D. Pecin, M. Poggi. 2014. Efficient elementary and restricted non-elementary route pricing. *European Journal of Operational Research* **239**(1) 102–111.

Munari, P., A. Moreno, J. De La Vega, D. Alem, J. Gondzio, R. Morabito. 2019. The robust vehicle routing problem with time windows: compact formulation and branch-price-and-cut method. *Transportation Science* **53**(4) 1043–1066.

Nemirovski, A., A. Shapiro. 2006. Convex approximations of chance constrained programs. *SIAM Journal on Optimization* **17**(4) 969–996.

Oyola, J., H. Arntzen, D. L. Woodruff. 2017. The stochastic vehicle routing problem, a literature review, part ii: solution methods. *EURO Journal on Transportation and Logistics* **6**(4) 349–388.

Oyola, J., H. Arntzen, D. L. Woodruff. 2018. The stochastic vehicle routing problem, a literature review, part i: models. *EURO Journal on Transportation and Logistics* **7**(3) 193–221.

Park, J., B.-I. Kim. 2010. The school bus routing problem: A review. *European Journal of Operational Research* **202**(2) 311–319.

Pecin, D., C. Contardo, G. Desaulniers, E. Uchoa. 2017. New enhancements for the exact solution of the vehicle routing problem with time windows. *INFORMS Journal on Computing* **29**(3) 489–502.

Poggi, M., E. Uchoa. 2014. *Chapter 3: New Exact Algorithms for the Capacitated Vehicle Routing Problem*, chap. 3. Society for Industrial and Applied Mathematics, 59–86.

Righini, G., M. Salani. 2006. Symmetry helps: Bounded bi-directional dynamic programming for the elementary shortest path problem with resource constraints. *Discrete Optimization* **3**(3) 255–273.

Ritzinger, U., J. Puchinger, R. F. Hartl. 2016. A survey on dynamic and stochastic vehicle routing problems. *International Journal of Production Research* **54**(1) 215–231.

Rockafellar, R. T., S. Uryasev. 2002. Conditional value-at-risk for general loss distributions. *Journal of Banking & Finance* **26**(7) 1443–1471.

Rostami, B., G. Desaulniers, F. Errico, A. Lodi. 2021. Branch-price-and-cut algorithms for the vehicle routing problem with stochastic and correlated travel times. *Operations Research* **69**(2) 436–455.

Russell, R. A., T. L. Urban. 2007. Vehicle routing with soft time windows and erlang travel times. *Journal of the Operational Research Society* **59**(9) 1220–1228.

Ryan, D. M., B. A. Foster. 1981. An integer programming approach to scheduling. A. Wren, ed., *Computer Scheduling of Public Transport Urban Passenger Vehicle and Crew Scheduling*. North-Holland, 269–280.

Secomandi, N., F. Margot. 2009. Reoptimization approaches for the vehicle-routing problem with stochastic demands. *Operations Research* **57**(1) 214–230.

Sniedovich, M. 1981. Analysis of a preference order traveling salesman problem. *Operations Research* **29**(6) 1234–1237.

Solomon, M. M. 1987. Algorithms for the vehicle routing and scheduling problems with time window constraints. *Operations Research* **35**(2) 254–265.

Subramanyam, A., F. Mufalli, J. M. Laínez-Aguirre, J. M. Pinto, C. E. Gounaris. 2021. Robust multiperiod vehicle routing under customer order uncertainty. *Operations Research* **69**(1) 30–60.

Sungur, I., Y. Ren, F. Ordóñez, M. Dessouky, H. Zhong. 2010. A model and algorithm for the courier delivery problem with uncertainty. *Transportation Science* **44**(2) 193–205.

Taş, D., M. Gendreau, N. Dellaert, T. van Woensel, A. de Kok. 2014. Vehicle routing with soft time windows and stochastic travel times: A column generation and branch-and-price solution approach. *European Journal of Operational Research* **236**(3) 789–799.

Taş, D., N. Dellaert, T. van Woensel, T. de Kok. 2013. Vehicle routing problem with stochastic travel times including soft time windows and service costs. *Computers & Operations Research* **40**(1) 214–224.

Toth, P., D. Vigo, eds. 2014. *Vehicle Routing: Problems, Methods, and Applications, Second Edition*. Society for Industrial & Applied Mathematics (SIAM), Philadelphia.

Verweij, B., S. Ahmed, A. J. Kleywegt, G. Nemhauser, A. Shapiro. 2003. The sample average approximation method applied to stochastic routing problems: a computational study. *Computational Optimization and Applications* **24**(2-3) 289–333.

Vidal, T. 2017. Node, edge, arc routing and turn penalties: Multiple problems—one neighborhood extension. *Operations Research* **65**(4) 992–1010.

Vidal, T., T. G. Crainic, M. Gendreau, C. Prins. 2014. A unified solution framework for multi-attribute vehicle routing problems. *European Journal of Operational Research* **234**(3) 658–673.

Vidal, T., G. Laporte, P. Matl. 2020. A concise guide to existing and emerging vehicle routing problem variants. *European Journal of Operational Research* **286**(2) 401–416.

Wang, A., A. Subramanyam, C. E. Gounaris. 2021. Robust vehicle routing under uncertainty via branch-price-and-cut. *Optimization and Engineering* 1–54.

Wiesemann, W., D. Kuhn, M. Sim. 2014. Distributionally robust convex optimization. *Operations Research* **62**(6) 1358–1376.

Zhang, Y., R. Baldacci, M. Sim, J. Tang. 2019a. Routing optimization with time windows under uncertainty. *Mathematical Programming* **175**(1-2) 263–305.

Zhang, Y., Z. Zhang, A. Lim, M. Sim. 2021. Robust data-driven vehicle routing with time windows. *Operations Research* **69**(2) 469–485.

Zhang, Z., Z. Luo, H. Qin, A. Lim. 2019b. Exact algorithms for the vehicle routing problem with time windows and combinatorial auction. *Transportation Science* **53**(2) 427–441.

Zhu, S., M. Fukushima. 2009. Worst-case conditional value-at-risk with application to robust portfolio management. *Operations Research* **57**(5) 1155–1168.

This page is intentionally blank. Proper e-companion title page, with INFORMS branding and exact metadata of the main paper, will be produced by the INFORMS office when the issue is being assembled.

Glossary, MIP model, example, proofs of statements, additional implementation details and computational results

EC.1. Glossary and terminology

Table EC.1 Glossary of symbols used

Symbol	Meaning
$G=(V,A)$	digraph with vertex set $V=\{0,1,2,\ldots,n+m\}$
V_c	set of customers
V_d	set of end depots
q_i, $[e_i,l_i]$	demand and time window of vertex $i\in V$
m, Q	number of vehicles and vehicle capacity
d_{ij}, $\tilde{t}_{ij}$	cost and uncertain travel time of arc $(i,j)\in A$
B	budget value
$\mathcal{R}$, R_r, $V(R_r)$, $A(R_r)$	index set of routes; route, vertices visited, arcs traversed
$\mathcal{P}$, $\mathcal{S}=\{\boldsymbol{x}^p\}_{p\in\mathcal{P}}$	index set of feasible VRPTW solutions and associated characteristic vectors
$\rho(\cdot)$	riskiness-index function
$\boldsymbol{x}$	decision variables of model (1)
$\tau_i(R_s,\boldsymbol{t})$	service start time function of $i\in V$
$\xi_i(R_s,\boldsymbol{t})$	delay function at vertex $i\in V$
$\zeta_s(\rho,\tilde{\boldsymbol{t}})$	total riskiness index of route R_s
c_r, a_{ir}	cost and coefficients of route r
$\boldsymbol{y}$	decision variables of model (6)
$\Omega=\{1,2,\cdots,N\}$	sample set

Table EC.2 Riskiness indices

Term	Reference/Meaning
Riskiness index (RI)	Aumann and Serrano (2008)
Requirement violation index (RVI), $\rho_{RVI}(\tilde{\xi})$	Jaillet et al. (2016)
Essential riskiness index (ERI), $\rho_{ERI}(\tilde{\xi})$	Zhang et al. (2019a)
Service fulfillment risk index (SRI), $\rho_{SRI}(\tilde{\xi})$	Zhang et al. (2021)
Generalized riskiness index (GRI), $\rho_{GRI}(\tilde{\xi})$	New riskiness index introduced in this paper
Convex piecewise riskiness index (CPRI), $\rho_{CPRI}(\tilde{\xi})$	Special instance of the GRI

EC.2. MIP model of Zhang et al. (2021)

In this section, we describe the mixed-integer linear problem (MIP) used by Zhang et al. (2021) for the SRI.

Let $\mathcal{S}=\{\boldsymbol{x}^p\}_{p\in\mathcal{P}}$ be the set of all characteristic vectors associated with the solutions in $\mathcal{P}$, where $\boldsymbol{x}^p\in\mathcal{S}$ denotes the characteristic vector of solution $p\in\mathcal{P}$, and for a vertex $i\in V$, $r(p,i)$ denotes the route index of solution p to which the vertex belongs. Given a route $R_r=(i_0=0,i_1,\ldots,i_\nu,i_{\nu+1})$ with $r\in\mathcal{R}$ and vertices $i,j\in V(R_r)$ such that vertex j precedes i in the route, R_r^{ji} denotes path

$(j,\ldots,i)$ from vertex j up to vertex i. Moreover, $V(R_r^{ji})$ denotes the set of vertices visited and $A(R_r^{ji})$ denotes the set of arcs traversed from vertex j up to vertex i (we assume $V(R_r^{ii})=\{i\}$ and $A(R_r^{ii})=\emptyset$).

Given a solution $p\in\mathcal{P}$ and a realization $\boldsymbol{t}$ of travel times $\tilde{\boldsymbol{t}}$, it can be shown (see Zhang et al. 2021) that the following function determines the *service start time*, $\tau_i(\boldsymbol{x}^p,\boldsymbol{t})$, of vertex $i\in V$ under realization $\boldsymbol{t}$:

$$\tau_i(\boldsymbol{x}^p,\boldsymbol{t})=\max_{j\in V\left(R^{0i}_{r(p,i)}\right)}\left\{e_j+\sum_{a\in A\left(R^{ji}_{r(p,i)}\right)}t_a\right\}. \tag{EC.1}$$

Function $\tau_i(\boldsymbol{x}^p,\boldsymbol{t})$ is convex piecewise affine in $\boldsymbol{t}$ (see Zhang et al. 2021). Based on the service start time function, the *delay function* at vertex i is defined as

$$\bar{\xi}_i(\boldsymbol{x}^p,\boldsymbol{t})=\tau_i(\boldsymbol{x}^p,\boldsymbol{t})-l_i, \tag{EC.2}$$

and hence, a late service at vertex i occurs if and only if $\bar{\xi}_i(\boldsymbol{x}^p,\boldsymbol{t})>0$. Because the travel times $\tilde{\boldsymbol{t}}$ are uncertain, the delay function, $\bar{\xi}_i(\boldsymbol{x}^p,\tilde{\boldsymbol{t}})$, is also uncertain.

Let set $\mathcal{S}$ represent a set of constraints of the two-index (vehicle flow) formulation for the directed capacitated VRP proposed by Laporte et al. (1986), i.e.,

$$\mathcal{S}=\left\{\boldsymbol{x}\in\{0,1\}^{|A|}\;\middle|\;\begin{array}{ll}\displaystyle\sum_{a\in\delta^+(i)}x_a=1, & \forall i\in V_c,\\ \displaystyle\sum_{a\in\delta^-(i)}x_a=1, & \forall i\in V_c,\\ \displaystyle\sum_{a\in\delta^+(0)}x_a\le m, & \\ \displaystyle\sum_{a\in\delta^-(i)}x_a\le 1, & \forall i\in V_d,\\ \displaystyle\sum_{a\in\delta^+(T)}x_a\ge\left\lceil\frac{\sum_{i\in T}q_i}{Q}\right\rceil, & \forall T\subseteq V,|T|\ge 2.\end{array}\right\},$$

where $\delta^-(i)=\{(j,i)\in A\;:\;j\in V\backslash\{i\}\}$ and $\delta^+(i)=\{(i,j)\in A\;:\;j\in V\backslash\{i\}\}$. In the formulation, the first four set of constraints impose degree constraints on the vertices, whereas the last set of constraints are the capacity constraints.

Let η_i be a nonnegative continuous variable representing the SRI value associated with vertex $i\in V$. Zhang et al. (2021) reformulated problem (1) for the SRI as the following MIP problem:

$$\min\quad\sum_{i\in V}\eta_i \tag{EC.3a}$$

$$\text{s.t.}\quad\sum_{a\in A(R^{0i}_{r(p,i)})}(x_a-1)\rho_{SRI}(\bar{\xi}_i(\boldsymbol{y}^p,\tilde{\boldsymbol{t}}))+\rho_{SRI}(\bar{\xi}_i(\boldsymbol{y}^p,\tilde{\boldsymbol{t}}))\le\eta_i, \tag{EC.3b}$$

$$\forall\boldsymbol{y}^p\in\mathcal{S},i\in V:\rho_{SRI}(\bar{\xi}_i(\boldsymbol{y}^p,\tilde{\boldsymbol{t}}))<+\infty,$$

$$\sum_{a\in A(R^{0i}_{r(p,i)})} (x_a - 1) + 1 \le 0, \qquad \text{(EC.3c)}$$

$$\forall \boldsymbol{y}^p \in \mathcal{S}, i \in V : \rho_{SRI}(\bar{\xi}_i(\boldsymbol{y}^p, \tilde{\boldsymbol{t}})) = +\infty,$$

$$\boldsymbol{c}^\top \boldsymbol{x} \le B, \qquad \text{(EC.3d)}$$

$$\boldsymbol{x} \in \mathcal{S}, \qquad \text{(EC.3e)}$$

$$\boldsymbol{\eta} \in \mathbb{R}_+^{|V|}. \qquad \text{(EC.3f)}$$

The objective function (EC.3a) minimizes the sum of the SRI measures over all vertices. Constraints (EC.3b) and (EC.3c) define the correct values of variables η_i, $i \in V$, by imposing the optimality and feasibility of the SRI, respectively. Constraint (EC.3d) imposes the budget limit.

EC.3. Example of decision criteria for measuring lateness level

In this section, we present a VRPTW example to illustrate the performance of different decision criteria to measure lateness levels. Consider a network with four nodes: depot 0 and customers 1, 2, and 3. We abbreviate "with probability" as "w.p." and provide the (correlated) travel time matrix in Table EC.3. Only one vehicle with an infinite capacity is available. It departs from depot 0 at

Table EC.3 Travel time matrix (unit: minute)

nodes	**0**	**1**	**2**	**3**
0	0	100	100	$+\infty$
1	90 w.p. 40%, 110 w.p. 60%	0	90 w.p. 95%, 110 w.p. 5%	100
2	90 w.p. 95%, 120 w.p. 5%	90 w.p. 90%, 105 w.p. 10%	0	100
3	100	100	100	0

time 0, serves each customer exactly once, and returns to the depot. Suppose the time window for each customer is $[0, +\infty]$ and that for the depot is $[0, 400]$; hence, a deadline for returning to the depot is imposed. We can enumerate all candidate routes: $R_1 = (0,1,2,3,0), R_2 = (0,1,3,2,0), R_3 = (0,2,1,3,0), R_4 = (0,2,3,1,0), R_5 = (0,3,1,2,0)$, and $R_6 = (0,3,2,1,0)$. Based on Table EC.3, the travel time from node 0 to 3 is $+\infty$, suggesting that R_5 and R_6 cannot satisfy the deadline of 400 with 100% probability. We next compare the remaining four routes in Table EC.4. The arc travel times in Table EC.3 indicate that the returning time of route R_1 to the depot is 390 with 95% probability and 410 with 5% probability, using which the uncertain delay in Table EC.4 can be obtained.

From the results in Table EC.4, we observe that the lateness probability criterion cannot distinguish the difference between routes R_1 and R_2, although R_1 has a smaller lateness magnitude

Table EC.4 Comparing the decision criteria for the candidate routes

Route	Uncertain delay		Decision criteria					
	Realization	Probability	Lateness probability	Expected lateness duration	RVI	ERI	SRI	CPRI
R_1	-10 10	95% 5%	5%	0.5	3.4	0.53	0.59	3.46
R_2	-10 20	95% 5%	5%	1	7.37	1.05	1.18	6.92
R_3	-10 5	90% 10%	10%	0.5	2.18	0.56	0.63	2.28
R_4	-10 10	40% 60%	60%	6	$+\infty$	$+\infty$	$+\infty$	$+\infty$

than R_2. In contrast, the other decision criteria–expected lateness duration, Requirement Violation Index (RVI), Essential Riskiness Index (ERI), Service Fulfillment Risk Index (SRI), Convex Piecewise Riskiness Index (CPRI)–invariably prefer R_1 over R_2. The expected lateness duration is indifferent to R_1 and R_3, whereas the lateness probability criterion chooses R_1 because of its lower lateness probability. The riskiness indices ERI and SRI would prefer R_1 over R_3, whereas the RVI and the CPRI prefer R_3 over R_1. This is because the exponential disutility underlying the RVI and the CPRI penalize the lateness magnitude in an exponential manner, whereas the ERI and the SRI do this in a linear manner. Although the riskiness indices here seem to be abstract, they are related to the lateness probability guarantee, which is detailed in Section 3 and concretized in Example 2. Route R_4 is late from an expectation perspective. In this case, the lateness probability and the expected lateness duration criteria will tolerate it, whereas the riskiness indices will assert R_4 to be infeasible.

EC.4. Proof of statements

EC.4.1. Proof of Proposition 1

Given a route $r \in \mathcal{R}$ with $R_r = (i_0 = 0, i_1, i_2, \ldots, i_{\nu-1}, i_\nu, i_{\nu+1})$ and a realization of $\tilde{\boldsymbol{t}}$, denoted by $\boldsymbol{t}$, the service start time for each node $i_k \in V(R_r)$ can be computed as:

- $\tau_{i_0}(R_r, \boldsymbol{t}) = e_0$.
- $\tau_{i_1}(R_r, \boldsymbol{t}) = \max\{\tau_{i_0}(R_r, \boldsymbol{t}) + t_{i_0 i_1}, e_{i_1}\}$.
- $\tau_{i_2}(R_r, \boldsymbol{t}) = \max\{\tau_{i_1}(R_r, \boldsymbol{t}) + t_{i_1 i_2}, e_{i_2}\}$.
- ....
- $\tau_{i_\nu}(R_r, \boldsymbol{t}) = \max\{\tau_{i_{\nu-1}}(R_r, \boldsymbol{t}) + t_{i_{\nu-1} i_\nu}, e_{i_\nu}\}$.
- $\tau_{i_{\nu+1}}(R_r, \boldsymbol{t}) = \max\{\tau_{i_\nu}(R_r, \boldsymbol{t}) + t_{i_\nu i_{\nu+1}}, e_{i_{\nu+1}}\}$.

Therefore, for a node $i_k \in V(R_r)$, we derive:

$$\begin{aligned}\tau_{i_k}(R_r,\boldsymbol{t}) = \max\{\tau_{i_{k-1}}(R_r,\boldsymbol{t}) + t_{i_{k-1}\,i_k}, e_{i_k}\} = \\ \max\{\max\{\tau_{i_{k-2}}(R_r,\boldsymbol{t}) + t_{i_{k-2}\,i_{k-1}}, e_{i_{k-1}}\} + t_{i_{k-1}\,i_k}, e_{i_k}\} = \\ \dots \\ \max\{e_0 + t_{i_0\,i_1} + \dots + t_{i_{k-1}\,i_k}, e_1 + t_{i_1\,i_2} + \dots + t_{i_{k-1}\,i_k}, \dots, e_{i_{k-1}} + t_{i_{k-1}i_k}, e_{i_k}\},\end{aligned} \tag{EC.4}$$

or, equivalently

$$\tau_{i_k}(R_r,\boldsymbol{t}) = \max_{h=0,\dots,k}\left\{e_{i_h} + \sum_{l=h}^{k-1} t_{i_l\,i_{l+1}}\right\}.\square \tag{EC.5}$$

EC.4.2. Proof of Theorem 1

The different statements can be proved as follows.

i) *Monotonicity:* If $\mathbb{P}[\tilde{\xi}_1 \geq \tilde{\xi}_2] = 1, \forall \mathbb{P} \in \mathbb{F}$, then $\mathbb{P}[\tilde{\xi}_1/\alpha \geq \tilde{\xi}_2/\alpha] = 1, \forall \mathbb{P} \in \mathbb{F}, \alpha > 0$. Becuase $\phi(\cdot)$ is non-decreasing, we have $\mathbb{E}_{\mathbb{P}}[\phi(\tilde{\xi}_1/\alpha)] \geq \mathbb{E}_{\mathbb{P}}[\phi(\tilde{\xi}_2/\alpha)], \forall \mathbb{P} \in \mathbb{F}$, and therefore $\sup_{\mathbb{P}\in\mathbb{F}} \mathbb{E}_{\mathbb{P}}[\phi(\tilde{\xi}_1/\alpha)] \geq \sup_{\mathbb{P}\in\mathbb{F}} \mathbb{E}_{\mathbb{P}}[\phi(\tilde{\xi}_2/\alpha)]$. Hence, $\mathcal{Y}_1 \subseteq \mathcal{Y}_2$ where $\mathcal{Y}_i \triangleq \{\alpha > 0 | \sup_{\mathbb{P}\in\mathbb{F}} \mathbb{E}_{\mathbb{P}}[\phi(\tilde{\xi}_i/\alpha)] \leq \gamma\}, i = 1, 2$. Finally, we conclude that $\rho_{GRI}(\tilde{\xi}_1) = \inf \mathcal{Y}_1 \geq \inf \mathcal{Y}_2 = \rho_{GRI}(\tilde{\xi}_2)$.

ii) *Satisficing:* If $\mathbb{P}[\tilde{\xi} < 0] = 1, \forall \mathbb{P} \in \mathbb{F}$, then as $\alpha \to 0^+$, we have $\mathbb{P}[\tilde{\xi}/\alpha \to -\infty] = 1, \forall \mathbb{P} \in \mathbb{F}$, and $\mathbb{P}[\phi(\tilde{\xi}/\alpha) \to 0^+] = 1, \forall \mathbb{P} \in \mathbb{F}$, which implies that $\mathbb{E}_{\mathbb{P}}[\phi(\tilde{\xi}/\alpha)] \leq \gamma, \forall \mathbb{P} \in \mathbb{F}$, and that $\alpha = 0^+$ satisfies the constraint in (13). In addition, $\alpha > 0$; taking the infimum, we obtain $\rho_{GRI}(\tilde{\xi}) = 0$.

iii) *Infeasibility:* If $\sup_{\mathbb{P}\in\mathbb{F}} \mathbb{E}_{\mathbb{P}}[\tilde{\xi}] > 0$, then $\sup_{\mathbb{P}\in\mathbb{F}} \mathbb{E}_{\mathbb{P}}[\tilde{\xi}/\alpha] > 0$ for all $\alpha > 0$. Since $\phi(\xi) \geq \xi + 1$, we obtain $\sup_{\mathbb{P}\in\mathbb{F}} \mathbb{E}_{\mathbb{P}}[\phi(\tilde{\xi}/\alpha)] \geq \sup_{\mathbb{P}\in\mathbb{F}} \mathbb{E}_{\mathbb{P}}[\tilde{\xi}/\alpha] + 1 > 1$. Consequently, the constraint in (13) cannot be satisfied and $\rho_{GRI}(\tilde{\xi}) = \inf \emptyset = +\infty$.

iv) *Positive homogeneity:* For all $k > 0$, we have

$$\begin{aligned}\rho_{GRI}(k\tilde{\xi}) &= \inf\left\{\alpha > 0 \;\middle|\; \sup_{\mathbb{P}\in\mathbb{F}} \mathbb{E}_{\mathbb{P}}\left[\phi(k\tilde{\xi}/\alpha)\right] \leq \gamma\right\} \\ &= \inf\left\{(k\alpha) > 0 \;\middle|\; \sup_{\mathbb{P}\in\mathbb{F}} \mathbb{E}_{\mathbb{P}}\left[\phi(k\tilde{\xi}/(k\alpha))\right] \leq \gamma\right\} \\ &= k\inf\left\{\alpha > 0 \;\middle|\; \sup_{\mathbb{P}\in\mathbb{F}} \mathbb{E}_{\mathbb{P}}\left[\phi(\tilde{\xi}/\alpha)\right] \leq \gamma\right\} \\ &= k\rho_{GRI}(\tilde{\xi}),\end{aligned}$$

where the second equality holds by substituting α with $k\alpha$ without loss of generality.

v) *Convexity:* The GRI (13) can be equivalently rewritten as

$$\rho_{GRI}(\tilde{\xi}) = \inf\left\{\alpha > 0 \;\middle|\; \sup_{\mathbb{P}\in\mathbb{F}} \mathbb{E}_{\mathbb{P}}\left[g(\tilde{\xi}, \alpha)\right] \leq 0\right\}, \tag{EC.6}$$

where $g(\xi, \alpha) = \alpha\phi(\xi/\alpha) - \gamma\alpha$. Because $\phi(\xi)$ is convex in $\xi \in \mathbb{R}$, its perspective function $\alpha\phi(\xi/\alpha)$ for $\alpha > 0$ is then jointly convex in (ξ, α). Thus, $g(\xi, \alpha)$ is jointly convex in (ξ, α).

For notational convenience, we express $\alpha_1^\star \triangleq \rho_{GRI}(\tilde{\xi}_1), \alpha_2^\star \triangleq \rho_{GRI}(\tilde{\xi}_2)$ and $\alpha_\lambda \triangleq \lambda\alpha_1^\star + (1-\lambda)\alpha_2^\star$ for $\lambda \in [0, 1]$. By convexity we have

$$g(\lambda\xi_1 + (1-\lambda)\xi_2, \alpha_\lambda) \leq \lambda g(\xi_1, \alpha_1^\star) + (1-\lambda) g(\xi_2, \alpha_2^\star). \tag{EC.7}$$

Hence, $\forall \mathbb{P} \in \mathbb{F}$,

$$\begin{aligned} \mathbb{E}_{\mathbb{P}}[g(\lambda\tilde{\xi}_1 + (1-\lambda)\tilde{\xi}_2, \alpha_\lambda)] &\leq \lambda \mathbb{E}_{\mathbb{P}}[g(\tilde{\xi}_1, \alpha_1^\star)] + (1-\lambda)\mathbb{E}_{\mathbb{P}}[g(\tilde{\xi}_2, \alpha_2^\star)] \\ &\leq \lambda 0 + (1-\lambda)0 \\ &= 0, \end{aligned} \tag{EC.8}$$

where the second inequality holds because the constraint in (EC.6) implies $\mathbb{E}_{\mathbb{P}}[g(\tilde{\xi}_1, \alpha_1^\star)] \leq 0$ and $\mathbb{E}_{\mathbb{P}}[g(\tilde{\xi}_2, \alpha_2^\star)] \leq 0, \forall \mathbb{P} \in \mathbb{F}$.

Owing to the condition (EC.8) and the fact that $\alpha_\lambda = \lambda\alpha_1^\star + (1-\lambda)\alpha_2^\star > 0$, we conclude that α_λ is a feasible solution for the optimization problem underlying the definition (EC.6) of $\rho_{GRI}(\lambda\tilde{\xi}_1 + (1-\lambda)\tilde{\xi}_2)$ and thus $\rho_{GRI}(\lambda\tilde{\xi}_1 + (1-\lambda)\tilde{\xi}_2) \leq \alpha_\lambda$. The result then follows.

vi) *Subadditivity:* To prove the result, we note that

$$\rho_{GRI}(\tilde{\xi}_1 + \tilde{\xi}_2)/2 = \rho_{GRI}((\tilde{\xi}_1 + \tilde{\xi}_2)/2) \leq (\rho_{GRI}(\tilde{\xi}_1) + \rho_{GRI}(\tilde{\xi}_1))/2,$$

where the equality is due to the positive homogeneity property and the inequality follows from the convexity when $\lambda = 1/2$.

vii) *Probability envelope:* Putting $\alpha^\star \triangleq \rho_{GRI}(\tilde{\xi})$, we have, $\forall \mathbb{P} \in \mathbb{F}$ and $\theta > 0$,

$$\begin{aligned} \mathbb{P}\big[\tilde{\xi} > \theta\big] &= \mathbb{P}\big[\tilde{\xi}/\alpha^\star > \theta/\alpha^\star\big] \\ &\leq \mathbb{P}\big[\phi(\tilde{\xi}/\alpha^\star) \geq \phi(\theta/\alpha^\star)\big] \\ &\leq \frac{\mathbb{E}_{\mathbb{P}}[\phi(\tilde{\xi}/\alpha^\star)]}{\phi(\theta/\alpha^\star)} \\ &\leq \frac{\gamma}{\phi\big(\theta/\alpha^\star\big)}. \end{aligned}$$

The first inequality holds because $\phi(\cdot)$ is non-decreasing, the second one owing to Markov's inequality and the fact that $\phi(\cdot)$ is strictly positive in $\mathbb{R}_+$, and the last inequality follows from the definition (13).□

EC.4.3. Proof of Proposition 2

By the convexity of function $\phi(\cdot)$, we have $N^{-1}\sum_{\omega\in\Omega}\phi(\xi^\omega)$ is convex in $\boldsymbol{\xi} = (\xi^\omega)_{\omega\in\Omega}$. Thus, its perspective, $\alpha N^{-1}\sum_{\omega\in\Omega}\phi(\xi^\omega/\alpha)$ for $\alpha > 0$, is jointly convex in $(\boldsymbol{\xi}, \alpha)$. Consequently, $g(\alpha) = \alpha N^{-1}\sum_{\omega\in\Omega}\phi(\xi^\omega/\alpha) - \alpha\gamma$ is convex in α, and subsequently the sublevel set, $\mathcal{M} \triangleq \{\alpha | g(\alpha) \leq 0\}$, is convex. Note that $\mathcal{M}$ is equivalent to $\{\alpha | \psi(\alpha) \leq \gamma\}$. Hence, the convexity of set $\mathcal{M}$ suggests the convexity of $\psi(\alpha)$.□

EC.4.4. Proof of Proposition 3

We first note that given a route $r \in \overline{\mathcal{R}}$, we have that $r \in \mathcal{R}$ because route set $\mathcal{R}$ satisfies the capacity and hard earliest service time window constraints. However, a route $r \in \mathcal{R}$ might not satisfy the

deadlines, l_i, of the time windows constraints under the mean travel times, $\boldsymbol{\mu}$. Therefore, $\overline{\mathcal{R}} \subseteq \mathcal{R}$. Below, we show that $\mathcal{R}_\rho \subseteq \overline{\mathcal{R}}$. Consider a route $r \in \mathcal{R}_\rho$. For each $i \in V(R_r)$, we have:

$$\begin{aligned} & \rho(\xi_i(R_r, \tilde{\boldsymbol{t}})) < +\infty \\ \Rightarrow \quad & \mathbb{E}_{\mathbb{P}}[\xi_i(R_r, \tilde{\boldsymbol{t}})] \leq 0 \\ \Rightarrow \quad & \mathbb{E}_{\mathbb{P}}[\tau_i(R_r, \tilde{\boldsymbol{t}}) - l_i] \leq 0 \\ \Rightarrow \quad & \mathbb{E}_{\mathbb{P}}[\tau_i(R_r, \tilde{\boldsymbol{t}})] \leq l_i \\ \Rightarrow \quad & \tau_i(R_r, \mathbb{E}_{\mathbb{P}}[\tilde{\boldsymbol{t}}]) \leq \mathbb{E}_{\mathbb{P}}[\tau_i(R_r, \tilde{\boldsymbol{t}})] \leq l_i. \end{aligned} \tag{EC.9}$$

The four implications result from the (i) infeasibility property, (ii) definition of the delay function (4), (iii) translation invariance of $\mathbb{E}_{\mathbb{P}}$, and (iv) property that the service start time function $\tau_i(R_r, \tilde{\boldsymbol{t}})$ is convex piecewise affine in $\tilde{\boldsymbol{t}}$ and Jensen's inequality. We conclude that $\mathcal{R}_\rho \subseteq \overline{\mathcal{R}} \subseteq \mathcal{R}$.□

EC.4.5. Proof of Theorem 2

Let $\mathcal{B} = \{r \in \mathcal{R}_\rho : y_r^* = 1\}$ be the index set of the routes of solution $\boldsymbol{y}^*$ of cost $z(FB(\mathcal{R}_\rho)) \leq B$ and, by contradiction, suppose that there exists $r' \in \mathcal{B}$ such that $\overline{c}_{r'} > B - \overline{z}$. Therefore, we have

$$\sum_{r\in\mathcal{B}} \overline{c}_r = \sum_{r\in\mathcal{B}} c_r - \sum_{r\in\mathcal{B}} \sum_{i\in V_c} b_{ir}\overline{u}_i - \sum_{r\in\mathcal{B}} \overline{u}_0. \tag{EC.10}$$

Because $\mathcal{B}$ represents a feasible solution of model $FB(\mathcal{R}_\rho)$, we have:

$$\sum_{r\in\mathcal{B}} \sum_{i\in V_c} b_{ir}\overline{u}_i + \sum_{r\in\mathcal{B}} \overline{u}_0 = \sum_{i\in V_c} \overline{u}_i + |\mathcal{B}|\overline{u}_0 \geq \sum_{i\in V_c} \overline{u}_i + m\overline{u}_0, \tag{EC.11}$$

where the last inequality holds since $|\mathcal{B}| \leq m$ and $\overline{u}_0 \leq 0$. The last term of the above inequality equals the cost of the dual solution, $\overline{z}$, and since $z(FB(\mathcal{R}_\rho)) = \sum_{r\in\mathcal{B}} c_r$ we obtain

$$z(FB(\mathcal{R}_\rho)) \geq \overline{z} + \sum_{r\in\mathcal{B}} \overline{c}_r. \tag{EC.12}$$

Because solution $\overline{\boldsymbol{u}}$ is a feasible dual solution, we have $\overline{c}_r \geq 0$, $\forall r \in \mathcal{B}$, and from inequality (EC.12), we derive

$$\begin{aligned} z(FB(\mathcal{R}_\rho)) \geq \overline{z} + \sum_{r\in\mathcal{B}} \overline{c}_r \geq \overline{z} + \overline{c}_{r'} > \\ \overline{z} + B - \overline{z} = B. \square \end{aligned} \tag{EC.13}$$

EC.5. Bisection algorithm for evaluating GRI

The bisection algorithm for evaluating the GRI is presented in Algorithm 1. Herein, becuase $+\infty$ is non-implementable, we use M to replace it in our implementation. Note that because $\psi(\alpha)$ is convex, its subgradient, $\mathrm{d}\psi(\alpha)/\mathrm{d}\alpha$, always exists. As a common argument, the bisection algorithm terminates in finite steps. Specifically, because each iteration cuts the search space, $[\varepsilon, M]$, by half, it takes at most $\lceil \log_2((M-\varepsilon)/\epsilon) \rceil$ iterations to terminate. For example, if $M = 10^3$ and $\varepsilon = \epsilon = 10^{-3}$, then the maximum number of iterations is 20.

Algorithm 1 Bisection for evaluating GRI

if $\sum_{\omega\in\Omega}\xi^{\omega}>0$ **then**
  return $+\infty$ ▷ By infeasibility property in Theorem 1
Let $\overline{\alpha}\leftarrow M$ and $\underline{\alpha}\leftarrow\varepsilon$ ▷ M is big number and ε is small positive number
if $\psi(\underline{\alpha})\leq\gamma$ **then**
  return 0 ▷ By definition in (15)
Initialize $\alpha^{\star}\leftarrow+\infty$ ▷ We use $\alpha^{\star}$ to restore GRI
if $\psi(\overline{\alpha})>\gamma$ **then** ▷ If yes, we find some feasible $\alpha\in(\underline{\alpha},\overline{\alpha})$ via bisection
  while $\overline{\alpha}-\underline{\alpha}>\epsilon$ **do** ▷ ϵ is tolerable error bound
    Let $\alpha\leftarrow(\underline{\alpha}+\overline{\alpha})/2$ ▷ α is tentative GRI
    if $\psi(\alpha)\leq\gamma$ **then** ▷ We already find a feasible α
      Let $\overline{\alpha}\leftarrow\alpha$ and **break**
    else ▷ α is infeasible. Continue bisection
      if $\mathrm{d}\psi(\alpha)/\mathrm{d}\alpha>0$ **then** ▷ By convexity of $\psi(\alpha)$, we have $\alpha^{\star}\notin[\alpha,\overline{\alpha}]$
        Let $\overline{\alpha}\leftarrow\alpha$
      else ▷ By convexity of $\psi(\alpha)$, we have $\alpha^{\star}\notin[\underline{\alpha},\alpha]$
        Let $\underline{\alpha}\leftarrow\alpha$
while $\overline{\alpha}-\underline{\alpha}>\epsilon$ **do** ▷ If we enter this loop, we must have $\psi(\underline{\alpha})>\gamma$ and $\psi(\overline{\alpha})\leq\gamma$
  Let $\alpha\leftarrow(\underline{\alpha}+\overline{\alpha})/2$
  if $\psi(\alpha)\leq\gamma$ **then** ▷ Such α is feasible
    Let $\overline{\alpha}\leftarrow\alpha$ and $\alpha^{\star}\leftarrow\alpha$
  else
    Let $\underline{\alpha}\leftarrow\alpha$
return $\alpha^{\star}$

EC.6. Comparing computational efficiency of Algorithm 1 and closed-form solution of Zhang et al. (2021) for evaluating SRI

In practice, the efficiency of the riskiness index calculation is particularly important because it is repeatedly performed several times in resolution methods. We conduct experiments for solving instances with 25 nodes using the SRI as the riskiness index. Specifically, we repeat the experiments in Table EC.5 by changing the riskiness index from the CPRI to the SRI, where the number, N, of samples is set as 200. We apply Algorithm 1 and the closed-form solution of Zhang et al. (2021), respectively, to evaluate the SRI. In Algorithm 1, we set $M=10^{3},\varepsilon=\epsilon=10^{-3}$. The total computational time used for evaluating the SRI in each instance and the average over all instances are shown in Figure EC.1.

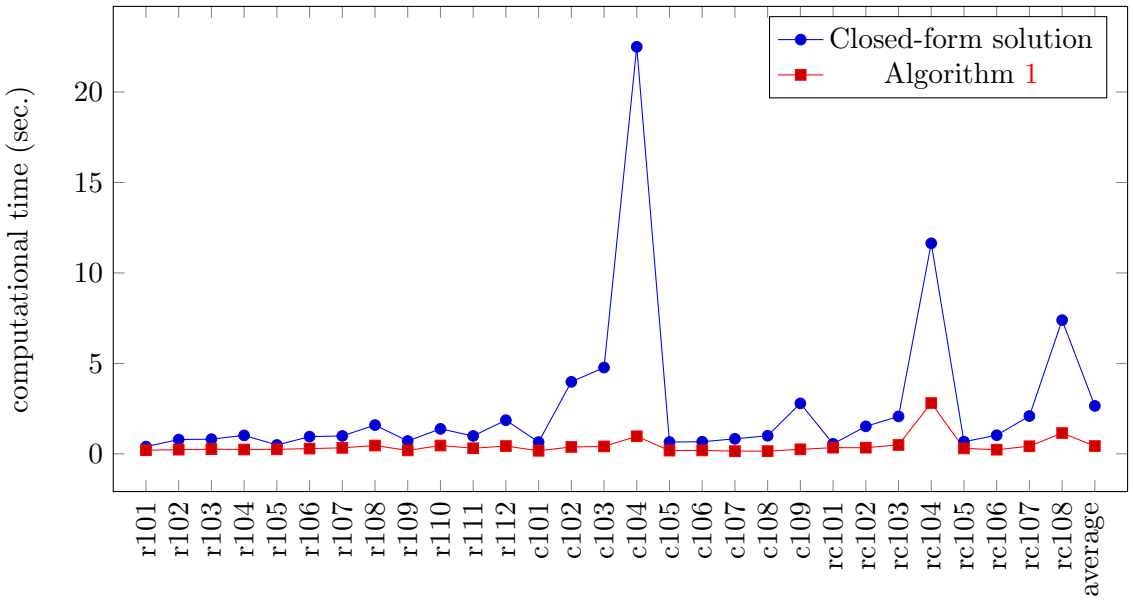

Figure EC.1 The total computational time for evaluating the SRI

Unexpectedly, Algorithm 1, although being more generally applicable than the closed-form solution, requires a shorter computational time for all instances. Specifically, the average over all instances is 0.43, approximately five times faster than that of the closed-form solution, 2.65 seconds. This probably is caused by the closed-form solution necessitating a sorting procedure with complexity $O(N \log N)$, which can be relatively time consuming.

EC.7. Implementation details

EC.7.1. Pricing algorithm

Let $v \leq 0$ be the dual variable associated with constraint (6d) of the LP relaxation of formulation $F_\rho(\mathcal{R}_\rho)$, and consider the dual vectors–$\boldsymbol{u}$, $\boldsymbol{\pi}$, $\boldsymbol{\eta}$ and $\boldsymbol{\varphi}$–introduced in Section 5.1.2. The pricing problem under the set of samples, Ω, needs computing

$$\min_{r\in\mathcal{R}_\rho}\Bigg\{\zeta_r(\rho,\tilde{\boldsymbol{t}})-\sum_{i\in V_c}a_{ir}u_i-u_0-c_rv-\sum_{(i,j)\in A}b_{ijr}\sum_{S\in\mathcal{S}_P:(i,j)\in\delta^+(S)}\pi_S- \sum_{(i,j)\in A}b_{ijr}\sum_{S\in\mathcal{S}_C:(i,j)\in\delta^+(S)}\eta_S-\sum_{C\in\mathcal{C}:|V(R_r)\cap C|\geq 2}\varphi_T\Bigg\}, \tag{EC.14}$$

where $\zeta_r(\rho,\tilde{\boldsymbol{t}})=\sum_{i\in V(R_r)}\rho(\xi_i(R_r,\tilde{\boldsymbol{t}}))$ and function $\rho(\xi_i(R_r,\tilde{\boldsymbol{t}}))$ is computed using Algorithm 1 presented in §3.3. The last three terms of the above expression account for the dual contributions of the 2PIs, CIs and SR3Is, respectively. Problem (EC.14) is an ESPPRC and can be effectively solved by a label-setting algorithm (Irnich and Desaulniers 2005) as follows:

We designed a forward dynamic programming-based algorithm, where a label L represents a partial path P starting at depot 0 and ending at vertex $i \in V$ and is composed of the following information commonly used in label-setting algorithms for VRPs:

- i: the last vertex in P.
- X: the set of vertices visited by P (also used to denote the sequence of vertices visited).
- c: the travel cost of P.
- $\overline{c}$: the reduced cost of P.
- w: the cumulative load along P.
- $\tau(\mu)$: the earliest time at which a service can start at vertex i under the mean travel time $\boldsymbol{\mu}$.
- $\mathcal{H}$: the set of binary resources associated with the SR3Is in set $\mathcal{C}$. For each SR3I inequality associated with a subset T, we consider one binary integer resource $\kappa : \mathcal{R}_\rho \to \{0,1\}$. $T(\kappa)$ and $\varphi(\kappa)$ denote the vertex subset defining the SR3I inequality and the associated dual variable, respectively.

In addition, the following two components are specifically introduced to deal with the riskiness index $\rho(\cdot)$:

- ζ: the cumulative riskiness index along P.
- $\{\tau(\omega)\}_{\omega\in\Omega}$: the earliest time at which service can start at vertex i under the different samples in set Ω.

The label extension rule for a label $L = (i, X, c, \overline{c}, w, \tau(\mu), \mathcal{H}, \zeta, \{\tau(\omega)\}_{\omega\in\Omega})$ is as follows. Let j be a vertex in set $V_c \cup \{n+1\} \setminus X$ such that $w + q_j \le Q$, $\tau(\mu) + \mu_{ij} \le l_j$ and $\zeta + \rho(\xi_j(P', \tilde{\boldsymbol{t}})) < +\infty$, where $\rho(\xi_j(P', \tilde{\boldsymbol{t}}))$ computes the riskiness index of path P' obtained by appending vertex j to the partial path P. If $j = n+1$, then path P' corresponds to a complete route. Otherwise, a new label L' is created to append vertex j to path P as follows:

$$i(L') = j, \tag{EC.15a}$$

$$X(L') = X(L) \cup \{j\}, \tag{EC.15b}$$

$$c(L') = c(L) + d_{ij}, \tag{EC.15c}$$

$$\overline{c}(L') = \overline{c}(L) + \rho(\xi_j((X,j), \tilde{\boldsymbol{t}})) - u_j - d_{ij}v - \overline{\pi}_{ij} - \sum_{\substack{\kappa\in\mathcal{H}\ s.t.\\ \kappa(L)=1,\, j\in T(\kappa)}} \varphi(\kappa), \tag{EC.15d}$$

$$w(L') = w(L) + q_j, \tag{EC.15e}$$

$$\tau(\mu)(L') = \max\{e_j, \tau(\mu)(L) + \mu_{i(L)j}\}, \tag{EC.15f}$$

$$\kappa(L') = \begin{cases} \mathrm{mod}(\kappa(L)+1, 2), & \text{if } j \in T(\kappa) \\ \kappa(L), & \text{otherwise} \end{cases}, \tag{EC.15g}$$

$$\zeta(L') = \zeta(L) + \rho(\xi_j((X,j), \tilde{\boldsymbol{t}})), \tag{EC.15h}$$

$$\tau(\omega)(L') = \max\{e_j, \tau(\omega)(L) + t_{ij}^{\omega}\}, \forall \omega \in \Omega, \tag{EC.15i}$$

where $\overline{\pi}_{ij} = \sum_{S \in \mathcal{S}_P : (i,j) \in \delta^+(S)} \pi_S + \sum_{S \in \mathcal{S}_C : (i,j) \in \delta^+(S)} \eta_S$.

The algorithm starts with an initial label $L = (0, \emptyset, 0, -u_0, 0, 0, \{0\}_{\kappa \in \mathcal{H}}, 0, \{0\}_{\omega \in \Omega})$.

To reduce the number of labels to extend, the dominance rule below is proposed to identify the labels that can be safely discarded. This dominance rule extends that proposed for a deterministic VRPTW by Jepsen et al. (2008) to account for the riskiness index.

Dominance 1 *Let L_1 and L_2 be two labels with $i(L_1) = i(L_2)$. Label L_1 dominates label L_2 if*

(i) $X(L_1) \subseteq X(L_2)$,

(ii) $w(L_1) \leq w(L_2)$,

(iii) $\tau(\mu)(L_1) \leq \tau(\mu)(L_2)$,

(iv) $\tau(\omega)(L_1) \leq \tau(\omega)(L_2)$, $\forall \omega \in \Omega$,

(v) $\overline{c}(L_1) - \sum_{\kappa \in \mathcal{H} \, s.t. \, \kappa(L_1)=1, \kappa(L_2)=0} \varphi(\kappa) \leq \overline{c}(L_2)$,

and at least one of the above inequalities is strict.

Conditions (i)–(iv) ensure that the feasible extensions of L_1 are also feasible for L_2. Inequality (v) aims at considering all resources from which a common extension of L_1 and L_2 will result in increasing the reduced cost of L_1 without increasing that of L_2. Thus, the inequality represents the impossibility of the reduced cost of L_1 exceeding that of L_2. It follows that L_2 can be safely discarded as it will never produce paths better than those that can be produced by extending L_1.

Note that Proposition 3 causes condition (iv) of Dominance 1 to dominate condition (iii). However, condition (iii) can accelerate the computation. In addition, based on Proposition 3 and the infeasibility property, graph G can be reduced by removing arcs $(i,j) \in A$ such that $e_i + \mu_{ij} > l_j$ or $\mathbb{E}_{\mathbb{P}}[\max\{e_i + \tilde{t}_{ij}, e_j\}] > l_j$.

Our implementation of the above label-setting algorithm also relies on a state-of-the-art algorithm based on an *ng-set based decremental state space relaxation* (Martinelli et al. 2014) and *completion bounds* (Baldacci et al. 2011). In particular, the completion bounds are computed by disregarding the SR3Is and the computation of the riskiness indices. We omit the corresponding details for the sake of brevity.

EC.7.2. Generating set of routes $\overline{\mathcal{R}}_\rho$

Column or route enumeration-based methods have been shown to be particularly effective for routing problems (Baldacci et al. 2008, Costa et al. 2019). To enumerate the set of routes $\overline{\mathcal{R}}_\rho$ at Step 2 of the exact algorithm, we use two different enumeration strategies.

The first strategy is based on a simple adaptation of the label-setting algorithm used to compute the dual solution $(\boldsymbol{u}, \boldsymbol{\pi}, \boldsymbol{\eta}, \boldsymbol{\varphi})$ (see §5.1.2) in Step 2 of the exact algorithm. More precisely, the

algorithm is modified to generate the largest route set $\hat{\mathcal{R}} = \{r \in \overline{\mathcal{R}} : \overline{c}_r \leq B - \overline{z}\}$, where the reduced cost of a route $r \in \overline{\mathcal{R}}$ is computed as

$$\overline{c}_r = c_r - \sum_{i \in V_c} a_{ir} u_i - u_0 - \sum_{(i,j) \in A} b_{ijr} \sum_{S \in \mathcal{S}_P : (i,j) \in \delta^+(S)} \pi_S - \sum_{(i,j) \in A} b_{ijr} \sum_{S \in \mathcal{S}_C : (i,j) \in \delta^+(S)} \eta_S - \sum_{C \in \mathcal{C} : |V(R_r) \cap C| \geq 2} \varphi_T \Bigg\}, \tag{EC.16}$$

and the final route set $\overline{\mathcal{R}}_\rho$ is computed as $\overline{\mathcal{R}}_\rho = \{r \in \hat{\mathcal{R}} : \rho(\xi_i(R_r, \tilde{\boldsymbol{t}})) < +\infty, \forall i \in V(R_r)\}$. Specifically, the set of routes $\hat{\mathcal{R}}$ is further reduced by (a posteriori) removing it from the set the routes that are infeasible for the infeasibility property.

In the second strategy, the computations of the riskiness index and the infeasibility property are embedded into a label-setting algorithm based on the algorithm used to solve formulation $F_\rho(\mathcal{R}_\rho)$ (see §EC.7.1). In this case, the reduced cost computed using (EC.15d) is modified to

$$\overline{c}(L') = \overline{c}(L) + d_{ij} - u_j - \overline{\pi}_{ij} - \sum_{\substack{\kappa \in \mathcal{H} \text{ s.t.} \\ \kappa(L)=1,\, j \in T(\kappa)}} \varphi(\kappa). \tag{EC.17}$$

In addition, Dominance 1 is modified as follows:

Dominance 2 *Let L_1 and L_2 be two labels with $i(L_1) = i(L_2)$. Label L_1 dominates label L_2 if*

(i) $X(L_1) = X(L_2)$,

(ii) $\tau(\mu)(L_1) \leq \tau(\mu)(L_2)$,

(iii) $\tau(\omega)(L_1) \leq \tau(\omega)(L_2)$, $\forall \omega \in \Omega$,

(iv) $\overline{c}(L_1) - \sum_{\substack{\kappa \in \mathcal{H} \text{ s.t.} \\ \kappa(L_1)=1, \kappa(L_2)=0}} \varphi(\kappa) \leq \overline{c}(L_2)$,

(v) $c(L_1) \leq c(L_2)$.

It is worth noting that the two strategies also differ in the dynamic programming strategy used to generate the labels. The first strategy relies on a bidirectional strategy, by which first, forward and backward labels are computed and subsequently joined to form complete routes. In the second strategy, although the infeasible labels are fathomed timely, the labels are generated in a forward manner. The motivation is that when the riskiness index is accounted into the reduced cost computation (as in the second strategy), the computation of the backward labels is difficult owing to the computation of the riskiness index. Based on experiments aimed at selecting the best strategy (see §6), we adopted the second strategy to perform the route enumeration. Finally, two different routes visiting the same customers may have the same riskiness index, particularly in the first option. To further reduce the number of routes generated, the following dominance rule is also used:

Table EC.5 Results of EXM under the CPRI on instances with 25 customers

							Step 1		Step 2		Step 3			
Name	B	$\underline{z}$	z^*	$\%gap$	$\%cost$	t_{tot}	$\%lb$	t	$\lvert\overline{\mathcal{R}}_\rho\rvert$	t	Method	z_{heu}	$nodes$	t
c101	200.87	7.36	7.36	0.00	95.24	0.92	95.24	0.59	1389	0.26	MIP	-	-	0.02
c102	199.82	7.19	7.19	0.00	95.24	3.67	95.24	1.26	8334	1.87	MIP	-	-	0.08
c103	199.82	0.86	0.86	0.00	97.04	5.32	95.24	1.95	2351	2.57	MIP	-	-	0.70
c104	196.25	0.00	0.00	0.00	99.16	13.96	95.24	2.19	18073	10.61	MIP	-	-	0.52
c105	200.87	0.00	0.00	0.00	95.24	1.29	95.24	0.87	2073	0.32	MIP	-	-	0.03
c106	200.87	17.67	17.67	0.00	95.24	1.03	95.24	0.60	1734	0.31	MIP	-	-	0.02
c107	200.87	0.00	0.00	0.00	98.62	1.51	95.24	0.73	4108	0.56	MIP	-	-	0.05
c108	200.87	0.00	0.00	0.00	95.24	2.10	95.24	1.21	2977	0.72	MIP	-	-	0.04
c109	200.87	0.00	0.00	0.00	95.68	3.72	95.24	1.49	1954	1.99	MIP	-	-	0.12
r101	647.96	40.83	40.83	0.00	99.77	0.83	95.24	0.47	294	0.17	MIP	-	-	0.18
r102	574.46	9.02	9.02	0.00	99.35	1.37	95.24	0.68	1501	0.49	MIP	-	-	0.14
r103	477.33	10.73	10.73	0.00	98.55	1.80	95.24	0.73	1689	0.58	MIP	-	-	0.38
r104	437.75	12.79	12.79	0.00	99.60	2.31	95.24	0.85	2246	0.80	MIP	-	-	0.59
r105	557.02	9.90	9.90	0.00	99.73	1.05	95.24	0.57	736	0.24	MIP	-	-	0.19
r106	488.67	18.76	18.76	0.00	99.39	2.87	95.24	1.42	2196	0.78	MIP	-	-	0.60
r107	445.52	14.16	14.16	0.00	98.76	2.96	95.24	1.07	2429	0.82	MIP	-	-	1.00
r108	417.17	6.61	6.61	0.00	98.50	6.48	95.24	1.93	4682	1.61	MIP	-	-	2.70
r109	463.37	10.97	10.97	0.00	98.54	1.22	95.24	0.62	1117	0.37	MIP	-	-	0.19
r110	466.31	1.86	1.86	0.00	98.73	5.22	92.17	1.74	7422	1.99	MIP	-	-	1.29
r111	450.24	5.58	5.58	0.00	99.66	2.76	95.24	1.33	2354	0.73	MIP	-	-	0.62
r112	412.65	2.17	2.17	0.00	99.14	8.21	95.24	3.52	4355	1.84	MIP	-	-	2.69
rc101	484.16	39.79	39.79	0.00	99.93	1.97	95.24	0.92	1422	0.41	MIP	-	-	0.59
rc102	369.39	155.57	155.57	0.00	99.60	2.31	95.24	0.74	1454	1.50	MIP	-	-	0.02
rc103	349.44	8.66	8.66	0.00	98.87	4.05	95.24	1.10	1316	2.84	MIP	-	-	0.02
rc104	321.93	8.91	8.91	0.00	99.90	14.48	95.24	1.41	7902	12.68	MIP	-	-	0.11
rc105	431.87	18.81	18.81	0.00	98.71	1.51	95.24	0.71	1495	0.64	MIP	-	-	0.11
rc106	362.78	4.94	4.94	0.00	98.13	1.54	95.24	0.82	869	0.67	MIP	-	-	0.01
rc107	313.22	0.54	0.54	0.00	99.20	2.99	95.24	0.99	957	1.94	MIP	-	-	0.01
rc108	309.23	1.82	1.82	0.00	99.86	7.87	95.24	1.46	832	6.36	MIP	-	-	0.01

Dominance 3 *A route $r_1 \in \overline{\mathcal{R}}_\rho$ dominates a route $r_2 \in \overline{\mathcal{R}}_\rho$ if the following conditions are satisfied:*

(i) $V(R_{r_1}) \cap V_c = V(R_{r_2}) \cap V_c$,

(ii) $c_{r_1} \leq c_{r_2}$,

(iii) $\zeta_{r_1}(\rho, \tilde{\boldsymbol{t}}) \leq \zeta_{r_2}(\rho, \tilde{\boldsymbol{t}})$.

EC.8. Additional computational results

EC.8.1. Detailed results of EXM under CPRI

This section presents the detailed results of the EXM based on the new CPRI obtained by solving the benchmark instances.

Tables EC.5, EC.6 and EC.7 list the results obtained for the instances involving 25, 50 and 100 nodes, respectively. For each instance, the tables provide the name of the instance, value of budget B, best lower bound obtained at the end of the exact method ("$\underline{z}$"), CPRI of the optimal solution or the CPRI of the best solution found ("z^*"), and percentage gap $\%gap$ with respect to the optimal solution value, computed as $100 \times (z^* - \underline{z})/z^*$. The $\%gap$ is equal to zero if the instance is solved to optimality. The tables also list the percentage deviation, $\%cost$, of the total routing cost, c, computed as $100 \times c/B$, and the total computing time in seconds of the EXM ("t_{tot}"). For Step 1, column $\%lb$ provides the percentage deviation of the initial lower bound, lb, computed

Table EC.6 Results of EXM under the CPRI on instances with 50 customers

							Step 1		Step 2		Step 3			
Name	B	$\underline{z}$	z^*	$\%gap$	$\%cost$	t_{tot}	$\%lb$	t	$\lvert\overline{\mathcal{R}}_\rho\rvert$	t	Method	z_{heu}	$nodes$	t
c101	380.52	7.40	7.40	0.00	95.24	2.16	95.24	1.04	14081	0.75	MIP	-	-	0.12
c102	379.47	7.17	7.17	0.00	97.90	11.46	95.24	1.88	55706	7.10	MIP	-	-	1.02
c103	379.47	1.13	1.13	0.00	98.11	236.49	95.24	3.78	302842	214.16	iBPC	inf	2	18.54
c104	375.90	0.00	-	-	-	14400.00	95.24	11.89	Δ_{max}	480.24	BPC	inf	10	13538.01
c105	380.52	0.00	0.00	0.00	97.03	4.88	95.24	1.41	32467	2.08	MIP	-	-	0.47
c106	380.52	18.68	18.68	0.00	95.66	22.53	95.24	1.44	44989	3.00	MIP	-	-	16.90
c107	380.52	0.00	0.00	0.00	97.81	4.66	95.24	1.44	25305	1.14	MIP	-	-	1.66
c108	380.52	0.00	0.00	0.00	96.11	34.78	95.24	2.52	35764	3.13	MIP	-	-	28.16
c109	380.52	0.00	0.00	0.00	99.47	45.83	95.24	4.26	101458	28.90	iBPC	0.00	18	12.66
r101	1096.20	50.64	50.64	0.00	99.89	2.14	95.24	1.27	5494	0.51	MIP	-	-	0.28
r102	954.45	53.57	53.57	0.00	99.99	29.43	95.24	1.18	60395	9.96	MIP	-	-	17.07
r103	811.54	46.67	46.67	0.00	99.90	177.83	95.14	5.19	307828	115.14	iBPC	114.53	95	57.50
r104	656.67	26.77	26.77	0.00	99.91	1256.01	95.24	12.76	1246194	684.67	iBPC	inf	101	558.57
r105	944.26	8.26	8.26	0.00	99.98	9.41	95.96	3.07	20485	2.03	MIP	-	-	3.88
r106	832.65	14.15	14.15	0.00	99.86	133.81	94.77	2.69	166012	41.00	iBPC	66.22	202	90.12
r107	746.66	29.71	29.71	0.00	99.98	469.75	95.83	19.33	521649	254.09	iBPC	inf	48	196.32
r108	648.59	4.86	-	-	-	14400.00	93.64	32.23	Δ_{max}	783.95	BPC	inf	2	13855.71
r109	826.14	7.98	7.98	0.00	99.87	117.57	94.76	9.26	193186	37.68	iBPC	inf	55	70.62
r110	731.85	10.77	10.77	0.00	99.94	89.26	95.24	4.90	177707	44.72	iBPC	inf	40	39.63
r111	742.56	6.17	6.17	0.00	99.82	323.40	95.24	12.46	487192	166.84	iBPC	inf	101	144.09
r112	661.71	14.25	14.25	0.00	99.79	1252.27	95.46	113.08	1306765	658.62	iBPC	inf	72	480.56
rc101	991.20	18.05	18.05	0.00	99.85	11.16	95.23	2.46	13217	1.56	MIP	-	-	6.74
rc102	863.62	58.50	58.50	0.00	99.45	104.85	95.16	5.14	59922	34.66	MIP	-	-	63.68
rc103	746.45	56.10	56.10	0.00	99.81	286.87	95.24	4.62	71738	93.47	MIP	-	-	187.09
rc104	573.09	18.77	18.77	0.00	99.39	220.35	95.73	3.20	28147	215.76	MIP	-	-	0.64
rc105	898.06	33.98	33.98	0.00	99.86	38.02	95.24	3.35	31201	10.34	MIP	-	-	23.61
rc106	759.36	196.67	196.67	0.00	97.95	30.93	95.24	4.25	13858	7.65	MIP	-	-	18.68
rc107	674.84	57.91	57.91	0.00	99.99	59.83	94.88	4.57	13598	38.87	MIP	-	-	15.82
rc108	628.00	51.56	51.56	0.00	99.94	144.59	95.24	8.39	15590	113.34	MIP	-	-	22.44

as $100 \times lb/B$. For Step 2, column $|\overline{\mathcal{R}}_\rho|$ reports the cardinality of the set of routes generated by the route enumeration phase; we report Δ_{max} whenever $|\overline{\mathcal{R}}_\rho| \geq \Delta_{max}$. Concerning Step 3, column "Method" indicates the method that is used in solving the instance: "MIP" (general MIP solver, Step 3.a), "iBPC" (implicit BPC, Step 3.b), and "BPC" (BPC, Step 3.c). In addition, for Step 3, the tables tabulate the CPRI of the best solution found by the heuristic algorithm during the BPC (for "iBPC" or "BPC") (we report "-" if the upper bound is not computed and "inf" if the heuristic fails to compute a valid upper bound). They also specify the number of nodes of the BPC executed in Step 3.b or 3.c ("*nodes*"). Finally, for each step of the EXM, the tables report the corresponding computing times ("t").

EC.8.2. Effectiveness of the different EXM components

In this section, we describe the investigation of the effectiveness of the route enumeration step of the EXM. More specifically, we compared the following three versions of the EXM: (i) with the use of the bidirectional label-setting algorithm (see Strategy 1, §EC.7.2), (ii) with the use of the forward label-setting algorithm (see Strategy 2), and (iii) without the use of the route enumeration phase, wherein the EXM works as a pure BPC. The three versions of the EXM were tested on the 25 and 50 node instances.

Table EC.7 Results of EXM under the CPRI on instances with 100 customers

							Step 1		Step 2		Step 3			
Name	B	$\underline{z}$	z^*	$\%gap$	$\%cost$	t_{tot}	$\%lb$	t	$\lvert\overline{\mathcal{R}}_\rho\rvert$	t	Method	z_{heu}	$nodes$	t
c101	868.66	12.01	12.01	0.00	99.29	14400.00	95.24	3.32	1048792	47.54	iBPC	293.25	401	14350.81
c102	868.66	2.85	-	-	-	14400.00	95.24	8.92	Δ_{max}	542.80	BPC	-	2	13814.17
c103	867.62	0.07	-	-	-	14400.00	95.24	17.76	Δ_{max}	526.88	BPC	-	2	13862.08
c104	864.04	0.00	-	-	-	14400.00	95.24	47.95	Δ_{max}	499.83	BPC	-	7	13235.56
c105	868.66	0.00	0.00	0.00	97.77	342.28	95.24	5.85	3069085	164.47	iBPC	0	3	171.94
c106	868.66	14.04	14.04	0.00	99.20	14396.47	95.24	5.96	2270867	174.89	iBPC	-	212	14215.61
c107	868.66	0.00	0.00	0.00	99.54	919.60	95.24	7.87	7282608	440.07	iBPC	0	5	471.61
c108	868.66	0.00	-	-	-	14400.00	95.24	8.85	Δ_{max}	485.36	BPC	-	18	12401.99
c109	868.66	0.00	0.00	0.00	99.53	595.97	95.24	19.36	Δ_{max}	576.14	BPC	0.00	1	0.45
r101	1719.59	197.97	197.97	0.00	99.98	212.38	93.73	5.73	689596	69.42	iBPC	-	197	137.22
r102	1539.93	116.52	574.85	79.73	0.00	14400.00	93.27	6.48	Δ_{max}	708.90	BPC	574.85	10	13657.27
r103	1269.13	84.20	799.80	89.47	0.00	14400.00	94.94	20.23	Δ_{max}	674.26	BPC	799.8	3	13683.75
r104	1020.08	0.00	-	-	-	14400.00	95.27	850.59	Δ_{max}	655.75	BPC	-	1	12889.45
r105	1423.07	37.09	-	-	-	14400.00	95.03	32.22	Δ_{max}	756.68	BPC	-	15	13539.98
r106	1296.33	31.36	-	-	-	14400.00	95.12	62.21	Δ_{max}	790.53	BPC	-	4	13509.95
r107	1117.83	33.10	-	-	-	14400.00	94.76	74.76	Δ_{max}	656.89	BPC	-	1	13651.64
r108	978.91	0.00	-	-	-	14400.00	94.70	1126.61	Δ_{max}	842.91	BPC	-	1	12426.07
r109	1204.25	26.42	-	-	-	14400.00	94.94	70.46	Δ_{max}	643.50	BPC	-	3	13662.57
r110	1121.40	23.19	-	-	-	14400.00	95.12	146.27	Δ_{max}	707.85	BPC	-	1	13524.76
r111	1101.13	28.46	-	-	-	14400.00	94.88	149.37	Δ_{max}	707.67	BPC	-	1	13525.03
r112	996.03	0.00	-	-	-	14400.00	94.88	4651.92	Δ_{max}	748.49	BPC	-	1	9003.80
rc101	1700.79	107.90	107.90	0.00	99.99	1581.74	95.24	26.35	2184102	323.23	iBPC	-	131	1232.14
rc102	1530.27	75.47	-	-	-	14400.00	95.23	98.88	Δ_{max}	891.46	BPC	-	6	13382.00
rc103	1320.90	55.64	-	-	-	14400.00	95.22	390.29	Δ_{max}	812.11	BPC	-	1	13205.63
rc104	1188.91	0.00	-	-	-	14400.00	94.97	1669.96	Δ_{max}	708.54	BPC	-	1	12016.88
rc105	1589.39	110.05	-	-	-	14400.00	95.24	35.25	Δ_{max}	998.15	BPC	-	6	13335.11
rc106	1441.34	47.50	-	-	-	14400.00	94.71	180.24	Δ_{max}	991.72	BPC	-	2	13187.63
rc107	1268.19	18.56	-	-	-	14400.00	95.24	101.83	Δ_{max}	821.99	BPC	-	1	13469.65
rc108	1169.91	0.00	-	-	-	14400.00	94.84	641.48	Δ_{max}	789.03	BPC	-	1	12965.04

Tables EC.8 and EC.9 summarize the results obtained by the different versions of the EXM, where the notations of the different columns are as previously described and the last row of each table provides the average results. Columns $\underline{z}$ and z^* report the values of the lower bounds and the solution values of Tables EC.5 and EC.6, respectively.

The results of the comparison noticeably show the advantage of using the route enumeration phase in terms of the number of instances solved to optimality, either using Strategy 1 or 2. Indeed, the pure BPC variant cannot solve to optimality two 25 node instances and almost all 50 node instances. On the instances solved to optimality by the pure BPC, the other two variants require considerably shorter computing times. From the comparison of the two strategies, expectedly, the cardinalities of the corresponding sets of routes, $\overline{\mathcal{R}}_\rho$, are similar; however, Strategy 2 (forward label setting) is on average approximately three and nine times faster than Strategy 1 (bidirectional LS) on the 25 and 50 node instances, respectively.

EC.8.3. Sensitivity analyses on budget B and on number N of samples

To investigate the impacts of the budget value, B, and the number, N, of samples, we considered the 50 node instances solved by the EXM algorithm using different values of B and N.

Table EC.8 Effectiveness of the route enumeration phase on the 25 customer instances

			Bidirectional LS			Forward LS			Pure BPC		
Name	$\underline{z}$	z^*	$\lvert\overline{\mathcal{R}}_\rho\rvert$	t_{RE}	t_{tot}	$\lvert\overline{\mathcal{R}}_\rho\rvert$	t_{RE}	t_{tot}	$\underline{z}$	z^*	t_{tot}
c101	7.36	7.36	1389	0.60	1.30	1389	0.25	0.92	7.36	7.36	252.84
c102	7.19	7.19	8334	15.41	16.96	8334	1.85	3.67	7.07	7.19	14400.00
c103	0.86	0.86	2351	7.84	10.35	2351	2.56	5.32	0.68	3.42	14400.00
c104	0.00	0.00	18073	45.58	49.12	18073	10.59	13.96	0.00	0.00	845.34
c105	0.00	0.00	2073	1.05	1.89	2073	0.32	1.29	0.00	0.00	0.12
c106	17.67	17.67	1734	0.71	1.40	1734	0.30	1.03	17.67	17.67	218.38
c107	0.00	0.00	4108	1.98	3.00	4108	0.55	1.51	0.00	0.00	0.13
c108	0.00	0.00	2977	4.19	5.69	2977	0.71	2.10	0.00	0.00	0.15
c109	0.00	0.00	1954	5.33	6.98	1954	1.98	3.72	0.00	0.00	0.14
r101	40.83	40.83	294	0.33	0.96	294	0.16	0.83	40.83	40.83	654.85
r102	9.02	9.02	1501	1.35	2.40	1501	0.48	1.37	9.02	9.02	609.04
r103	10.73	10.73	1689	1.58	2.77	1689	0.58	1.80	10.73	10.73	1323.28
r104	12.79	12.79	2246	2.31	3.88	2246	0.79	2.31	12.79	12.79	7074.47
r105	9.90	9.90	736	0.50	1.27	736	0.24	1.05	9.90	9.90	305.71
r106	18.76	18.76	2193	2.16	4.36	2196	0.77	2.87	18.76	18.76	1128.18
r107	14.16	14.16	2429	2.56	4.43	2429	0.81	2.96	14.16	14.16	4271.98
r108	6.61	6.61	4682	5.75	10.85	4682	1.60	6.48	6.61	6.61	3098.87
r109	10.97	10.97	1117	0.86	1.82	1117	0.36	1.22	10.97	10.97	2006.67
r110	1.86	1.86	7422	7.46	10.77	7422	1.98	5.22	1.86	1.86	1591.12
r111	5.58	5.58	2354	2.23	4.33	2354	0.73	2.76	5.58	5.58	1235.67
r112	2.17	2.17	4355	5.00	11.81	4355	1.82	8.21	2.17	2.17	4771.95
rc101	39.79	39.79	1422	1.05	2.50	1422	0.40	1.97	39.79	39.79	454.15
rc102	155.57	155.57	1454	3.59	4.42	1454	1.49	2.31	155.57	155.57	4284.12
rc103	8.66	8.66	1316	8.12	9.38	1316	2.83	4.05	8.66	8.66	2269.30
rc104	8.91	8.91	7901	21.58	23.39	7902	12.67	14.48	8.91	8.91	12198.88
rc105	18.81	18.81	1495	2.09	3.01	1495	0.63	1.51	18.81	18.81	1617.63
rc106	4.94	4.94	869	2.48	3.36	869	0.66	1.54	4.94	4.94	158.16
rc107	0.54	0.54	957	4.82	5.85	957	1.94	2.99	0.54	0.54	2329.60
rc108	1.82	1.82	832	6.40	7.90	832	6.35	7.87	1.82	1.82	13648.48
	14.33	14.33	3112	5.69	7.45	3112	1.94	3.70	14.32	14.42	3281.01

More specifically, for the budget value, B, we compared the results of the default setting (i.e., $B = 1.05 \times opt$, where opt is the optimal cost of the deterministic VRPTW) with two alternatives values, $B = 1.01 \times opt$ and $B = 1.03 \times opt$. For the number, N, of samples, we compared the default value of $N = 200$ adopted in our experiments with two alternative values $N = 500$ and $N = 1000$. Tables EC.10 and EC.11 summarize the obtained results; the notations of the different columns are the same as in the previous tables, and the last line of each table reports the average values.

The results reported in Table EC.10 show that the EXM is particularly sensitive to the value of budget, B, which controls the quality of the final solution in terms of the total routing cost. Therefore, it is particularly relevant for a decision maker interested in the analysis of the trade-off between the service quality, addressed by the CPRI in the EXM, and the cost. Managerially, a low cost budget B results in a high (or at least equal) value z^* of the CPRI, which represents a tradeoff between the cost and the service level, consistent with our expectation. Computationally, a low value of B implies a high efficiency of the EXM, as displayed by the average computing times. The main cause of this is that the cardinality of the set of routes, $\overline{\mathcal{R}}_\rho$, is significantly reduced for low

Table EC.9 Effectiveness of the route enumeration phase on the 50 customer instances

			Bidirectional LS			Forward LS			Pure BPC		
Name	$\underline{z}$	z^*	$\lvert\overline{\mathcal{R}}_\rho\rvert$	t_{RE}	t_{tot}	$\lvert\overline{\mathcal{R}}_\rho\rvert$	t_{RE}	t_{tot}	$\underline{z}$	z^*	t_{tot}
c101	7.40	7.40	14081	2.32	3.65	14081	0.74	2.16	7.40	7.40	353.44
c102	7.17	7.17	55706	88.68	93.16	55706	7.08	11.46	6.79	7.17	14400.00
c103	1.13	1.13	302801	3421.4	3441.55	302842	214.15	236.49	0.73	-	14400.00
c104	0.00	-	Δ_{max}	56.04	14400.00	Δ_{max}	480.19	14400.00	0.00	-	14400.00
c105	0.00	0.00	32465	14.92	18.31	32467	2.06	4.88	0.00	0.00	0.24
c106	18.68	18.68	44989	17.6	36.87	44989	2.99	22.53	18.68	18.68	439.11
c107	0.00	0.00	25305	11.11	14.00	25305	1.13	4.66	0.00	0.00	0.33
c108	0.00	0.00	35764	43.29	76.70	35764	3.11	34.78	0.00	0.00	369.46
c109	0.00	0.00	101461	197.58	210.73	101458	28.87	45.83	0.00	0.00	0.31
r101	50.64	50.64	5494	2.05	3.89	5494	0.50	2.14	50.64	50.64	515.71
r102	53.57	53.57	60348	67.78	80.77	60395	9.95	29.43	53.57	53.57	10679.34
r103	46.67	46.67	307716	662.6	725.22	307828	115.12	177.83	46.39	111.29	14400.00
r104	26.77	26.77	1245420	3250.51	4592.46	1246194	684.65	1256.01	24.88	647.81	14400.00
r105	8.26	8.26	20485	11.54	18.73	20485	2.02	9.41	8.26	8.26	1381.75
r106	14.15	14.15	165937	241.64	310.65	166012	40.99	133.81	13.13	66.17	14400.00
r107	29.71	29.71	521655	1142.62	1430.55	521649	254.07	469.75	29.59	-	14400.00
r108	4.86	-	Δ_{max}	14774.4	14400.00	Δ_{max}	783.77	14400.00	4.86	-	14400.00
r109	7.98	7.98	193088	182.33	263.52	193186	37.66	117.57	7.98	7.98	13165.90
r110	10.77	10.77	177666	209.64	251.80	177707	44.70	89.26	10.76	-	14400.00
r111	6.17	6.17	487137	814.49	954.76	487192	166.82	323.40	5.73	-	14400.00
r112	14.25	14.25	1306923	2941.3	3444.82	1306765	658.59	1252.27	9.76	-	14400.00
rc101	18.05	18.05	13216	10.37	19.10	13217	1.55	11.16	18.05	18.05	1810.30
rc102	58.50	58.50	59920	217.37	282.84	59922	34.64	104.85	53.76	-	14400.00
rc103	56.10	56.10	71742	569.75	1322.45	71738	93.46	286.87	54.37	-	14400.00
rc104	18.77	18.77	28151	785.39	790.33	28147	215.75	220.35	0.00	-	14400.00
rc105	33.98	33.98	31199	69.36	95.37	31201	10.32	38.02	33.98	33.98	6713.28
rc106	196.67	196.67	13861	57.66	79.83	13858	7.64	30.93	160.13	-	14400.00
rc107	57.91	57.91	13596	276.05	298.66	13598	38.86	59.83	57.45	-	14400.00
rc108	51.56	51.56	15591	504.88	542.49	15590	113.33	144.59	0.00	-	14400.00
	27.58	29.44	198212	1056.71	1662.18	198251	139.82	1169.66	23.34	64.44	9663.07

B values. Nevertheless, the problem can become infeasible as shown by the infeasible instances (marked with "inf" in the table), and therefore a trade-off must be identified.

Table EC.11 lists the results obtained by varying the sample size, concerning the instances for which the EXM can compute the optimal solution for each different sample size. The increase in the number, N, of samples has a marginal effect on the number of routes generated during the enumeration phase, as shown by the average cardinalities of sets $\overline{\mathcal{R}}_\rho$ under the different sample sizes. The number of samples directly impacts the complexity of the pricing problem, because the computation of the CPRI and the dominance rules depend on the number of samples. Indeed, the average computing time under the 1000 samples case is approximately thrice that in the 200 samples case, where most of the additional time is spent by the route enumeration phase (see column t_{RE}).

To better understand the impact of the number, N, of samples on the CPRI, we additionally perform out-of-sample evaluation using another 10,000 independent samples and report the results ("$\hat{z}$"). As shown, with the increase in the number of samples, the in-sample z^* increases and the out-of-sample $\hat{z}$ decreases, suggesting that the *optimizer's curse* (or *overfitting effect*) is alleviated and

Table EC.10 Sensitivity analysis on the budget B

Name	$B = 1.01 \times opt$					$B = 1.03 \times opt$					$B = 1.05 \times opt$				
	z^*	$\%gap$	$\lvert\overline{\mathcal{R}}_\rho\rvert$	t_{RE}	t_{tot}	z^*	$\%gap$	$\lvert\overline{\mathcal{R}}_\rho\rvert$	t_{RE}	t_{tot}	z^*	$\%gap$	$\lvert\overline{\mathcal{R}}_\rho\rvert$	t_{RE}	t_{tot}
c101	7.40	0.00	1050	0.20	1.29	7.40	0.00	5923	0.48	1.81	7.40	0.00	14081	0.74	2.16
c102	7.35	0.00	1807	0.33	2.28	7.17	0.00	13932	1.72	4.10	7.17	0.00	55706	7.08	11.46
c103	1.30	0.00	2235	24.44	27.57	1.13	0.00	51247	67.87	73.13	1.13	0.00	302842	214.15	236.49
c104	0.00	0.00	1068	129.76	142.27	0.00	0.00	Δ_{max}	985.28	2111.93	-	-	Δ_{max}	480.19	14400.00
c105	0.00	0.00	1529	0.22	1.58	0.00	0.00	10146	0.71	2.50	0.00	0.00	32467	2.06	4.88
c106	18.68	0.00	1352	0.19	1.65	18.68	0.00	12930	0.72	2.37	18.68	0.00	44989	2.99	22.53
c107	0.00	0.00	907	0.18	1.69	0.00	0.00	8661	0.62	2.26	0.00	0.00	25305	1.13	4.66
c108	0.00	0.00	297	0.20	2.72	0.00	0.00	5549	0.79	3.39	0.00	0.00	35764	3.11	34.78
c109	0.00	0.00	620	0.57	5.83	0.00	0.00	14494	4.00	9.35	0.00	0.00	101458	28.87	45.83
r101	inf	0.00	574	0.19	1.77	82.75	0.00	2758	0.34	2.21	50.64	0.00	5494	0.50	2.14
r102	inf	0.00	1164	0.31	1.67	78.63	0.00	13155	2.33	5.12	53.57	0.00	60395	9.95	29.43
r103	93.84	0.00	3347	0.83	6.17	70.33	0.00	57111	16.61	61.33	46.67	0.00	307828	115.12	177.83
r104	58.55	0.00	4114	2.69	16.85	42.74	0.00	166902	58.85	136.68	26.77	0.00	1246194	684.65	1256.01
r105	inf	0.00	121	0.29	4.26	161.59	0.00	4407	1.07	8.24	8.26	0.00	20485	2.02	9.41
r106	95.75	0.00	4579	1.02	5.40	23.05	0.00	35871	5.60	24.27	14.15	0.00	166012	40.99	133.81
r107	187.96	0.00	740	2.51	21.19	100.19	0.00	60509	28.20	121.78	29.71	0.00	521649	254.07	469.75
r108	51.73	0.00	165900	83.78	290.03	13.88	0.00	1721109	1001.27	1858.30	-	-	Δ_{max}	783.77	14400.00
r109	32.51	0.00	4530	1.37	9.80	15.87	0.00	47980	9.39	47.28	7.98	0.00	193186	37.66	117.57
r110	inf	0.00	1169	0.34	3.79	55.16	0.00	26502	4.76	102.47	10.77	0.00	177707	44.70	89.26
r111	inf	0.00	2376	2.03	15.60	16.89	0.00	64590	19.81	48.48	6.17	0.00	487192	166.82	323.40
r112	109.36	0.00	3059	22.80	133.74	41.86	0.00	164109	128.91	380.76	14.25	0.00	1306765	658.59	1252.27
rc101	inf	0.00	2234	0.61	4.83	48.32	0.00	9664	1.21	13.12	18.05	0.00	13217	1.55	11.16
rc102	127.85	0.00	2756	1.05	6.84	59.02	0.00	23414	11.32	38.87	58.50	0.00	59922	34.64	104.85
rc103	164.38	0.00	1665	3.05	7.98	82.94	0.00	15986	28.67	62.08	56.10	0.00	71738	93.46	286.87
rc104	47.38	0.00	210	29.59	32.62	20.96	0.00	4747	80.33	83.41	18.77	0.00	28147	215.75	220.35
rc105	112.08	0.00	2138	0.56	4.07	51.39	0.00	14319	3.69	23.86	33.98	0.00	31201	10.32	38.02
rc106	inf	0.00	1048	0.53	4.26	196.67	0.00	5874	4.27	14.49	196.67	0.00	13858	7.64	30.93
rc107	453.84	0.00	639	8.21	12.41	87.92	0.00	3735	21.71	29.05	57.91	0.00	13598	38.86	59.83
rc108	inf	0.00	393	11.65	19.87	64.69	0.00	3966	38.91	47.81	51.56	0.00	15590	113.33	144.59
		0.00	7366	11.36	27.24		0.00	89734	85.71	143.51			198251	139.82	1169.66

Table EC.11 Sensitivity analysis on the sample size

Name	$N = 200$					$N = 500$					$N = 1000$				
	z^*	$\hat{z}$	$\overline{\mathcal{R}}_\rho$	t_{RE}	t_{tot}	z^*	$\hat{z}$	$\overline{\mathcal{R}}_\rho$	t_{RE}	t_{tot}	z^*	$\hat{z}$	$\overline{\mathcal{R}}_\rho$	t_{RE}	t_{tot}
c101	7.40	8.94	14081	0.74	2.16	7.29	8.94	14464	1.30	3.33	8.28	8.94	16722	3.51	5.55
c102	7.17	6.95	55706	7.08	11.46	6.40	6.95	73970	35.93	41.41	6.77	6.95	105335	114.56	121.75
c103	1.13	1.04	302842	214.15	236.49	1.06	1.04	145297	136.51	149.06	1.02	1.04	189254	332.34	346.60
c105	0.00	0.00	32467	2.06	4.88	0.00	0.00	32512	2.62	4.75	0.00	0.00	32485	6.52	8.79
c106	18.68	18.30	44989	2.99	22.53	18.03	18.30	28865	2.38	5.04	17.96	18.30	14431	3.48	5.70
c107	0.00	0.22	25305	1.13	4.66	0.00	0.22	36254	2.90	5.99	0.00	0.22	36253	8.92	13.19
c108	0.00	0.24	35764	3.11	34.78	0.00	0.24	81015	10.63	26.59	0.00	0.00	52747	23.88	60.64
c109	0.00	0.00	101458	28.87	45.83	0.00	0.00	96973	61.21	137.68	0.00	0.00	91674	133.08	277.19
r101	50.64	50.39	5494	0.50	2.14	51.27	50.39	5168	0.98	2.43	51.04	50.39	5384	3.02	5.53
r102	53.57	58.38	60395	9.95	29.43	55.36	58.38	70598	34.25	50.91	56.05	56.73	69672	76.49	93.91
r103	46.67	55.61	307828	115.12	177.83	50.62	48.19	273568	261.11	319.45	48.19	47.36	251828	527.22	590.13
r105	8.26	11.24	20485	2.02	9.41	9.35	9.76	19709	5.57	12.65	9.64	9.76	19707	10.12	16.27
r106	14.15	22.82	166012	40.99	133.81	16.67	21.01	164509	86.94	166.92	17.17	18.85	177959	220.93	274.00
r107	29.71	45.59	521649	254.07	469.75	29.65	35.20	558209	615.04	861.98	33.74	35.20	555116	1350.30	1680.39
r109	7.98	16.83	193186	37.66	117.57	11.31	14.02	179720	76.93	157.81	11.93	12.54	205671	194.44	278.04
r110	10.77	13.87	177707	44.70	89.26	13.00	13.87	170206	101.19	153.57	14.76	13.87	163295	221.68	269.52
r111	6.17	10.51	487192	166.82	323.40	7.74	13.14	504275	406.71	543.18	7.94	10.51	558623	987.94	1125.87
rc101	18.05	17.55	13217	1.55	11.16	17.59	17.55	13476	3.17	9.27	16.89	17.55	13281	8.88	16.57
rc102	58.50	56.51	59922	34.64	104.85	53.68	56.51	48992	39.61	81.27	54.84	56.51	50885	169.39	230.88
rc103	56.10	55.62	71738	93.46	286.87	54.55	56.99	67621	162.59	559.84	55.05	55.62	64272	480.43	927.92
rc104	18.77	23.91	28147	215.75	220.35	19.94	23.62	24300	378.50	381.76	20.72	23.52	19307	773.70	777.56
rc105	33.98	37.05	31201	10.32	38.02	41.94	37.05	32338	17.61	110.47	41.59	37.05	35297	66.94	140.83
rc106	196.67	197.85	13858	7.64	30.93	180.58	197.85	14391	14.53	31.63	176.41	198.09	12484	38.60	59.48
rc107	57.91	61.90	13598	38.86	59.83	61.69	61.90	22104	82.78	100.26	63.95	61.90	31372	281.20	297.11
rc108	51.56	51.16	15590	113.33	144.59	51.04	52.44	13675	218.52	239.01	50.70	51.16	30050	573.68	596.23
	30.15	32.90	111993	57.90	104.48	30.35	32.14	107688	110.38	166.25	30.59	31.68	112124	264.45	328.79

the accuracy is improved, respectively. Although the results show the benefit of using more samples, the improvement is marginal and associated with the consequence of increased computational burden. Thus, a sample size of 200 may suffice for many real-world applications.